# 5. SITE 698[1]

Shipboard Scientific Party[2]

## Hole 698A

**Date occupied:** 17 March 1987

**Date departed:** 19 March 1987

**Time on hole:** 2 days, 9 hr

**Position:** 51°27.51′S; 33°05.96′W

**Bottom felt (rig floor; m; drill-pipe measurement):** 2138.0

**Distance between rig floor and sea level (m):** 10.50

**Water depth (drill-pipe measurement from sea level; corrected m):** 2138

**Total depth (rig floor; corrected m):** 2375.0

**Penetration:** 237.0

**Number of cores:** 27

**Total length of cored section (m):** 237.0

**Total core recovered (m):** 52.26

**Core recovery (%):** 22

**Oldest sediment cored:**
**Depth sub-bottom (m):** 200.15
**Nature:** sandy mud
**Age:** Campanian or older
**Measured velocity (km/s):** 2.4

**Basement:**
**Depth sub-bottom (m):** 210.43–237.0
**Nature:** sparsely phyric, holocrystalline basalt, trachytic to subtrachytic basalt, and ferro(?)basalt with slight to pervasive veining and variable amounts of alteration products overlying a weathered basalt
**Measured velocity (km/s):** 4.2–5.28 for basalt, 1.8 for weathered basalt regolith

**Principal results:** Site 698 is near the eastern edge of the shallowest part of the Northeast Georgia Rise (51°27.51′S, 33°05.96′W) at a water depth of 2128 m. The primary objectives of the site were largely tectonic in nature: to determine the age, nature, and subsidence history of basement; to establish the possible role of the Northeast Georgia Rise as a Late Cretaceous/early Tertiary convergent boundary between the Malvinas plate and the South American plate; and to determine the temporal relationship between subduction at the Northeast Georgia Rise and southern Andean Orogeny. These objectives are also important for evaluating the influence of the Northeast Georgia Rise and other regional plateaus and ridges as Late Cretaceous–Paleogene obstructions to deep-water interchange between the Weddell and South Atlantic basins.

Early departure from port and rapid transit resulted in the gain of 2.3 days of operational time used to drill this lower priority site. A single hole was rotary (RCB) cored (to ensure basement penetration in the time allotted) in 2 days and 9 hr, from 17 to 19 March 1987. Hole 698A consists of 27 cores to a depth of 237 mbsf with 22% recovery. Weather conditions were excellent. Drilling terminated 27.6 m into basement.

The sequence recovered at Site 698 consists of a surface residual-lag deposit of ice-rafted detritus above a thick, pelagic carbonate sequence of nannofossil ooze, nannofossil chalk, and limestone. Common chert stringers and nodules, which occur throughout the carbonate section, hampered sediment recovery. Basement consists of fine-grained, sparsely phyric, holocrystalline basalt, trachytic to subtrachytic basalt, and ferro(?)basalt overlying a hematite-rich basaltic regolith. The dominant lithologies in the stratigraphic sequence and their ages are as follows:

0–4.25 mbsf: ice-rafted gravel of mixed lithologies and rock types of probable Pliocene-Quaternary age

4.25–42 mbsf: foraminifer-bearing nannofossil ooze of late early to early middle Eocene age

42–146.5 mbsf: foraminifer-bearing chalk of Maestrichtian to early Eocene age

146.5–190.5 mbsf: very-fine-grained limestone of Campanian to Maestrichtian age

200–200.15 mbsf: sandy mud of probable Campanian age

209.5–219.28 mbsf: sparsely phyric, holocrystalline basalt (Core 114-698A-24R) and trachytic to subtrachytic basalt and ferro(?)basalt (Core 114-698A-25R), with slight to pervasive veining and variable amounts of alteration products

219.28–237 mbsf: extremely weathered basalt (regolith) in which the original Fe-Mg minerals have been completely altered to hematite, with some microbreccia containing fragments of altered (to serpentine) basaltic material.

The smooth and layered acoustic basement on the Northeast Georgia Rise may be attributed to, at least in its upper part, interbedded altered basalt flows and the highly weathered (subaerially?) basaltic regolith. A sandy mud above basement may represent a transgressive sand incorporating some eroded weathered basalt. Sparse nannofossils in this sandy mud suggest a Campanian age, if they are not downhole contaminants. A 9.5-m recovery gap occurs between the sandy mud and the base of the overlying pelagic carbonate sequence of probable Campanian age. Initial subsidence of the Northeast Georgia Rise must have occurred during the Campanian or earlier, as benthic foraminifers throughout the carbonate sequence overlying basement are indicative of water depths no less than lower bathyal, >1000 m below sea level (mbsl). If the Northeast Georgia Rise was a Cretaceous convergent boundary between the Malvinas and South American plates, the cessation of any subduction must have occurred prior to or during the early Campanian.

An apparently uninterrupted sequence of pelagic carbonate accumulated on the subsiding basement of the Northeast Georgia Rise during the Campanian/Maestrichtian to early middle to late early Eocene. Unfortunately, the Cretaceous/Tertiary boundary was not recovered in adjacent cores of late Maestrichtian and Danian age. The sequence contains nodular chert horizons and displays progressive lithification from nannofossil ooze to limestone. Sedimentation rates for the early Paleogene are 6–9 m/m.y. The Late Cretaceous–early Paleogene surface waters were well oxygenated, and there are indications that the low-energy benthic environment periodically experienced oxygen-reduced conditions. Relative climatic warmth is indicated by calcareous microfossil assemblages, which include discoasters.

In spite of poor recovery, the section is relatively undisturbed. The section will provide an important Late Cretaceous to early Paleogene reference point for biostratigraphic, biogeographic, and isotopic studies of the antarctic-subantarctic region by the scientists of ODP Legs 113 and 114.

Correlation of Site 698 to site survey seismic lines reveals a major deformational episode in the western part of the Northeast Georgia Rise, which has downfaulted strata of post-early middle Eocene age.

---

[1] Ciesielski, P. F., Kristoffersen, Y., et al., 1988. *Proc. ODP, Init. Repts.*, 114: College Station, TX (Ocean Drilling Program).

[2] Shipboard Scientific Party is as given in the list of Participants preceding the contents, with the addition of M. Perfit, Department of Geology, University of Florida, Gainesville, FL 32611.

The similarities in the seismic character of the younger effected strata with that of sections drilled on the Maurice Ewing Bank suggest that deformation occurred during the Miocene. This event may be related to Miocene compression between the South Georgia block and the Northeast Georgia Rise.

## BACKGROUND AND OBJECTIVES

Site 698 (51°27.51′S, 33°05.96′W; 2128 m water depth; Figs. 1 and 2) is near the eastern edge of the apex of the Northeast Georgia Rise, an oceanic plateau of mid-Cretaceous to Paleocene age. This second priority site was not scheduled to be drilled unless operation time additional to that required for drilling the first priority sites became available. Early departure from port and rapid transit resulted the accumulation of sufficient time for drilling the site. In spite of being considered lower priority, Site 698 was anticipated to yield evidence that would answer major questions regarding the history of the Malvinas plate. Although the shallow water depth at this site (~2128 mbsl) made the sedimentary sequence of the rise an attractive target for obtaining well-preserved pelagic sediments, the small amount of drilling time available for this site (approximately 2 days) required the selection of a thin sedimentary sequence (~200 m) to ensure that the more important basement objectives would be reached.

Single-channel seismic-reflection profiles (Figs. 2 and 3) indicate the presence of a more than 1-s-thick (two-way traveltime [TWT]) sequence of sediments, which is thinned by erosional truncation toward the flanks of the shallowest part of the rise. Acoustic basement is very smooth and shows evidence of layering in its upper part.

A thin veneer of Pliocene-Quaternary sediment was anticipated to cover unconformably the lower, well-bedded seismic sequence at Site 698. Piston cores taken on the Northeast Georgia Rise (Fig. 3), including some in close proximity to Site 698, recovered 1.5 to 8.0 m of mid-Gilbert to Brunhes Chronozone sediment, consisting of muddy diatomaceous ooze or diatomaceous mud, rich in sand- and pebble-size ice-rafted detritus (Fig. 4; P. Ciesielski, unpubl. data). Within 10 to 15 m below seafloor (mbsf), Paleogene sediments were anticipated to represent the lower well-bedded seismic sequence. Expected lithologies in this sequence were chalk, biosiliceous chalk, and zeolitic clay. The age of the oldest sediments blanketing the Northeast Georgia Rise at this site and elsewhere was inferred to be Late Cretaceous or older, from the tectonic position of the Northeast Georgia Rise within a domain of oceanic crust generated by seafloor spreading in the Cretaceous magnetic quiet zone. The major unconformity is tentatively related to enhanced circulation in the late Oligocene/early Miocene as a consequence of the opening of the Drake Passage. The basement may consist of basalt flows with intercalated sediments because the site is only 5 km away from a small volcano and the seismic data show clear evidence of layering in the vicinity of the sediment/basement contact (Fig. 2).

Site 698 is approximately 60 to 100 km south of the mean present-day Antarctic Convergence Zone, which separates antarctic and subantarctic surface-water masses (Fig. 5). Figures 6 and 7 show the location of Site 698 plotted against modern hydrologic data from the region between the eastern extremity of the Falkland Plateau and the Islas Orcadas Rise. The site is just to the north of the potential temperature and salinity line shown in Figure 6. In the vicinity of the site, the temperature of modern surface waters is near 2°C and decreases to −0.5°C below 4000 m.

The seafloor at the site is presently under the influence of Circumpolar Deep Water (CPDW), which flows eastward through the Drake Passage and then bends northward toward the Northeast Georgia Rise from east of South Georgia Island. During the Late Cretaceous to early Paleogene, the seafloor may have been in subantarctic to temperate surface waters, deepening to intermediate water depth during the Paleogene and finally subsiding to the depth of the CPDW (or its precursor) during the early Neogene.

Surface productivity over the site was expected to have been influenced by subantarctic or temperate surface waters until the middle to late Neogene. Since that time surface productivity has probably been under the influence of subantarctic and antarctic surface waters. Ice-rafted detritus was expected to be sparse, except in the thin upper Neogene cap overlying the unconformity where it was concentrated as a residual lag from strong CPDW flow.

### Site Objectives

Site 698 objectives were as follows:

1. To determine the subsidence history of the Northeast Georgia Rise. Sediment lithologic and paleontologic characteristics were to be used to interpret the rate of subsidence of this oceanic plateau. Interpretation of the subsidence rates in terms of the lithospheric stress and thermal state could contribute to better understanding of the mechanisms that generated this feature. The rates of subsidence of the Northeast Georgia Rise, as well as the Islas Orcadas Rise and Meteor Rise, are essential for evaluating the role of these plateaus as possible major obstructions to deep water during the Late Cretaceous–Paleogene (Figs. 8–10).

2. To determine the geologic history of the Northeast Georgia Rise and its relationship to the southern Andean Orogeny and the development of the Scotia Sea. LaBrecque and Hayes (1979) documented the existence of the Malvinas plate and its motion with respect to Africa in the Late Cretaceous. The extent of the Malvinas plate in the Late Cretaceous is uncertain because of the limited geophysical data in the region. Additionally, most of the Mesozoic crust from the western Indo-Atlantic Basin (except for that in the Georgia Basin) has been removed by convergence with the Falkland block and/or consumed as the South Sandwich subduction zone advanced eastward. The regional geology of the North Scotia Ridge and the Northeast Georgia Rise may allow a reconstruction of the Mesozoic history of the northern Indo-Atlantic Basin. The Andean Orogeny generated a mid-Cretaceous accretionary prism that extends 2000 km from Tierra del Fuego to South Georgia Island. The North Scotia Ridge may be interpreted as the remains of an accretionary prism that has subsequently been dissected by the generation of the Scotia Sea since the Oligocene. Plate tectonic analysis and marine geophysical data show the Northeast Georgia Rise may have been a portion of the convergent boundary between the Malvinas and South American plates that was active during the Southern Andean Orogeny. Figure 8 (from LaBrecque, 1986) displays the geometry and the amount of convergence predicted between the Malvinas plate and the South American plate during the Late Cretaceous. The model predicts nearly 1000 km of northward convergence in Tierra del Fuego (if the Malvinas plate extended as far west as Tierra del Fuego), as well as the proper sense of motion to generate the Northeast Georgia Rise. Therefore, this model can explain the Southern Andean Orogeny and link the North Scotia Ridge sediments to Weddell Basin development by attributing accretion of the sediments to the opposing (northern) flank of a spreading center that generated the present-day Weddell seafloor (J. L. LaBrecque, pers. comm., 1987).

The thin sedimentary sequence targeted at Site 698 also augments other major objectives of the leg. The anticipated recovery of Paleogene to Upper Cretaceous sediments at this site was

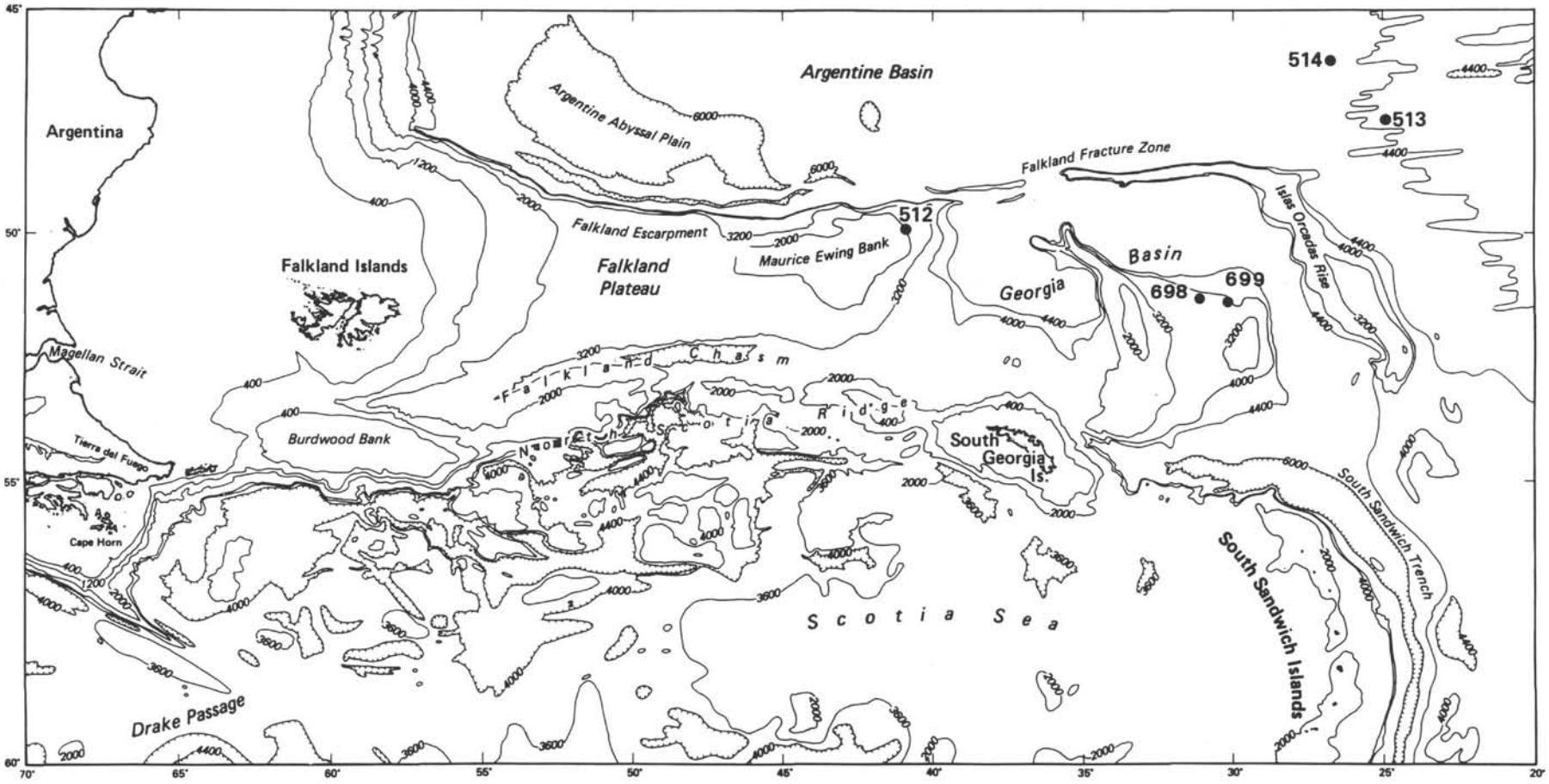


Figure 1. Bathymetric chart of the Georgia Basin region showing the location of ODP Sites 698 and 699, as well as previously drilled DSDP Sites 328 (Leg 36), 512, 513, and 514 (Leg 71).

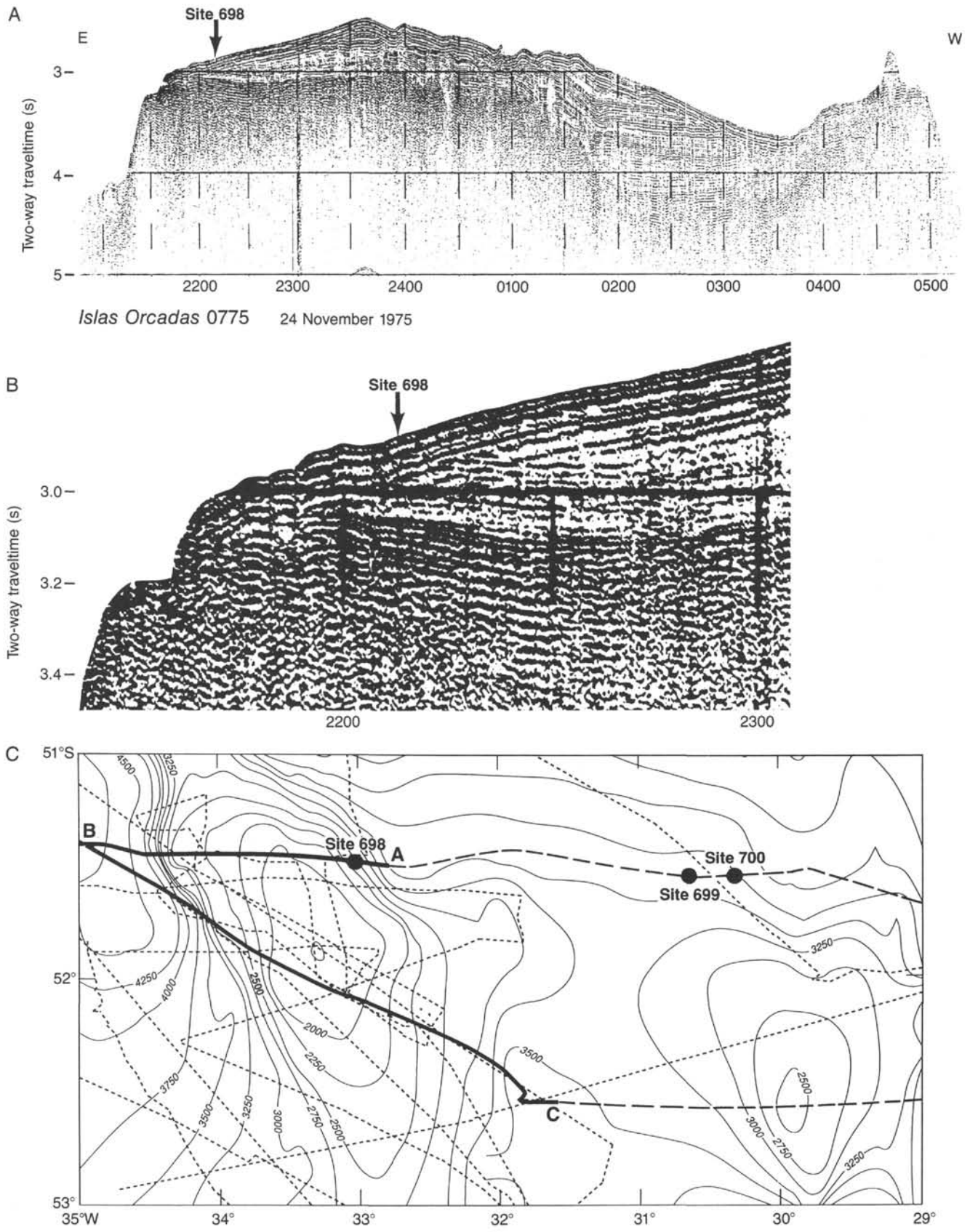


Figure 2. **A.** Location of Site 698 on the *Islas Orcadas* seismic-reflection profile across the Northeast Georgia Rise. **B.** Enlargement of the site area. **C.** Bathymetric map showing the location of the seismic line (A-B) shown above. Seismic reflection profiles A-B and B-C are shown in Figure 3 with piston core locations.

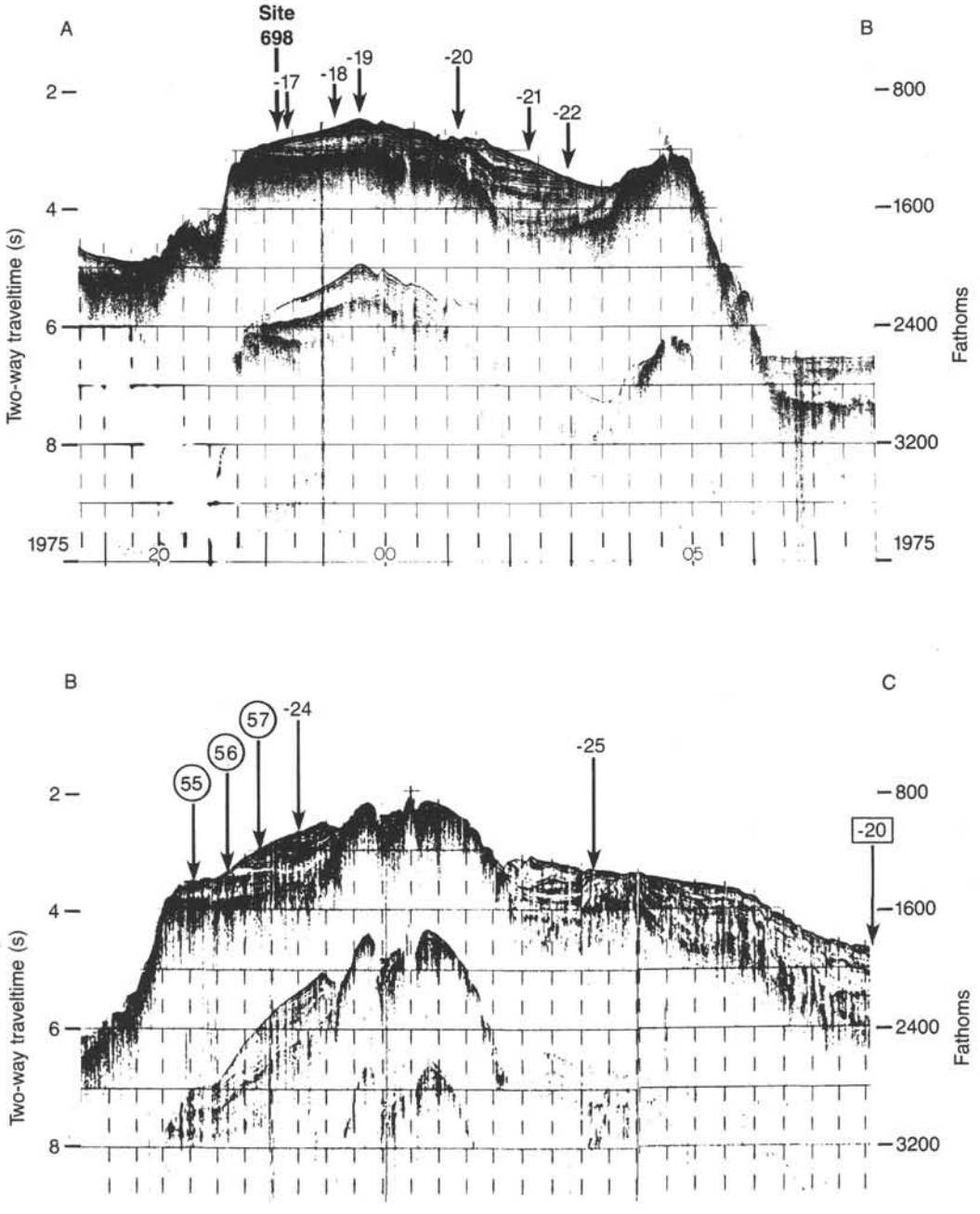


Figure 3. *Islas Orcadas* cruise 07-75 seismic-reflection profiles taken on an east to west (A-B) and west to east (B-C) track over the Northeast Georgia Rise. The location of Site 698 is shown on line A-B. Piston cores taken on these lines during *Islas Orcadas* cruises 07-75, 11-76, and 16-78 shown by arrows with core numbers (circled = 16-78; boxed = 07-75; unmarked = 11-76).

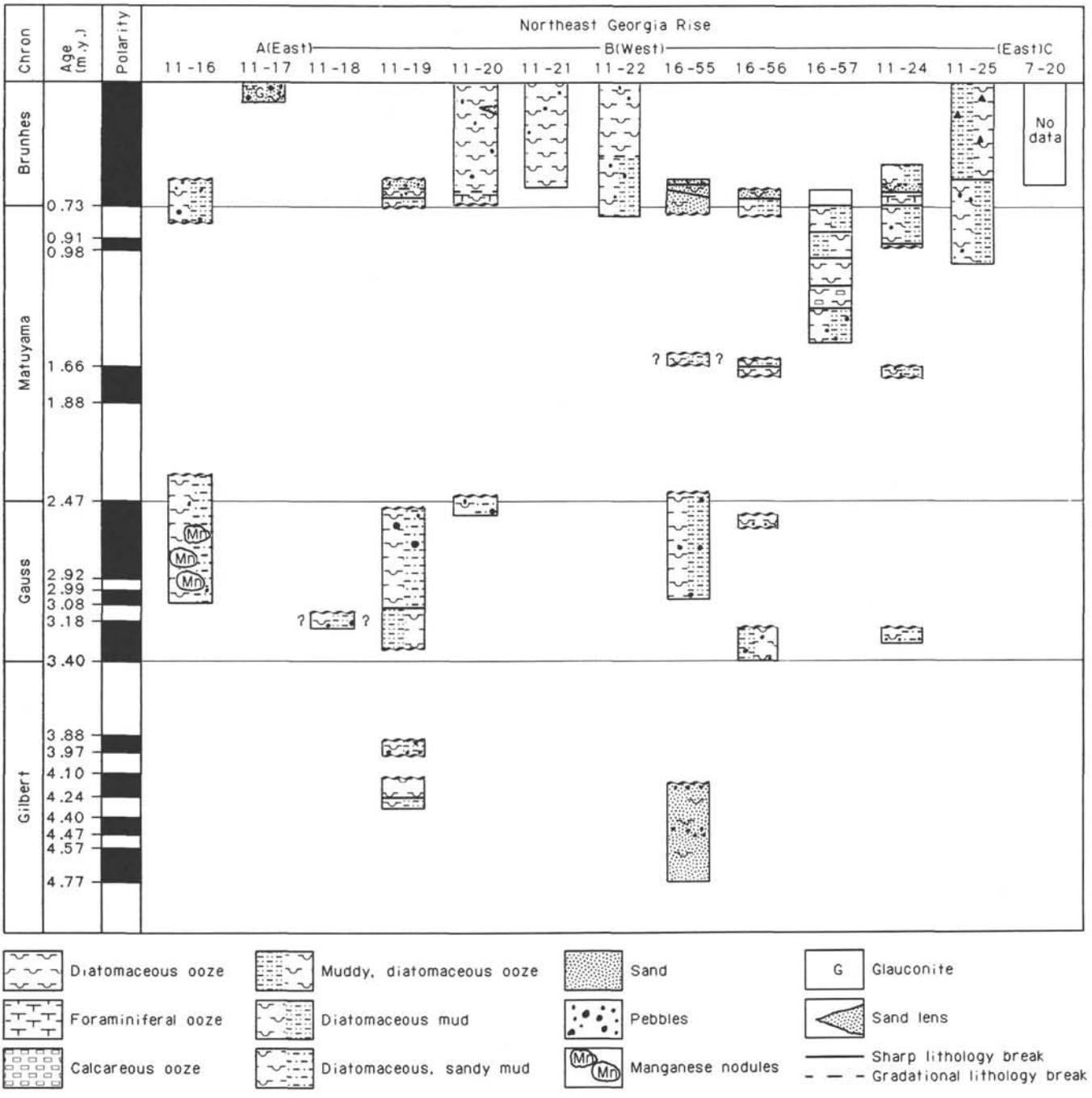


Figure 4. Biostratigraphic-magnetostratigraphic correlation of Northeast Georgia Rise piston cores with the geomagnetic polarity time scale. All cores failed to penetrate Pliocene-Quaternary sediments rich in ice-rafted detritus to reach near-surface disconformities visible on the seismic lines of Figures 2 and 3. The lithologies of the Pliocene-Quaternary sediments of all piston cores are represented.

to provide important information about the paleoceanographic and paleoclimatic development of the Southern Ocean. To date, the only cored sections recovering this interval from the Atlantic sector of the Southern Ocean outside the Falkland Plateau are from ODP Leg 113 (Sites 689 and 690 on the Maud Rise and short intervals from Sites 693 and 696; Barker, Kennett, et al., 1988). Little or no stratigraphic representation exists for the early to middle Paleocene and early to middle Eocene throughout the Southern Ocean. Cretaceous and Paleogene sediments recovered here and at other Leg 114 sites would be used in conjunction with sediments of similar age recovered from antarctic Leg 113 to:

1. Develop an integrated high-latitude siliceous and calcareous microfossil stratigraphy for the antarctic and subantarctic, which would also be correlated to lower latitude standard microfossil zonal schemes;
2. Interpret the climatic, paleoceanographic, and glacial history of the antarctic margin and subantarctic/antarctic of the South Atlantic sectors of the Southern Ocean; and

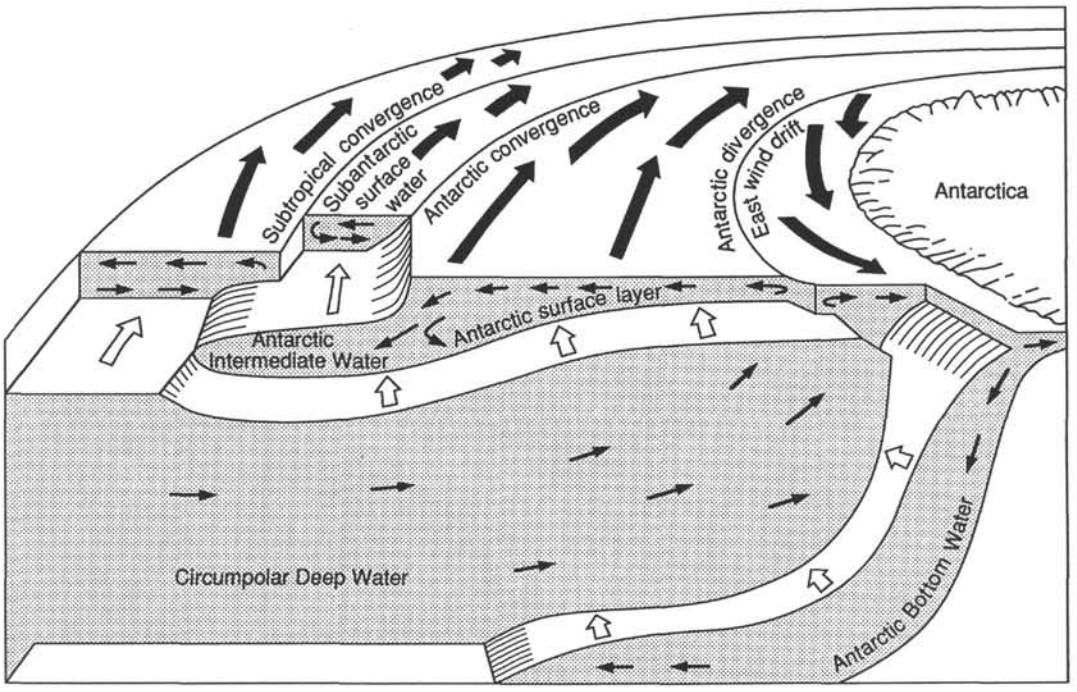


Figure 5. Schematic representation of major surface and subsurface water masses of the Southern Ocean (from Gordon, 1971).

3. Document the evolution and biogeographic distribution of high-latitude microfossil faunas and floras.

Of particular importance at this site is the evaluation of the subsidence history of the Northeast Georgia Rise. The effects of this feature and other aseismic ridges, plateaus, and fracture zones on Late Cretaceous to Paleogene oceanic interchange of antarctic-South Atlantic waters are also major factors.

The drilling plans for Site 698 called for using the RCB system to basement. Drilling into basement would continue until bit distruction or until the designated time at which the *JOIDES Resolution* would have to depart to reach Site 699 on or close to the precruise schedule. Heat-flow measurements were to be conducted if allowed by the the sediment characteristics.

## OPERATIONS

Site 698 was a bonus site, to be drilled only if time was available both for drilling and for the transit to arrive at Site 699 on schedule. *JOIDES Resolution* left port on 14 March 1987 nearly 2 days ahead of schedule, and the average transit speed enroute to the first site was 12.6 kt. At this point Leg 114 was well ahead of schedule, and we decided to stop at Site 698. The objective was to continuously core from the mudline down to and into basement. Because time was extremely limited, the hole was cored only with the RCB system. The advanced hydraulic piston core (APC) and extended core barrel (XCB) systems would have recovered a higher volume of core with less disturbance but would not have enabled the recovery of basement material. There was not enough time to trip the drill string and change coring systems; the Navidrill coring system was considered too new and developmental to deploy at this site.

Site 698 was spudded-in on 18 March 1987 in a water depth of 2138 m. A total of 237 m of penetration was achieved, with a recovery of 52.3 m (22.1%) (Table 1). Recovery at this site was plagued from the start. The hole was spudded-in on a gravel pavement directly overlying a foraminifer nannofossil ooze. The soft, easily washable nature of the ooze did not lend itself well to the RCB method, and the formation was laced with chert stringers that further complicated coring. Recovery would be good within in a core barrel until chert was reached, which would jam the core catcher, preventing further recovery. On several occasions chert fragments became packed in the throat of the bit, resulting in a zero-recovery core and necessitating an additional wireline run with a bit deplugger before coring operations could continue. Another problem experienced in this hole was that the core barrel was prevented from properly seating and latching, assumably by chert fragments lodging above the bit throat. This material could have been dislodged from the previous core barrel during retrieval. After Core 114-698A-23R came up empty, a chisel-nose center bit was deployed. Upon retrieval we determined that this assembly did not latch in. A second barrel, with a hollow bit deplugger on the end, was dropped. This barrel became lodged in the outer core barrel and could not be retrieved. After an overpull of about 3000 lb, the overshot disengaged and the sand line was retrieved. A second attempt to retrieve the stuck barrel ended in success after pulling in excess of 7500 lb over line weight. Upon retrieval the deplugger was found to contain approximately 10 cm of highly altered basalt. Fresh basalt was subsequently recovered in Core 114-698A-24R at 209.5 mbsf. Three more cores were taken recovering alternating fresh and highly weathered basalt until we reached a total depth of 237.0 mbsf. At this point coring operations ended and the drill string was tripped out of the hole. At 2230 hr the vessel was secured and underway. Several hours were taken to conduct a geophysical survey prior to setting course for the next site.

The weather experienced at Site 698 was extremely favorable up until the trip out of the hole. At this time the seas began building and the wind velocity continued to climb. While under way to Site 699, a full-fledged force 10 storm climaxed with winds gusting to 53 kt.

## LITHOSTRATIGRAPHY

The sedimentary sequence recovered at Site 698 consists of pelagic carbonates, grading from nannofossil ooze near the top of the hole through nannofossil chalk to limestones near the bottom of the hole (Fig. 11). Chert nodules and chert horizons increase irregularly in frequency toward the base of the hole.

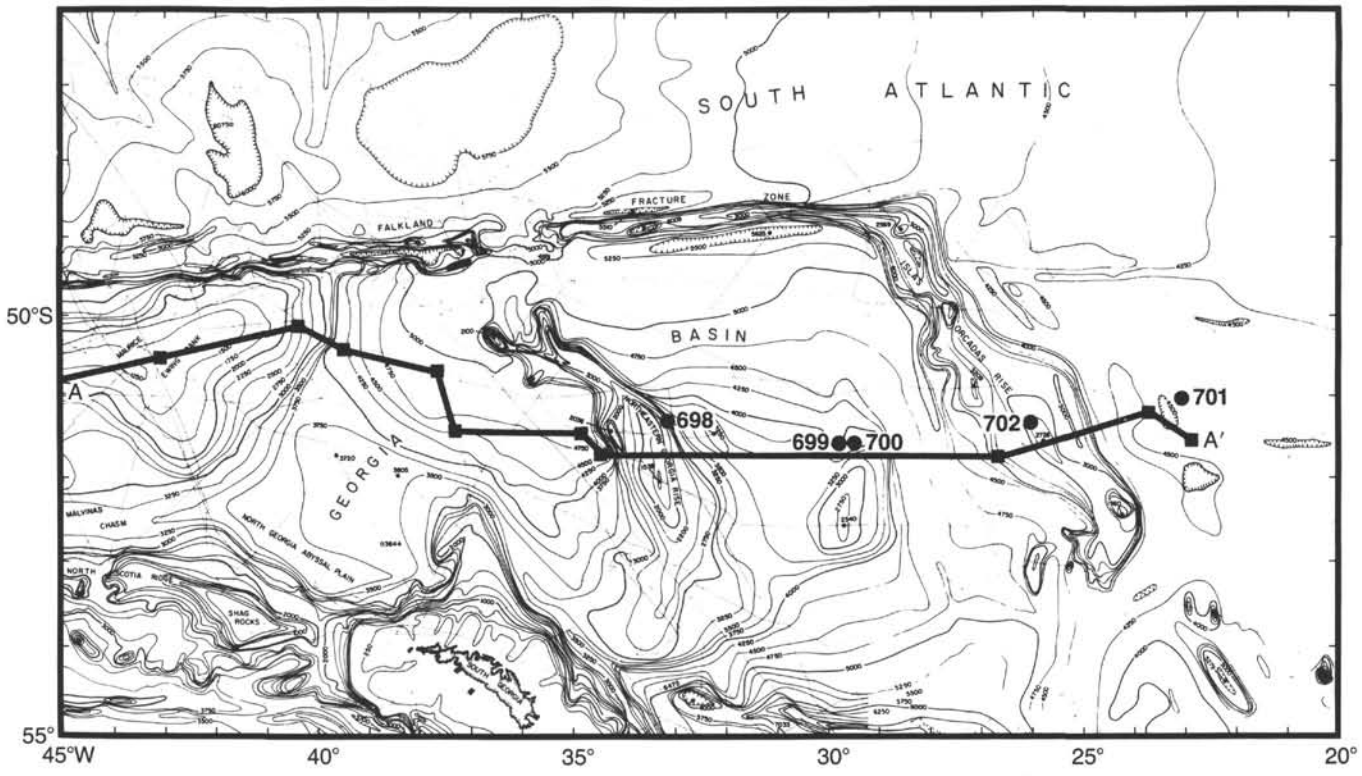


Figure 6. Map showing the location of Sites 698–702 relative to hydrographic transects. Data from transect A-A' are shown in Figure 7 (from Mead, 1982).

Ice-rafted debris occurs only in a gravel layer at the surface, but its thickness is indeterminable because of drilling disturbance. The basal termination of the sequence includes interlayered soil-like sediments, basalts, hematite-rich claystone (derived from weathered basalts?), and completely weathered basalts. The complete sequence is subdivided into three units, as shown in Table 2. Recovery at this site was fair to poor, ranging from 0% in three cores (Cores 114-698A-18R, 114-698A-19R, and 114-698A-22R) to 57.8% in Core 114-698A-24R.

### Unit I: Core 114-698A-1R through Sample 114-698A-2R-1, 25 cm; Depth: 0–4.25 mbsf; Age: Pliocene(?)-Quaternary.

Unit I was recovered only in the core catcher of Core 114-698A-1R and (as downcore slump) in Core 114-698A-2R. Material from Unit I also occurred in deeper cores as downhole contamination. The unit consists of a gravel lag deposit composed of chert pieces and dropstones (sandstone, gneiss), as well as one manganese nodule. The pebbles are embedded in a matrix of white, foraminifer-bearing nannofossil ooze that constitutes the beginning of the underlying lithostratigraphic unit. Because of severe drilling disturbance and mixing of various lithologies, the thickness of Unit I cannot be reliably determined. Its thickness is estimated to range from a few tens of centimeters to several meters, but should not exceed about 4 m.

### Unit II: Sample 114-698A-2R-1, 25 cm, through Core 114-698A-21R; Depth: 4.25–190.5 mbsf; Age: earliest middle or early Eocene–Late Cretaceous.

Unit II is a sequence of nannofossil oozes, chalks, and limestones with intercalated cherts. The unit is 186 m thick and has been subdivided into three subunits based on the degree of lithification, that is, the relative dominance of ooze, chalk, and limestone. Although the boundaries of these subunits are somewhat arbitrary, this division should reflect the relative degree of lithification from top to bottom. Individual subunits are described below.

The unit is characterized by (nearly) uninterrupted pelagic sedimentation, completely dominated by the deposition of nannofossil ooze. Ash, diatom, and radiolarian components are minor contributors to the total sediment volume and decrease in importance with depth in the section.

#### *Subunit IIA: Sample 114-698A-2R-1, 25 cm, through Core 114-698A-5R; Depth: 4.25–42 mbsf; Age: earliest middle(?)-early Eocene.*

This subunit consists predominantly of foraminifer-bearing nannofossil ooze, with foraminifers ranging from sparse, particularly in the first 9.5 m of the subunit, to foraminifer-rich in the remainder of the subunit. An interesting minor lithology is represented by a radiolarian-foraminifer-bearing ooze (i.e., both the radiolarian and foraminifer components qualify as minor components). This lithology was noted only in Section 114-698A-3R, CC (23 mbsf), but may occur elsewhere.

The color of the nannofossil ooze is white to "off-white," but is not depicted in the Munsell color chart. The radiolarian-bearing variety is light gray (5Y 7/1). The color boundary of the small intercalations of the radiolarian-bearing ooze with the overlying nannofossil ooze is sharp but uneven.

The highest (youngest) occurrence of chert in this unit is at Sample 114-698A-2R, CC, 12–17 cm (7.57–7.59 mbsf; Fig. 12). A single piece of chert, white (10YR 8/2), marks the beginning of progressive chertification downhole (see the following "Chertification" discussion). Cherts become significant in Section 114-698A-5R-1, CC (32.5–42.0 mbsf).

In Section 114-698A-5R-2 (34–35.5 mbsf), mottling caused by burrowing organisms (e.g., *Planolites*) becomes obvious (Fig. 13). This is a feature that predominates throughout the next subunit (IIB).

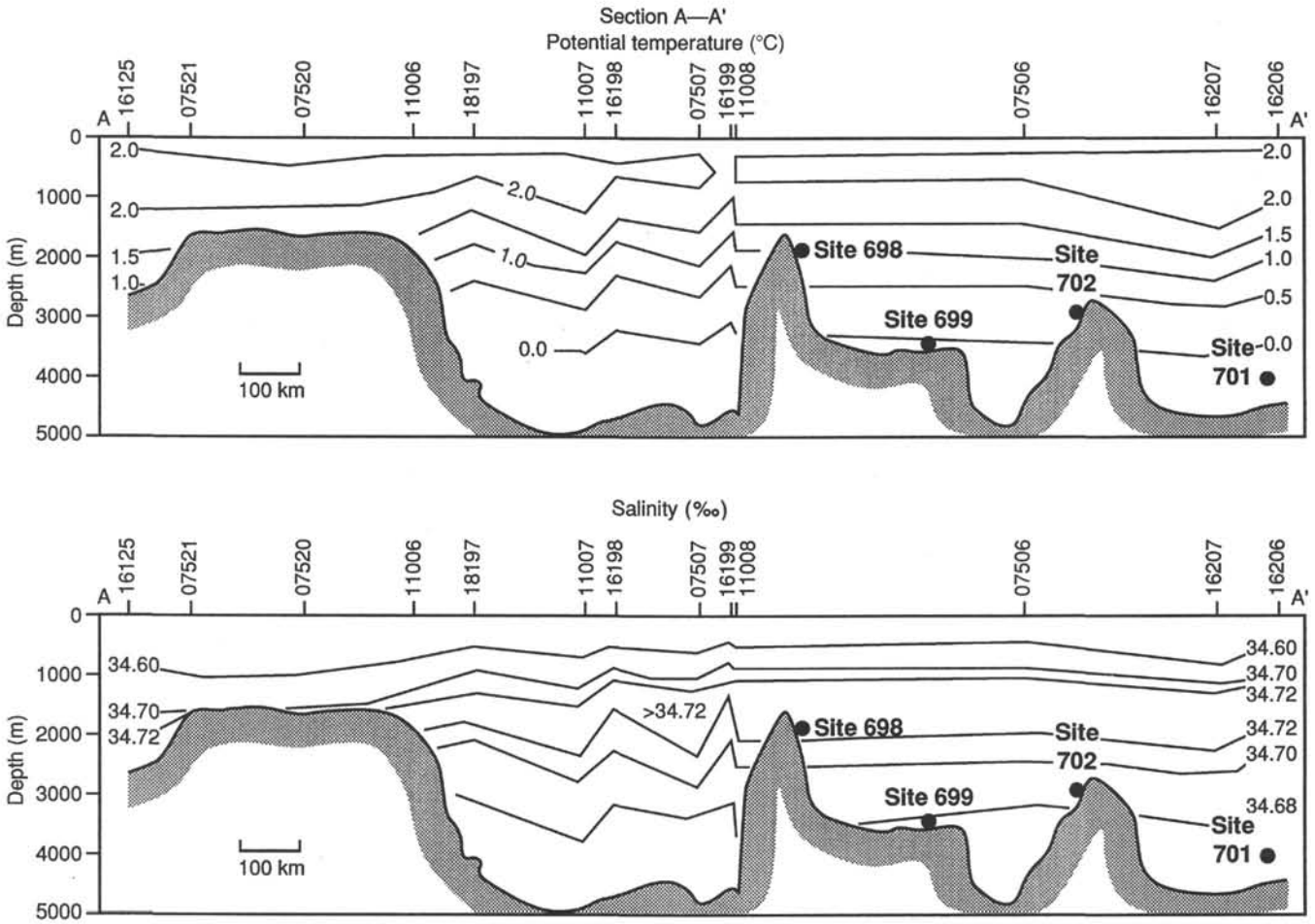


Figure 7. Potential temperature and salinity data along transect A-A' on map in Figure 6. Modern potential temperature and salinity at the seafloor at Site 698 are ~1.0°C and 34.72‰, respectively. These values are close to the mean values for CPDW (0.62°C, 34.65‰; Mead, 1982).

***Subunit IIB: Cores 114-698A-6R through 114-698A-16R; Depth: 42–146.5 mbsf; Age: early Eocene–late Maestrichtian.***

Subunit IIB consists of foraminifer-bearing chalk, ranging in color from white (no color code) to white (5Y 8/1) to light gray (5Y 7/1). Minor varieties include foraminifer-bearing nannofossil ooze, intercalated with chalk in a seemingly random fashion but disappearing toward the bottom of the unit. Chert intercalations become increasingly significant downsection, ranging in color from gray (5Y 7/2) to light gray (5Y 7/1).

Mottling is prominent throughout this subunit, for example, in Sections 114-698A-6R-1 and 114-698A-6R-2 (42–45 mbsf) (Figs. 14 and 15), 114-698A-8R-1 (61–62.5 mbsf), 114-698A-9R-1 and 114-698A-9R-2 (70.5–73.5 mbsf), and so forth, down to the base of the section. This bioturbation is present in all recovered sections, and is probably present throughout the uncored intervals. Burrowing becomes intense in Section 114-698A-6R, is dominated by *Zoophycos* in Section 114-698A-12R (Figs. 16 and 17), and is prevalent throughout the lower part of this subunit (Figs. 18 through 20) (see "Ichnology," this section).

***Subunit IIC: Cores 114-698A-17R through 114-698A-21R; Depth: 146.5–190.5 mbsf; Age: Late Cretaceous.***

This subunit is composed of very fine-grained limestone, occurring in two slightly different colors: light gray (5Y 7/1), moderately to highly bioturbated, with thin layering, and white (5Y 8/1), faintly to moderately bioturbated. The light gray limestone has fewer than 10% minor constituents, such as volcanic ash, radiolarians, diatom fragments, zeolites, and clay. The white limestone has no minor constituents. Another color variation occurs in Section 114-698A-21R as individual horizons, which are light greenish gray (5GH 6/1).

Chert, light gray (5Y 7/1) to gray (5Y 6/1), occurs in increasing importance toward the bottom of the subunit (see "Chertification").

## Unit III: Cores 114-698A-23R through 114-698A-27R; Depth: 200.0–237.0 mbsf; Age: Late Cretaceous or older.

Unit III is 37 m thick (because of very poor recovery, this figure is highly uncertain) and is subdivided into several subunits because of the diverse lithologies recovered. The thicknesses may range from 15 cm to 9.5 or even up to 19 m (no recovery in Core 114-698A-22R) for Subunit IIIA, and up to about 20 m for Subunit IIIB. The hole was terminated with Core 114-698A-27R, but there was no recovery in the lower sections of this core. However, we must emphasize that recovery was so spotty as to preclude reliable estimates of actual thicknesses.

Although both sedimentary and volcanic rock types (and transitional lithologies) were encountered, they will be treated here as one unit. Drilling employing low-disturbance methods (such as the XCB system) would have undoubtedly enabled better stratigraphic resolution of this very interesting succession.

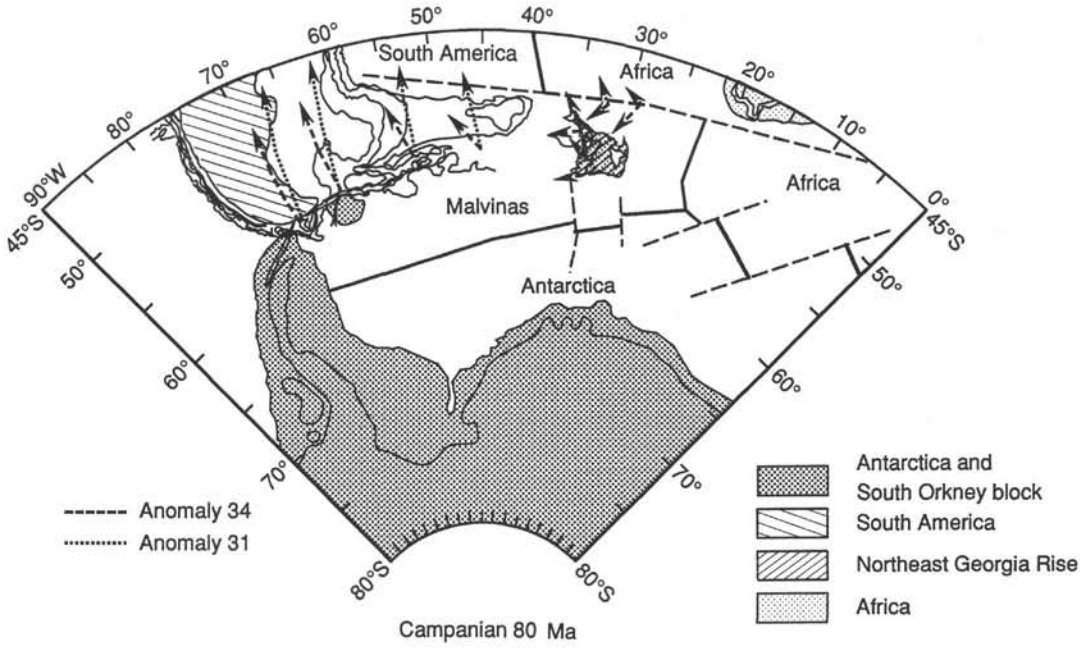


Figure 8. Plate boundaries and convergence directions for the southwest Atlantic during the Campanian/Santonian boundary (Chron C34). Spreading-center location determined from magnetic anomaly locations. Convergence vectors show direction and total motion during Chrons C34 and C31 based on the poles of rotation determined from LaBrecque and Hayes (1979) and Ladd (1974). The bases of the convergence vectors are plotted along the North Scotia Ridge and Northeast Georgia Rise. Note that the total convergence may have reached 1000 km near Tierra del Fuego from the Santonian to Maestrichtian. Polarity of the subduction zone was likely southward-dipping along the North Scotia Ridge and west-facing along the Northeast Georgia Rise.

***Subunit IIIA: Core 114-698A-23R; Depth: 200.0–200.15 mbsf; Age: Late Cretaceous.***

This unit is a sandy mud, of dark olive (5Y 3/2) color. We interpret it to be either a weathering (subaerial?) product of the underlying basalt or a part of a transgressive facies. It contains a few nannofossils and chalk fragments that represent downhole contamination. The nature of the contact between this subunit and the overlying limestone is unknown because there was no recovery in Core 114-698A-22R.

***Subunit IIIB: Core 114-698A-24R through Sample 114-698A-26R-1, 28 cm; Depth: 209.5–219.28 mbsf; Age: Late Cretaceous or older.***

This unit represents the upper boundary of basement consisting of sparsely phyric, holocrystalline basalt (Core 114-698A-24R), trachytic and subtrachytic basalt, and ferro(?)basalt (Core 114-698A-25R). Colors are greenish gray (5BG 6/1), dark gray (7.5YR N5/), and very dark gray (7.5YR N3/1). Phenocrysts, where present, are 1–9 mm long. Vesicles of 1–3 mm occur in some parts and seem to be stretched and preferentially oriented. In Core 114-698-25R-2, ferromagnesian minerals are also preferentially oriented. Sample 114-698A-25R-2, 110–112 cm, contains large anhedral and subhedral opaques, microphenocrysts of plagioclase, and slightly zoned pyroxene crystals in clots. Several sets of fractures are present. Alteration and mineralization are common, but are more common in the horizontal fracture set. Several amygdules and distensive fracture networks are filled with calcite and zeolites.

One piece of polymict conglomerate occurs at 209.0–209.06 mbsf. The exact derivation of this conglomerate is enigmatic. It may be drilling contaminant, despite its size (i.e., filling the liner).

***Subunit IIIC: Sample 114-698A-26R-1, 28 cm, through the bottom of hole, Core 114-698A-27R; Depth: 219.28–237 mbsf; Age: Late Cretaceous or older.***

This subunit consists of hematite-rich claystone at the top, but it is badly disturbed by drilling and contains much drilling slurry. The top of the subunit is a microbreccia containing fragments of altered (to serpentine) basalt, with a hematite matrix and common opaques. The claystone grades down into material that could be interpreted as completely weathered basalt. Authigenic material in this horizon consists of claystone clasts of dark brown (7.5YR 3/2) to dark reddish brown color (5YR 2.5/1). Some of these clasts, particularly when viewed microscopically, have retained textural characteristics of the parental basaltic rock, although altered to serpentine. Vesicles and altered phenocrysts are still visible (Fig. 21). Weathering has completely altered the original Fe-Mg minerals, forming hematite. There probably was also a phase of albitization, with some of these materials subsequently filling vesicles.

Unfortunately, the exact relationship of the contact with the overlying basalt was completely destroyed by rotary drilling, changing the original succession to a slurry. Fortuitously, some of the original material survived in the form of clasts and is similar to the highly altered vesicular basalt recovered on the western escarpment of the Northeast Georgia Rise during the site surveys by *Polar Duke* (P. Ciesielski, pers. comm., 1987).

## Chertification

Nodular chert horizons are common at Site 698 from Cores 114-698A-2R through 114-698A-24R (Table 3). The chert nodules are embedded within nannofossil chalks and limestones that are depauperate or devoid of volcanic or biogenic silica. The age of the nodule-bearing sediment ranges from late Eo-

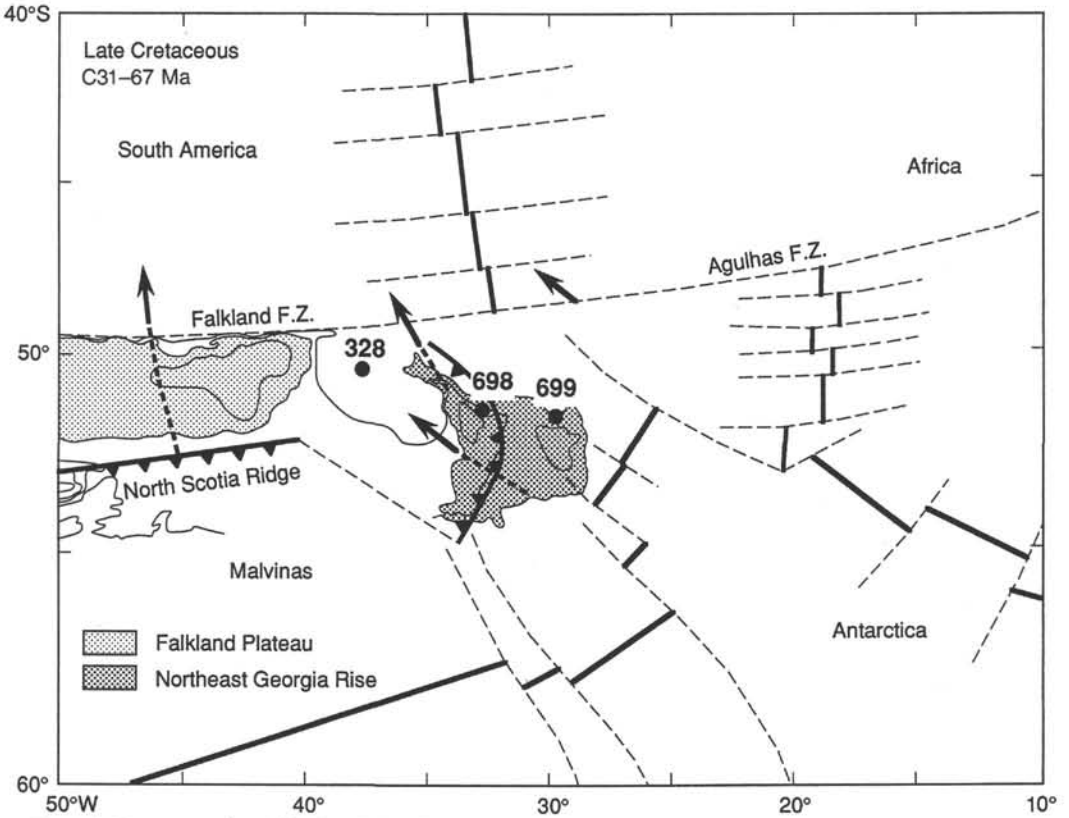


Figure 9. Reconstruction of the Leg 114 region of the southwest Atlantic for the Late Cretaceous (Chron C31, 67 Ma) with the positions of Sites 698, 699, and 328. Spreading-center locations based on magnetic anomaly locations and SEASAT gravity field. Supporting data are presented in the OMD Region 13 Synthesis (LaBrecque, 1986).

cene to Late Cretaceous. Nodules and chert horizons range in size from a few centimeters to 14 cm. In most cases, the contact between the chert nodules and carbonate sediments is abrupt, although contacts are suspect in many places because of discontinuous coring at this site. The first occurrence of a chert nodule is shown in Figure 12 (from the core catcher of Core 114-698A-2R). The contact with the upper nannofossil ooze is probably not in place. The zoned chert nodule consists of a light gray inner core surrounded by a thin, darker outer rind (1–2 mm thick). In previous descriptions of nodules from deep-sea chalks, zoning typically consists of an inner quartz core surrounded by a thin rind of disordered cristobalite or a mixture of cristobalite and cryptocrystalline chalcedony (Wise and Weaver, 1974).

The genesis of nodular chert in pelagic carbonates has been extensively studied, and several theories have been proposed. Most models of chertification require mobilization of silica within interstitial pore waters by the dissolution of radiolarians, diatoms, or volcanic glass contained within the host carbonate sediment. Silica is then precipitated in the interstices of the chalk/limestone matrix and replaces the groundmass of the carbonate rock (Wise and Weaver, 1974). This leads to the development of a dense opaline nucleus with dissolution and expulsion of carbonate from the nodule. The nodule continues to grow by accretion, and all remaining pore spaces are filled until the supply of silica is exhausted. With time and increased diagenesis, the fine-crystalline cristobalite matrix inverts to quartz.

Figure 22 shows a 14-cm chert horizon from Sample 114-698A-9R-1, 8–19 cm, consisting of four fragments. The third fragment resembles a nodule mosaic, consisting of dark gray chert, lighter gray chert, and white carbonate. The chalk inclusions probably represent carbonate material that was trapped during the chertification process and was not replaced by silica. The various shadings of gray may represent varying degrees of carbonate replacement by silica. In Piece 4 (114-698A-9R-1, 4–10 cm), an injection infilling of chert is almost completely enveloped by the nannofossil chalk matrix. These chert nodules and included carbonate at Site 698 vividly illustrate the origin of chert nodules through diagenetic replacement of carbonate in pelagic sequences.

## Ichnology

Sediments drilled at Site 698 are very-fine-grained calcareous oozes or chalks that show various degrees of bioturbation unless destroyed by compaction and diagenesis. In the upper part of the cored section, bioturbation is difficult to observe, and only fine variations in color (mottling) occur in the white ooze. Intense bioturbation first appears in Sample 114-698A-5R-2, 51–77 cm (Fig. 23) and continues downsection. Successive bioturbated intervals occur throughout the sedimentary column, in places showing intensive modification of the former sediment.

Bioturbation was identified in the following intervals:

- 114-698A-5R-2, 51–77 cm (Fig. 12): first clear evidence of extensive bioturbation; mainly *Planolites*
- 114-698A-5R-2, 89–101 cm (Fig. 13): oblique and horizontal *Endichnia* of "wandering feeding" pattern; *Planolites, Cylindrichnus*
- 114-698A-6R-1, 0–17 cm (Fig. 14): *Planolites* and oblique furrows
- 114-698A-6R-1, 67–75 cm (Fig. 15): *Planolites* and oblique furrows
- 114-698A-12R-6, 108–118 cm (Fig. 16): mainly *Zoophycos*, well developed
- 114-698A-12R-1, 122–135 cm (Fig. 17): mainly *Zoophycos*

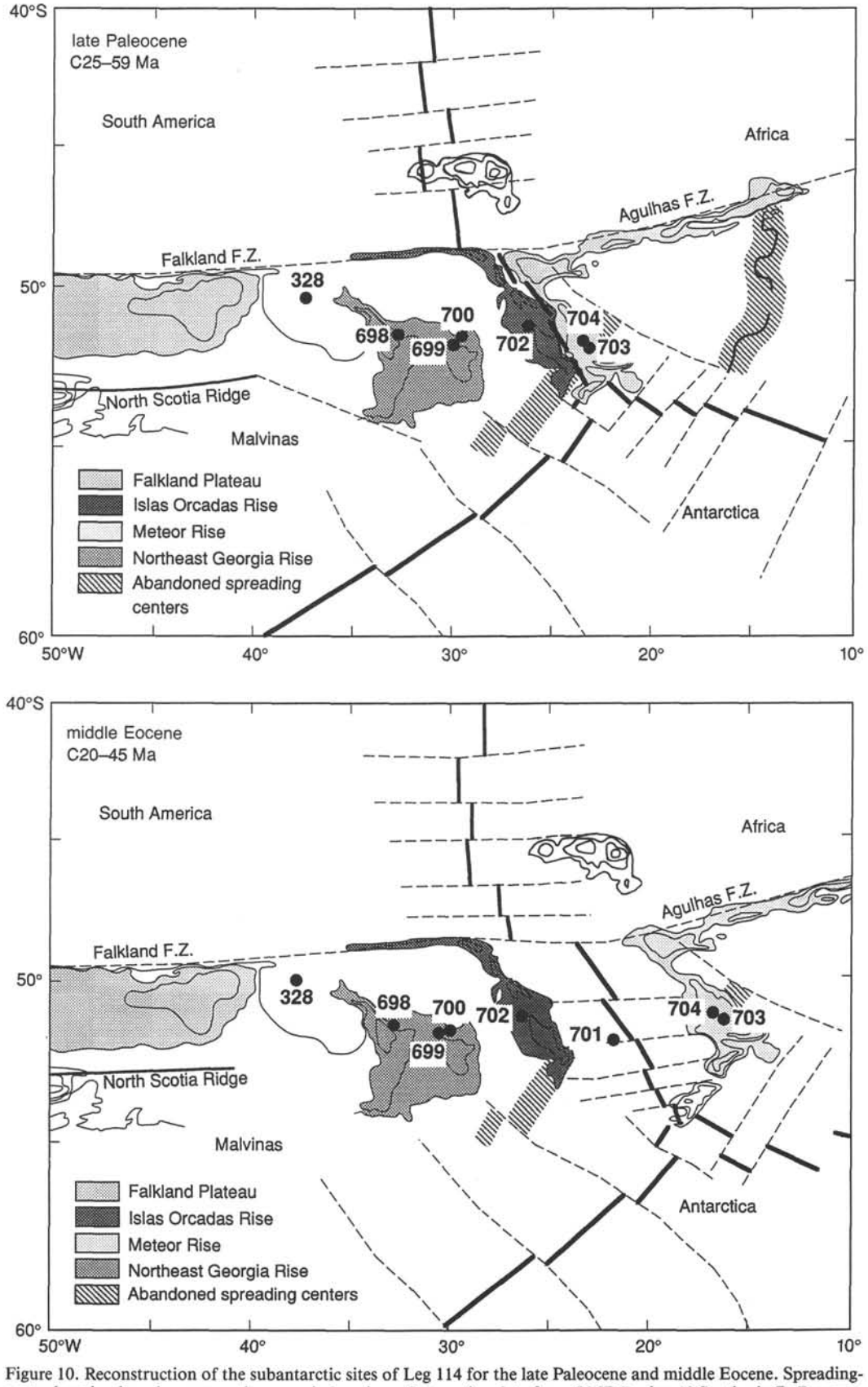


Figure 10. Reconstruction of the subantarctic sites of Leg 114 for the late Paleocene and middle Eocene. Spreading-center location based on magnetic anomaly locations. Supporting data from OMD Region 13 Synthesis (LaBrecque, 1986).

**Table 1. Site 698 coring summary.**

| Core no. | Date (March 1987) | Local time | Depth (mbsf) | Length cored (m) | Length recovered (m) | Recovery (%) |
|---|---|---|---|---|---|---|
| 1R | 18 | 0300 | 0–4.0 | 4.0 | 0.10 | 2.5 |
| 2R | 18 | 0415 | 4.0–13.5 | 9.5 | 3.66 | 38.5 |
| 3R | 18 | 0505 | 13.5–23.0 | 9.5 | 2.05 | 21.6 |
| 4R | 18 | 0615 | 23.0–32.5 | 9.5 | 1.39 | 14.6 |
| 5R | 18 | 0705 | 32.5–42.0 | 9.5 | 2.99 | 31.5 |
| 6R | 18 | 0805 | 42.0–51.5 | 9.5 | 3.17 | 33.3 |
| 7R | 18 | 0850 | 51.5–61.0 | 9.5 | 0.18 | 1.9 |
| 8R | 18 | 0945 | 61.0–70.5 | 9.5 | 1.84 | 19.3 |
| 9R | 18 | 1040 | 70.5–80.0 | 9.5 | 3.17 | 33.3 |
| 10R | 18 | 1115 | 80.0–89.5 | 9.5 | 3.05 | 32.1 |
| 11R | 18 | 1200 | 89.5–99.0 | 9.5 | 0.15 | 1.6 |
| 12R | 18 | 1305 | 99.0–108.5 | 9.5 | 1.82 | 19.1 |
| 13R | 18 | 1355 | 108.5–118.0 | 9.5 | 0.90 | 1.0 |
| 14R | 18 | 1435 | 118.0–127.5 | 9.5 | 0.82 | 8.6 |
| 15R | 18 | 1520 | 127.5–137.0 | 9.5 | 1.70 | 17.9 |
| 16R | 18 | 1600 | 137.0–146.5 | 9.5 | 3.60 | 37.9 |
| 17R | 18 | 1645 | 146.5–156.0 | 9.5 | 3.25 | 34.2 |
| 18R | 18 | 1720 | 156.0–165.5 | 9.5 | 0 | 0 |
| 19R | 18 | 1820 | 165.5–175.0 | 9.5 | 0 | 0 |
| 20R | 18 | 2005 | 175.0–181.0 | 6.0 | 1.23 | 20.5 |
| 21R | 18 | 2120 | 181.0–190.5 | 9.5 | 2.60 | 27.3 |
| 22R | 18 | 2310 | 190.5–200.0 | 9.5 | 0 | 0 |
| 23R | 19 | 0115 | 200.0–209.5 | 9.5 | 0.10 | 1.1 |
| 24R | 19 | 0700 | 209.5–213.5 | 4.0 | 2.31 | 57.8 |
| 25R | 19 | 1000 | 213.5–219.0 | 5.5 | 3.94 | 71.6 |
| 26R | 19 | 1215 | 219.0–228.5 | 9.5 | 0.76 | 8.0 |
| 27R | 19 | 1445 | 228.5–237.0 | 8.5 | 8.29 | 97.5 |
| | | | | 237.0 | 52.26 | |

114-698A-15R-1, 36–49 cm (Fig. 18): *Planolites*
114-698A-15R-1, 100–112 cm (Fig. 19): *Planolites*
114-698A-16R-1, 27–37 cm (Fig. 20): *Chondrites*
114-698A-21R-1, 135–150 cm (Fig. 24): *Planolites*

In all observed intervals, bioturbation is very clear, sometimes affecting several tens of centimeters of sediment. Upper as well as lower contacts are generally diffuse. Ichnological communities are extensively developed, but it must be noted that, in some cases, a species is dominant over other bioturbant organisms. For example, *Zoophycos* appears to be very well represented in some intervals of Core 114-698A-12R-1 (Figs. 16 and 17).

These observations show that the rate of sedimentation was low, allowing for extensive development of ichnological communities, unperturbed by rapid fluxes of terrigenous components. In other cases "wandering feeding" into the sediment is predominant, and the remaining poorly bioturbated sediment is darker, showing that the initial sediment was richer in organic content than the white calcareous ooze. In these cases, bioturbation is more intense, corresponding to a rapidly increasing *Endichnia* community.

In conclusion, the observed ichnological communities show that:

1. The calcareous oozes, as well as the more diagenetically evolved chalks and limestones, were deposited slowly and that sedimentation periodically occurred under oxygen-reduced conditions (but only with respect to microhorizons; the predominant character of the sediment indicates well-oxygenated conditions throughout). This second type of sedimentation is reflected by the intensively burrowed intervals, as well as the occurrence of small *Chondrites* communities (Sample 114-698A-16R-1, 30–36 cm; Fig. 20) (Bromley and Ekdale, 1984).
2. No crisis occurred to modify radically the rate of sedimentation or the geochemical conditions near the seafloor. Ichnological communities remained quite constant through time.
3. Significant erosional events are not discernible, at least not within the limits set by core recovery.

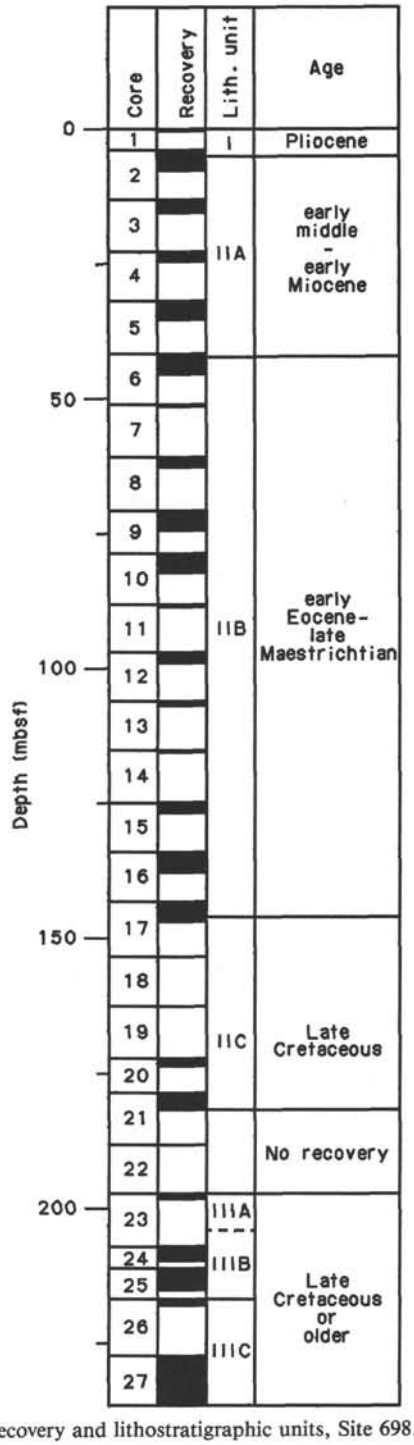


Figure 11. Recovery and lithostratigraphic units, Site 698.

## Conclusions and Paleoenvironmental Interpretation

The overall impression conveyed by the sedimentary column is one of remarkable uniformity, with minor fluctuations. The sedimentary sequence as well as the good-quality seismic records do not reflect significant tectonic or climatic events below the lower Eocene.

Pending more detailed studies of the basalt of Unit III, the available material suggests flows without pillowing over an extensively developed red regolith and hematitic claystone. The nature of the regolithic material suggests an environment conducive to intensive chemical weathering, such as a tropical climate, on a surface that favored retention of local weathering

**Table 2. Lithostratigraphic units at Site 698.**

| Unit/ Subunit | Lithology | Depth (mbsf) | Age |
|---|---|---|---|
| I | Ice-rafted detritus (gravel) | 0–4.25 | Pliocene? |
| IIA | Nannofossil ooze | 4.25–42.0 | early middle–early Eocene |
| IIB | Nannofossil chalk | 42.0–146.5 | early Eocene–late Maestrichtian |
| IIC | Limestone | 146.5–190.5 | Late Cretaceous |
| IIIA | Sandy mud | 200–200.15 | |
| IIIB | Basalt | 209.5–219.28 | Late Cretaceous or older |
| IIIC | Hematite-rich claystone | 219.28–237.0 | |

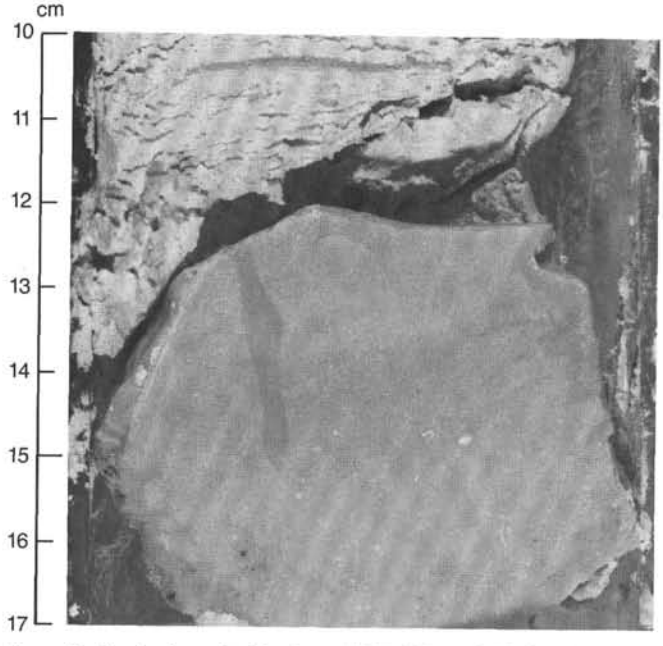


Figure 12. Single piece of white chert (10YR 8/2) at the highest (youngest) occurrence of this lithology (Sample 114-698A-2R, CC (10–17 cm)).

products. The association of basalt flows with sediments may be analogous to the basalt-volcanogenic sediment associations represented by landward-dipping reflector sequences, albeit in a different tectonic setting. Subaerial exposure of the local package may have been caused simply by the accumulation of volcanic lithologies. After cessation of volcanism and renewed weathering represented by Subunit IIIA, the sea transgressed. This relative change in sea level may have been caused by isostatic adjustment, eustatic change of sea level, or a combination of these and other circumstances.

No coralline structures were observed, suggesting that water depth increased initially to beyond the euphotic zone, but the seafloor remained above the carbonate compensation depth (CCD) during the entire interval represented by the lithostratigraphic column below Unit I. The widespread nannofossil lithologies (and their diagenetic derivatives, see Fig. 25) suggest warm water and perhaps the absence of a well-developed thermocline (and consequently, pycnocline), favoring the settling of nannofossil tests, perhaps as fecal pellets, to the seafloor. Whether or not the predominance of nannofossils signifies unproductive surface water is unresolved. We have no information on primary productivity or the residence times of nutrients. In any event, siliceous primary producers were present, but their scarcity indicates the absence of upwelled, colder water. In addition, the siliceous tests that became incorporated into the sedimentary column were subjected to diagenetic processes leading to their dissolution with time and to the formation of cherts.

Whatever the structure of this Cretaceous-Paleogene ecosystem, enough organic matter reached the seafloor to support a benthic community. It is suggested that the horizons reflecting intense bioturbation may represent periods of reduced, but not absent, oxygenation. The increasing paucity of burrows going upsection may perhaps be the result of slowly increasing water depth, resulting in the increasing degradation of organic matter as it settled through the deeper water column.

The lack of a significant influx of terrigeneous matter during the period of deposition is a result of the elevation of the depositional site above the surrounding seafloor. This is in contrast to Deep Sea Drilling Project (DSDP) Site 328 in the deep West Georgia Basin, in which a thick sequence of Upper Cretaceous to Eocene zeolitic clays and claystones is present.

The youngest calcareous sediments at the drill site are of Eocene age. How much sediment has been eroded is unknown. Undoubtedly, the Miocene development of oceanic circulation, characterized by an overall trend toward greater thermal gradients and intensifying geostrophic and thermohaline circulation, led to nondeposition and additional erosion in this area. Certainly, the winnowed character of the ice-rafted debris (lag gravel) of unknown age at the top of the sequence justifies this conclusion. Modern oceanographic conditions were shown to preclude the accumulation of any significant amounts of late Neogene terrigeneous or biogenic sediments at this Northeast Georgia Rise site, Falkland Plateau, and Islas Orcadas Rise (Ciesielski et al., 1982; Ciesielski and Wise, 1977; P. Ciesielski, unpubl. data).

## BIOSTRATIGRAPHY

### Biostratigraphic Synthesis

#### *Biostratigraphy*

Based on observations made mainly from core-catcher samples from the sequence recovered at Site 698, calcareous microfossils (both planktonic and benthic foraminifers and nannofossils) are abundant, rich in taxonomic diversity, and exhibit moderate to good preservation. Siliceous microfossils were recovered only from a few samples (Fig. 26) and are common and well preserved almost exclusively in the upper Paleocene.

Silica dissolution is observed in Sections 114-698A-1R, CC, through 114-698A-5R, CC, resulting in preservation of only the resistant, siliceous forms. Although preservation of nannofossils was poor in both Sections 114-698A-6R, CC, and 114-698A-7R, CC, an early Eocene age is tentatively assigned to these sections.

Sample 114-698A-9R-1, 52–53 cm, through Section 114-698A-12R, CC, are assigned a late Paleocene age based on both calcareous and siliceous microfossils. Whereas Section 114-698A-

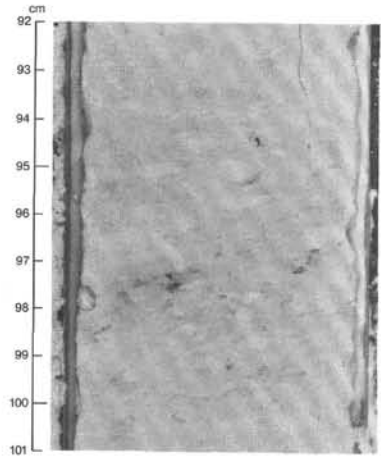


Figure 13. "Wandering feeding" bioturbation, mainly *Planolites* and some *Cylindrichnus* (Sample 114-698A-5R-2, 92–101 cm). Note that bioturbation is greater in the darker sediment than in the overlying nannofossil chalk.

13, CC, is interpreted to be early Paleocene (NP3–4) in age, a late Maestrichtian nannoflora was identified from Sample 114-698A-14R-1, 1 cm. Thus, the Cretaceous/Tertiary boundary is located in the unrecovered interval between the bottom of Core 114-698A-13R and the top of Sample 114-698A-14R-1, 1–2 cm. It is unfortunate that recovery for this critical boundary in Core 114-698A-13R was only 1%.

In the underlying Mesozoic section, the following ages are determined:

| Interval | Nannofossils | Planktonic foraminifers |
|---|---|---|
| 114-698A-14R-1, 1–2 cm, and 114-698-15R, CC | late Maestrichtian | |
| 114-698A-16R, CC, and 114-698A-17R, CC | middle Maestrichtian to late Campanian | Maestrichtian to Campanian |
| 114-698A-21R, CC | middle Maestrichtian to late Campanian | Campanian |
| 114-698A-23R, CC | middle Maestrichtian to late Campanian | |

A list of identified microfossil datums is given in Table 4.

### *Paleoenvironment*

The thick sequence of carbonate sediments from Site 698 indicates that sedimentation at this site was above the lysocline and, judging from the benthic foraminifer assemblages, at a lower bathyal paleodepth. Furthermore, the site experienced a cool to temperate environment with warm influences in the Campanian–early Maestrichtian, the latest Maestrichtian, and the latest early Eocene.

### *Sedimentation Rate*

In calculating the sedimentation rate for Site 698 (Fig. 27), nannofossil data are adopted in conjunction with the time scale prepared by Berggren et al. (1985) for the Paleogene and Hallam et al. (1985) for the Cretaceous. The nannofossil zonations provide the most detailed zonal scheme available among the studied microfossil groups.

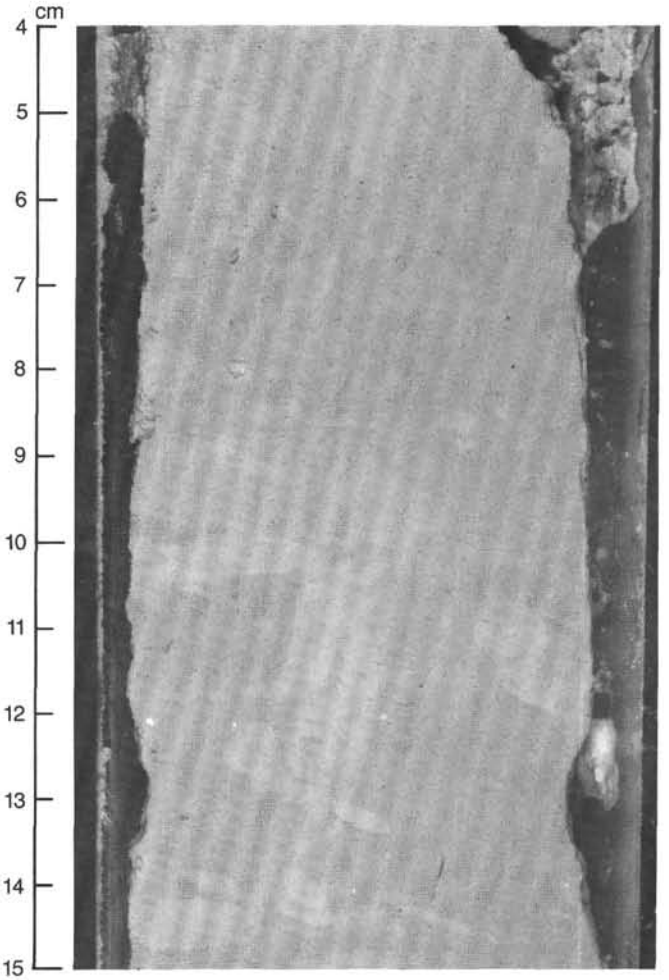


Figure 14. Bioturbated interval, mainly by *Planolites* (Sample 114-698A-6R-1, 4–15 cm). Note conspicuous vertical furrow.

The sedimentation rates thus calculated from Site 698 are ~8 m/m.y. during the Paleogene and 4–5 m/m.y. during the Late Cretaceous.

## Calcareous Nannofossils

Nineteen core-catcher and eight other core samples were examined from Hole 698A for nannofossils. Most of the samples are fossiliferous, but the nannofossil floras are generally of low diversity. The nannofossil floras are assigned to the zonation schemes of Martini (1971) and Sissingh (1977), as described in the "Explanatory Notes" chapter, this volume.

### *Biostratigraphy*

Section 114-698A-1R, CC, to Sample 114-698A-3R-1, 20–21 cm, are assigned to NP14 (middle lower Eocene). The three samples from this interval contain *Discoaster lodoensis* and *Discoaster sublodoensis*. The first appearance datum (FAD) of the latter species defines the NP14/13 boundary.

Section 114-698A-3R, CC, lies between the FAD of *D. sublodoensis* and the last appearance datum (LAD) of *Tribrachiatus orthostylus*; these two events define the NP13 Zone (lower Eocene). The occurrence of *T. orthostylus* in Sections 114-698A-4R, CC, to 114-698A-8R, CC, indicates the presence of the NP12–10 Zones (lower Eocene). The absence of the species that define the bases of NP12 and NP11 prevents any subdivision of this interval.

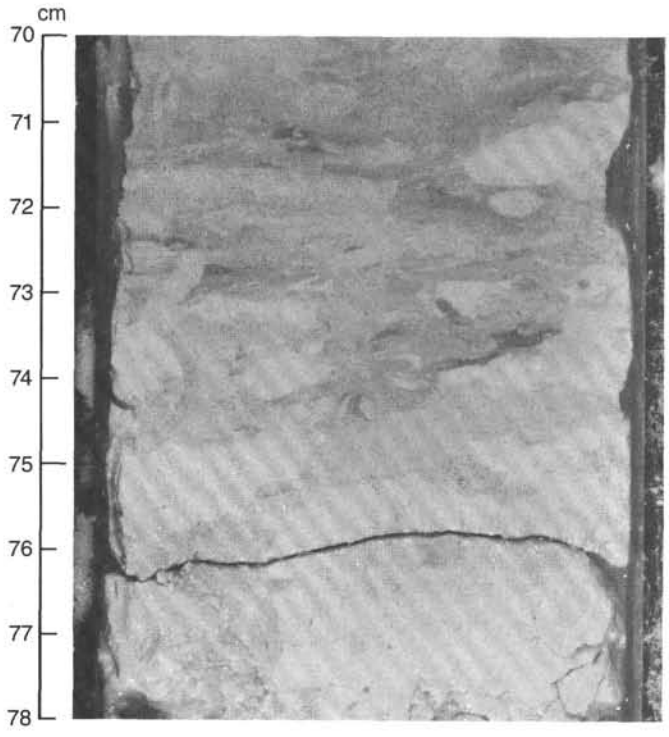


Figure 15. *Planolites, Cylindrichnus*, and oblique furrows (Sample 114-698A-6R-1, 70–78 cm). Note the surrounding darker sediment.

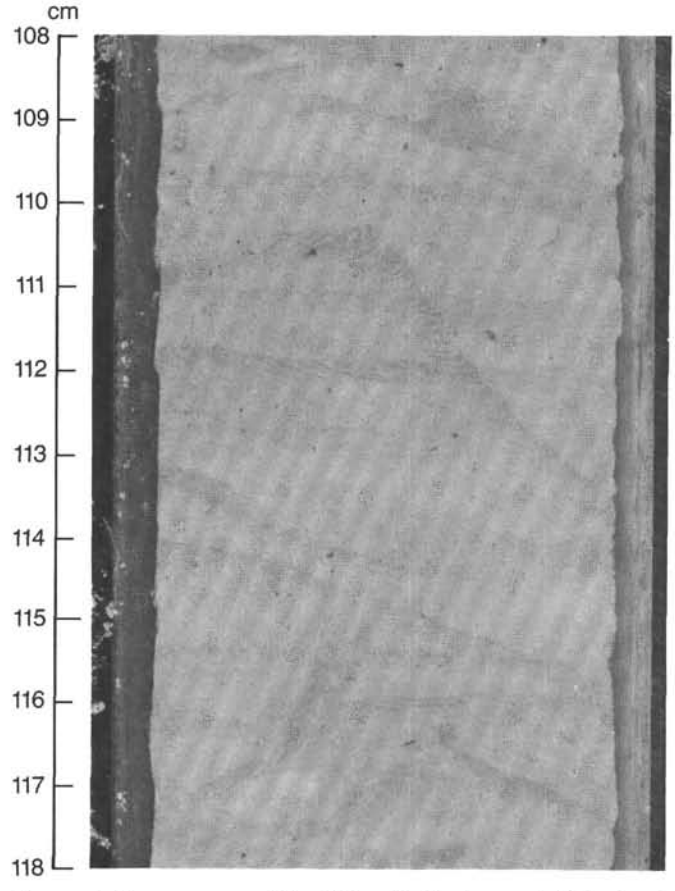


Figure 16. Homogeneous white chalk with development of dominant ichnological "tribe" of *Zoophycos* (Sample 114-698A-12R-1, 108–118 cm).

The co-occurrence of *Fasciculithus tympaniformis* and *Discoaster multiradiatus* in Samples 114-698A-9R-1, 52–53 cm, to 114-698A-10R-1, 66–67 cm, is taken to indicate the presence of NP9 (upper Paleocene). The top of this zone is defined by the FAD of *Tribrachiatus bramlettei*. This species is absent from the area of Site 698, so the LAD of *F. tympaniformis* is used instead.

The absence of *D. multiradiatus* and the presence of *Heliolithus riedelii* in Sample 114-698A-10R-2, 35–36 cm, to Section 114-698A-10R, CC, indicate the presence of NP8 (upper Paleocene).

Samples between Sections 114-698A-11R, CC, and 114-698A-12R, CC, continue to contain *F. tympaniformis* and are thus assigned to the NP7–5 Zones (upper Paleocene).

A single sample from Section 114-698A-13R, CC, is assigned to NP4–3 (upper lower Paleocene). It contains *Cruciplacolithus edwardsii, Prinsius martinii*, and *Hornibrookina teuriensis*; this last species has a reported range of NP3–5 (Perch-Nielsen, 1985). The zonal assignment is further refined by the stratigraphic position of this sample below the FAD of *F. tympaniformis*.

A stratigraphic break probably occurs between Section 114-698A-13R, CC, and Sample 114-698A-14R-1, 1–2 cm. This break separates the lower Paleocene from the upper Maestrichtian strata. The presence of *Nephrolithus frequens* between Sample 114-698A-14R-1, 1–2 cm, and Section 114-698A-15R, CC, indicates the presence of the *N. frequens* Zone (upper Maestrichtian). In this area, the stratigraphic range of *N. frequens* overlaps with that of *Reinhardtites levis*; Sissingh (1977) considered the two species to be mutually exclusive and defined the *Arkhangelskiella cymbiformis* Zone as an interval between the LAD of *R. levis* and the FAD of *N. frequens*. No such interval exists at this high latitude, probably because *N. frequens* has an earlier FAD. Thus, Sample 114-698A-14R-1, 1–2 cm, to Section 114-698A-15R, CC, are assigned to the *N. frequens* to *A. cymbiformis* Zones (upper Maestrichtian) and the interval from Section 114-698A-16R, CC, to Sample 114-698A-20R, 148–149 cm, to the *R. levis* Zone (middle lower Maestrichtian).

Section 114-698A-21R, CC, is assigned to the *Tranolithus orionatus* Zone (lower Maestrichtian–upper Campanian) because of the presence of *Broinsonia parca*.

Two samples examined from lower in the hole, bit Sample 114-698A-23R and Section 114-698A-27R, CC, are barren of calcareous nannofossils.

### *Paleoenvironment*

The nannofossil floras from the Paleogene cores contain only sporadic discoasters and common to abundant *Chiasmolithus* spp. These characteristics are typical of colder water, high-latitude assemblages. The Paleocene nannofossil floras are of low diversity but high abundance; this is also characteristic of cold-water assemblages but can be the result of selective dissolution. The common occurrence of *Zygrhablithus bijugatus* in the lower Eocene samples possibly indicates a water depth of less than 1000 m. This species is a Holococcolith, which Edwards (1973) reported as being included only in modern sediments deposited in less than 1000 m water depth.

The Cretaceous nannofossil floras recovered from Hole 698A are typically high-latitude assemblages. *N. frequens*, present in the upper Maestrichtian, is restricted to high- to midlatitudes (Worsley and Martini, 1970). *Biscutum magnum*, recovered from the Maestrichtian-Campanian interval, is also typical of high latitudes; it has been found in sediments from the southern

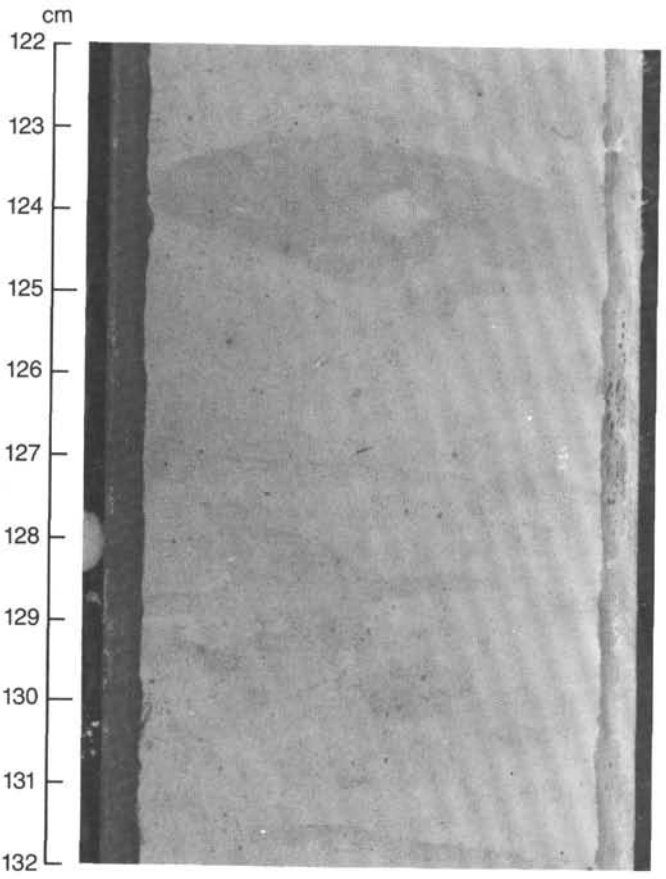


Figure 17. Burrows, dominantly *Zoophycos* (Sample 114-698A-12R-1, 122–132 cm).

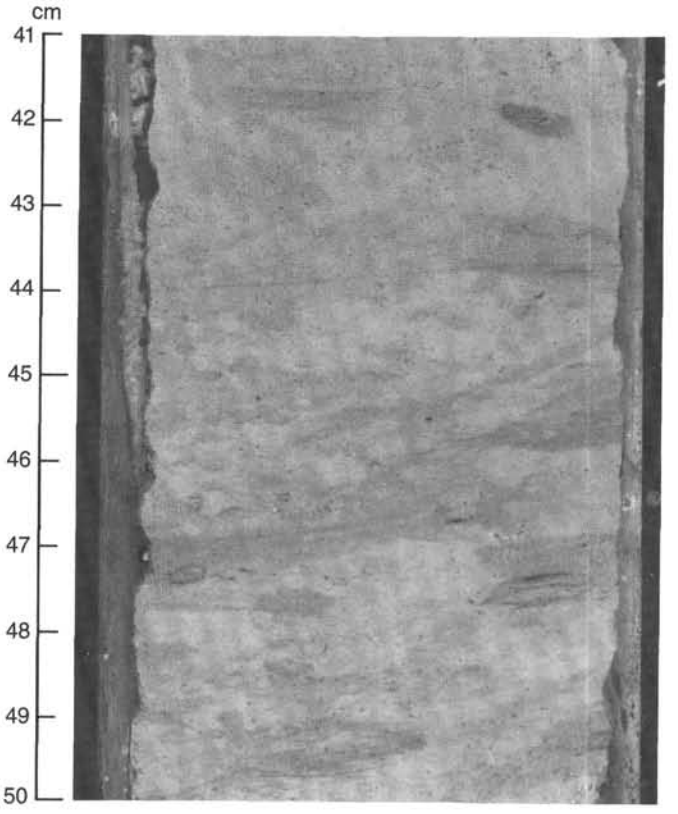


Figure 18. Typical *Planolites*. Dark hollow burrows bioturbating a white chalk (Sample 114-698A-15R-1, 41–50 cm).

South Atlantic (Wise and Wind, 1977) and southern England (Crux, 1982). Other high-latitude species from this interval include *Monomarginatus quaternarius* and *Teichorhabdus ethmos*.

### *Preservation*

The nannofossil floras throughout Hole 698A are overgrown with secondary calcite deposition.

## Planktonic Foraminifers

All core-catcher samples examined contain abundant planktonic foraminifers. They are the most representative organisms in the >45-μm size fraction, with the exception of Sections 114-698A-1R, CC, 114-698A-10R, CC, and 114-698A-11R, CC, in which radiolarians are dominant, and Sections 114-698A-14R, CC, and 114-698A-15R, CC, in which calcipherulids and benthic foraminifers prevail.

### *Biostratigraphy*

In the lower Eocene the *Morozovella crater* Zone of Jenkins' (1985) biozonation (see also "Explanatory Notes" chapter) was found between Section 114-698A-1R, CC, and Sample 114-698A-3R-2, 4–6 cm. The lower boundary is uncertain because of the poor recovery and discontinuity of the marker species. The assemblages are characterized by abundant *Planorotalites* in the >150-μm size fractions, as well as *Acarinina primitiva* and other acarininids, such as *Acarinina triplex, Acarinina aquiensis*, and *Acarinina esnaensis*. The occurrence of very rare middle- to low-latitude *Acarinina haynesi* and *Acarinina rohri jiparoensis* is indicative of relatively warm surface waters. The FAD of *Pseudohastigerina danvillensis* within this zone allows correlation to the P9 Zone (Blow, 1979). The underlying *Pseudohartigerina wilcoxensis* Zone extends downhole to Sample 114-698A-8R-1, 13–15 cm, and can be divided in P9–8 and P7–6 Zones by the first occurrence (FO) of *Acarinina pentacamerata* in Section 114-698A-6R, CC.

The interval between Sample 114-698A-8R-2, 14–16 cm, and Section 114-698A-11, CC, belongs to P5–4 of the upper Paleocene. This zonation is evidenced by the occurrence of *Subbotina pseudobulloides* and *Subbotina triloculinoides*, the evolutionary stage of acarininids, and absence of *P. wilcoxensis*; however, the marker species of the standard zonation was not noted. *Acarinina mckannai* and Chiloguembelinids are common.

The assemblages between Sample 114-698A-12R-1, 115–117 cm, and Section 114-698A-13, CC, are represented by *Globigerina daubjergensis, S. pseudobulloides, Subbotina fringa*, and *Globigerina varianta*, which are characteristic species of P1c–1b Zones, whereas Zone P1a is absent.

The uppermost part of Upper Cretaceous *Abathomphalus mayaroensis* Zone (Caron, 1985) extends from Section 114-698A-14R, CC, to Sample 114-698A-16R-2, 109–111 cm, and contains abundant *Abathomphalus* in association with common to abundant heavily ornamented forms such as *Rugoglobigerina rugosa* and *Globotruncana bulloides*. Rugoglobigerinids are also present in Section 114-698A-16R, CC, but the absence of any other marker species prevents the identification of standard zones. The Maestrichtian/Campanian boundary cannot be identified below this core-catcher sample. The assemblages are dominated by *Globigerinelloides*, small *Heterohelix, Archaeoglobigerina*

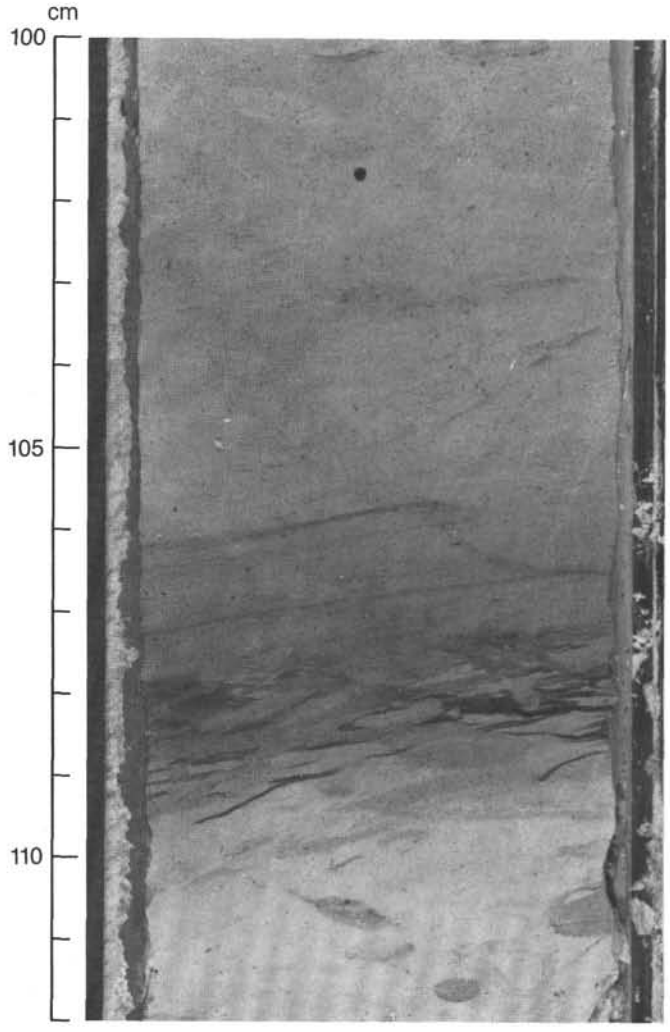


Figure 19. *Planolites* and possibly *Cylindrichnus* in a conspicuous, dark horizon. Note also *Teichichnus* (Sample 114-698A-15R-1, 100–112 cm).

*cretacea, Archaeoglobigerina blowi*, and *Hedbergella holmdelensis*. At the bottom of the hole in Section 114-698A-21R, CC, a similar assemblage was found enriched with some large globotruncanids, among which few *Marginotruncana pseudoemiliana* were identified, suggesting an early late Campanian age.

A possible hiatus may be near 99 mbsf, where P3 and P2 Zones are absent. However, calcareous nannofossil data (Table 4) suggest that sediment of this age (63.0–61.0 Ma) is present. A second hiatus brackets the Cretaceous/Tertiary boundary where the P1a Zone is absent between 118.0 and 118.05 mbsf.

### *Paleoenvironment*

The section investigated here is represented by carbonate sediments deposited above the foraminiferal lysocline in a cool to temperate environment, as suggested by the abundance of low-spired subbotinids and planorotalids, which are characteristic inhabitants of deep and intermediate water masses. Warm influences, however, are evident in the upper Maestrichtian and in the uppermost lower Eocene by the occurrence of low-latitude forms such as *Abathomphalus* and *Morozovella*.

### *Preservation*

The preservation of species is moderate or good in the Tertiary part of the sequence, but it is rather poor in the Cretaceous section. In general, planktonic foraminifers were not affected by intense dissolution, but differential dissolution is evidenced in the comparison of foraminiferal and radiolarian assemblages.

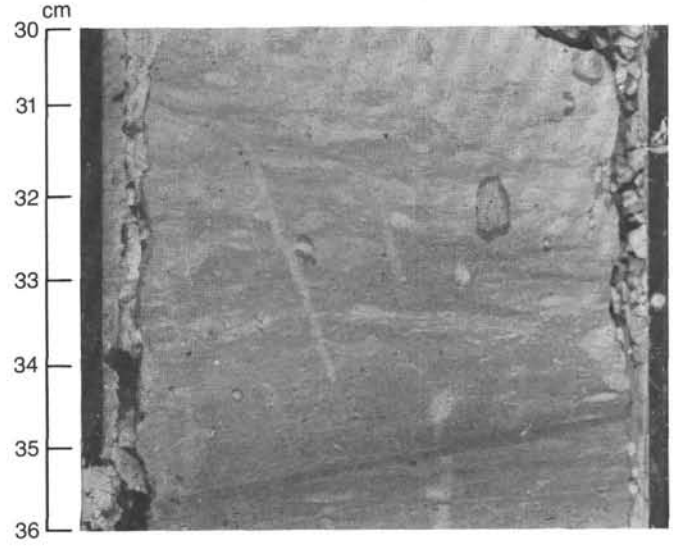


Figure 20. *Planolites* and *Chondrites* in an oxygen-reduced horizon of very low energy (Sample 114-698A-16R-1, 30–36 cm). Note that compaction was smooth to conserve delicate vertical burrow traces.

## Benthic Foraminifers

Benthic foraminifers in Hole 698A generally are abundant and well preserved. Evidence of contamination and reworking are negligible.

The Eocene assemblage found in Sections 114-698A-1R, CC, to 114-698A-7R, CC, is diverse and generally consistent downhole, with only minor fluctuations in faunal composition and relative abundance. The Eocene assemblage includes *Cibicidoides praemundulus, Cibicidoides eocaena, Cibicidoides havanensis, Cibicidoides micrus, Anomalinoides capitatus, Anomalinoides semicribratus, Bulimina semicostata, Bulimina aculeata, Bulimina tuxpomensis, Bulimina glomarchallengeri, Buliminella grata, Turrilina robertsi, Nuttallides truempyi*, and *Osangularia mexicana. Anomalinoides* spp., *Gyroidinoides* spp., *Lenticulina* spp., *Oridorsalis* spp., *Pleurostomella* spp., and *Pullenia* spp. are common in the Eocene samples recovered, as well as throughout the rest of the Hole 698A.

Evidence of a faunal transition to a Paleocene assemblage begins in Section 114-698A-8R, CC, with the occurences of *Anomalinoides praeacuta, Aragonia velascoensis, Bulimina velascoensis*, and *Cibicidoides hyphalus*, whereas much of the Eocene assemblage is still present. Sections 114-698A-9R, CC, through 114-698A-13R, CC, display a more typical Paleocene fauna dominated by *Stensioina beccariiformis* along with *C. hyphalus, Pullenia coryelli, A. praeacuta, A. velascoensis, B. velascoensis*, and a few occurrences of *Coryphostoma* cf. *midwayensis, Gyroidinoides quadratus, Neoflabellina semireticulata*, and *Neoflabellina jarvisi*.

The Maestrichtian-Campanian faunas found in Sections 114-698A-14R, CC, to 114-698A-17R, CC, and 114-698A-21R, CC, are characterized by *S. beccariiformis, Osangularia* sp., *P. coryelli, Pullenia jarvisi, Spiroplectammina spectabilis, Cibicidoides dayi*, and *Reusella szajnochae*.

Moderate to high abundances of *C. praemundulus, C. eocaena, A. capitatus, Hanzawaia ammophila, Lenticulina* spp., *O. mexicana*, and buliminids, along with very low abundances of deep-water species *Alabamina dissonata* and *Abyssamina poagi*,

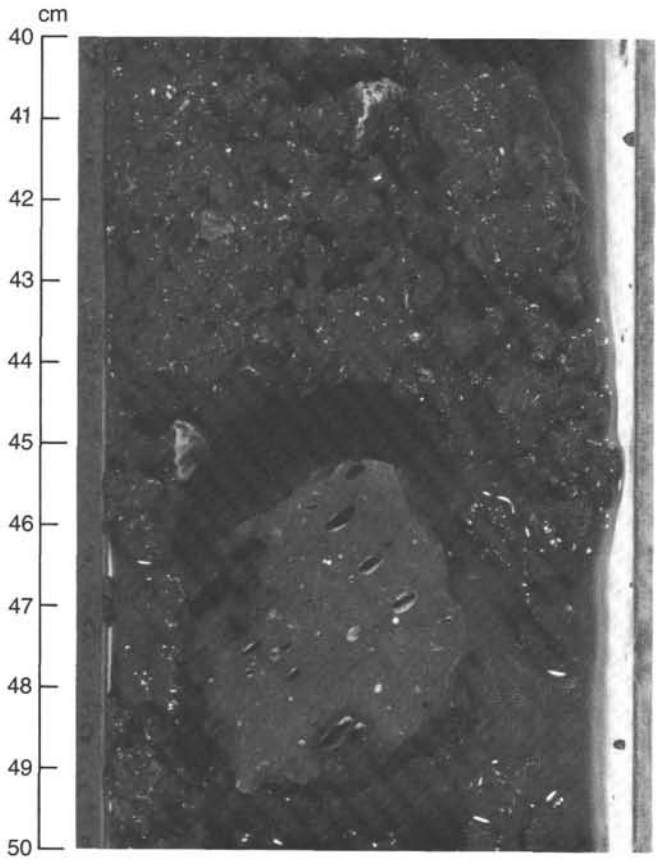


Figure 21. Clasts of completely weathered basalt in slurry (Sample 114-698A-27R-5, 40–50 cm). Note the original texture, including vesicles.

suggest a lower bathyal (1000–2000-m) depth in the Eocene. Similarly, Hole 698A bathymetric estimates for the Paleocene suggest a lower bathyal realm on the basis of moderate to high abundances of *S. beccariiformis, Lenticulina* spp., *Anomalinoides danica*, and *P. coryelli*.

## Diatoms

In Eocene and uppermost Paleocene chalks (Cores 114-698A-1R to 114-698A-9R), dissolution of Opal-A is severe. Practically all diatoms are dissolved and as a consequence, the silt fraction consists nearly entirely of clinoptilolite. Chert nodules are consistently present throughout this section. Only a few highly dissolution-resistant archaeomonadaceae were found. Single fragments of diatom valves were found in Section 114-698A-1R, CC, and in the ash-rich, silty gray-green mud of Section 114-698A-3R, CC. Clinoptilolite is present and dissolution of siliceous skeletons is evident in the latter sample. The more soluble siliceous microfossil groups, the diatoms and silicoflagellates, show signs of intense dissolution. Only valves and valve fragments of very dissolution-resistant species of diatoms are left. The presence of *Riedelia pacifica* suggests a late early Eocene to early middle Eocene age.

In the chalks of Cores 114-698A-10R to 114-698A-12R, siliceous microfossils dominate the HCl-insoluble residue. Diatoms are common to abundant and moderately well preserved. These cores are placed in the late Paleocene *Hemiaulus inaequilaterus* Zone of Gombos (1977). Stratigraphic marker species occurring in addition to the nominate species include *Hemiaulus incurvus, Triceratium gracillium* sensu Gombos (1977), and *Triceratium cellulosum* var. *simbirskianum*.

**Table 3. Chert horizons in Hole 698A.**

| Interval (core, section, cm) | Type | Thickness (cm) |
|---|---|---|
| 2R, CC (12–17) | Chert nodule | 5 |
| 3R, CC (8–17) | Chert nodule | 9 |
| 4R-1, 18–30 | Chert | 12 |
| 4R-1, 48–49 | Chert | 1 |
| 5R-1, 50–61 | Chert | 11 |
| 5R-2, 135–140 | Chert | 5 |
| 5R, CC (2–5) | Chert | 3 |
| 8R-1, 26–30 | Chert clasts (not *in situ*) | 4 |
| 9R-1, 5–17 | Chert (in place?) | 12 |
| 9R-2, 71–76 | Mottled chert | 5 |
| 9R, CC (4–7) | Chert | 3 |
| 10R-1, 20–30 | Chert | 10 |
| 12R-1, 75–83 | Reniform cherts | 8 |
| 12R, CC | Reniform cherts | |
| 13R, CC | Light gray porcellanite | |
| 14R-1, 36–45 | Chert | 9 |
| 14R-1, 59–62 | Chert nodule | 3 |
| 15R, CC | Chert nodules | |
| 16R-1, 43–46 | Chert nodule | 3 |
| 16R-2, 50–60 | Chert layer | 10 |
| 16R, CC | Reniform cherts | |
| 17R-1, 75–83 | Chert nodule | 8 |
| 17R-2, 31–40 | Chert | 9 |
| 20R, CC | Nodular chert | |
| 21R-1, 4–9 | Chert | 5 |
| 21R-1, 31–37 | Chert | 6 |
| 21R-1, 48–60 | Chert | 12 |
| 21R-1, 66–71 | Chert | 5 |
| 21R-1, 71–75 | Chert | 4 |
| 21R-1, 75–78 | Chert | 3 |
| 21R-1, 104–114 | Chert | 10 |
| 21R-2, 4–14 | Chert | 10 |
| 21R-2, 17–26 | Chert | 9 |
| 21R-2, 29–33 | Chert | 4 |
| 21R-2, 56–61 | Chert | 5 |
| 21R-2, 73–75 | Chert | 2 |
| 21R, CC | Two chert layers | |
| 24R-1, 0–4 | Chert | |

The upper Paleocene diatom assemblage is dominated by planktonic species. Only a few resting spores and shallow-water diatoms are found. This indicates a depositional environment with little input from nearshore areas.

From Core 114-698A-13R of early Paleocene age, the chalks alternate with centimeter-thick clay-rich chalk. Alternation becomes more prominent in the Upper Cretaceous (Cores 114-698A-14R to 114-698A-23R) where chert is also present. No diatoms were found in the core-catcher samples of these cores except for single, non-age-diagnostic species in Section 114-698A-15R, CC. Only the more dissolution-resistant archaeomonadaceae and radiolarians are present.

Cores 114-698A-24R and 114-698A-25R recovered basalt. No siliceous microfossils were found in the underlying red regolith.

## Radiolarians

The occurrence of radiolarians in Hole 698A is sporadic, limited to only a few samples in which their abundance ranges from common to abundant and their preservation is fairly good.

Radiolarians are absent in Section 114-698A-1R, CC. In Section 114-698A-2R, CC, radiolarian species including *Lychnocanoma babylonis turgidulum* and *Amphicraspedum pyxilum* were recognized. From Section 114-698A-3R, CC, *Phormocyrtis striata striata* and *Phormocyrtis striata exquisita* were observed in addition to the previous species, suggesting that the age of sediments is near the base of *P. s. striata* Zone (Sanfilippo et al., 1985) of lower Eocene. Unfortunately, other char-

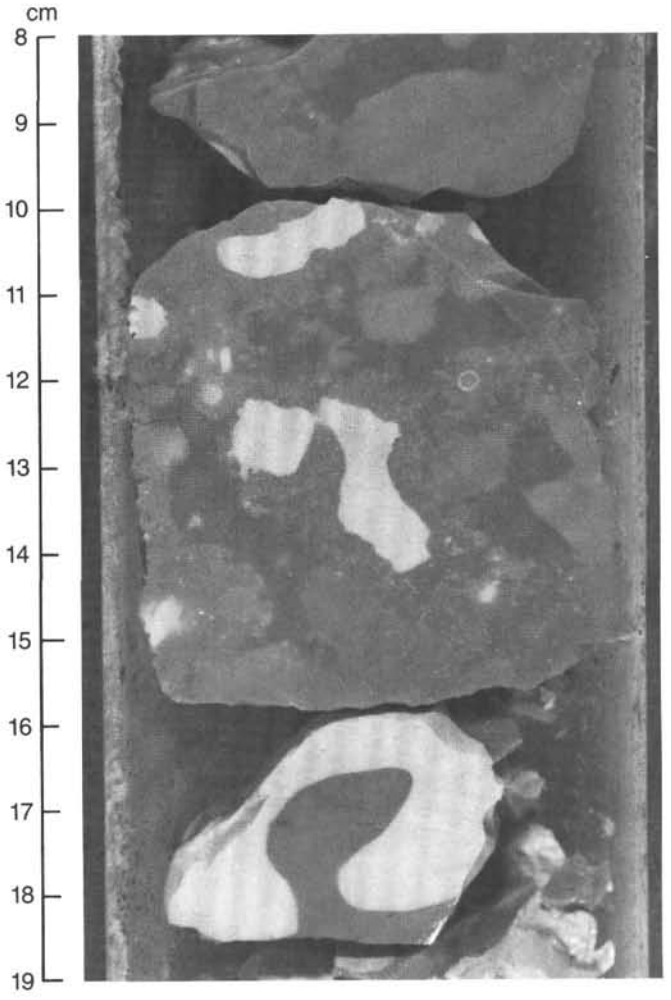


Figure 22. Chert horizon consisting of fragments; center fragment shows carbonate inclusions trapped during chertification (Sample 114-698A-9R-1, 8–19 cm).

acteristic species generally observed in the widely recognized standard zonation, which is based on results from tropical regions, are absent from the samples, thus preventing detailing their definite age assignment. From Section 114-698A-4R, CC, to the bottom of the hole, radiolarians are generally absent, except in Cores 114-698A-8R, 114-698A-10R, 114-698A-11R, and 114-698A-16R. In Cores 114-698A-8R, 114-698A-10R, and 114-698A-11R, radiolarians are abundant, their preservation is good, and the overall faunal composition is similar to the late Paleocene age assemblages recognized at Sites 552 (Westberg-Smith and Riedel, 1984) and 208 (Dumitrica, 1973). However, the absence of zonal index fossils belonging to species of genus *Buryella* again made it impossible to place the samples into existing zonal schemes.

In Section 114-698A-16R, CC, rare specimens of moderately well-preserved Cretaceous forms, including *Amphipyndax* sp., were observed, clearly indicating that the sediments are of Cretaceous age.

## Silicoflagellates

Specimens of silicoflagellates and ebridians were observed only in Sections 114-698A-3R, CC, 114-698A-8R, CC, 114-698A-10R, CC, and 114-698A-11R, CC. The occurrence of *Naviculopsis biapiculata* and *Naviculopsis constrica* in Section 114-698A-3R, CC, indicates that these sediments belong to the *N. constricta*

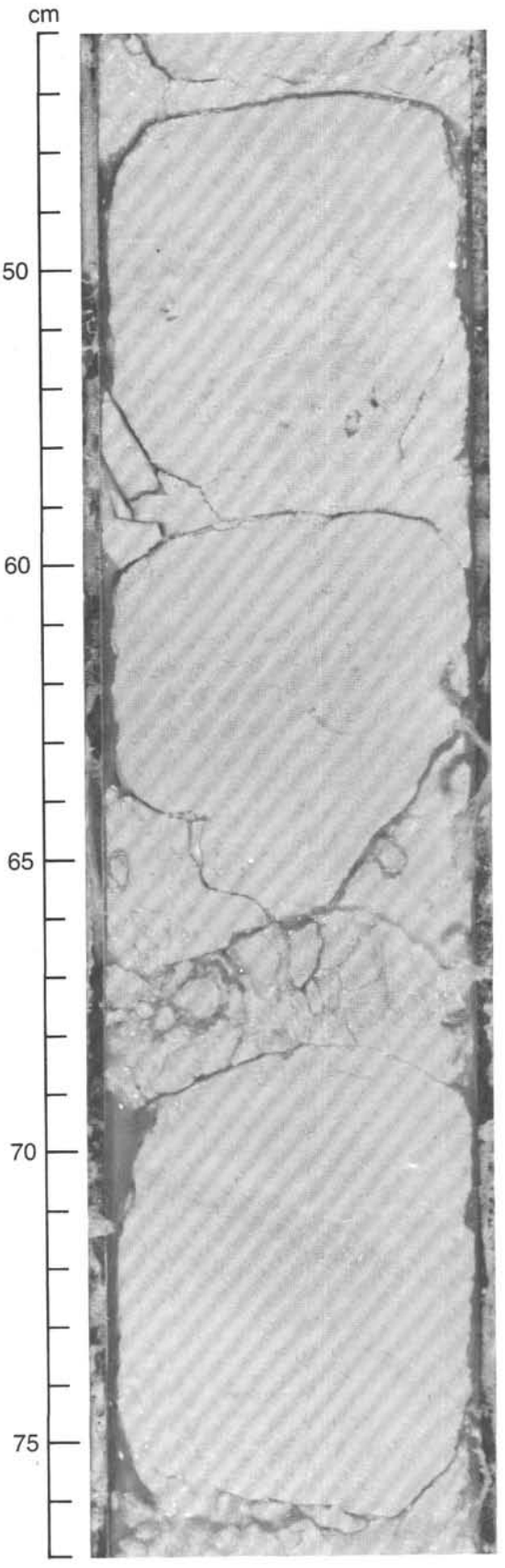


Figure 23. Nannofossil chalk, intensely bioturbated, with the first appearance of bioturbation, which is mainly *Planolites* (Sample 114-698A-5R, 46–77 cm).

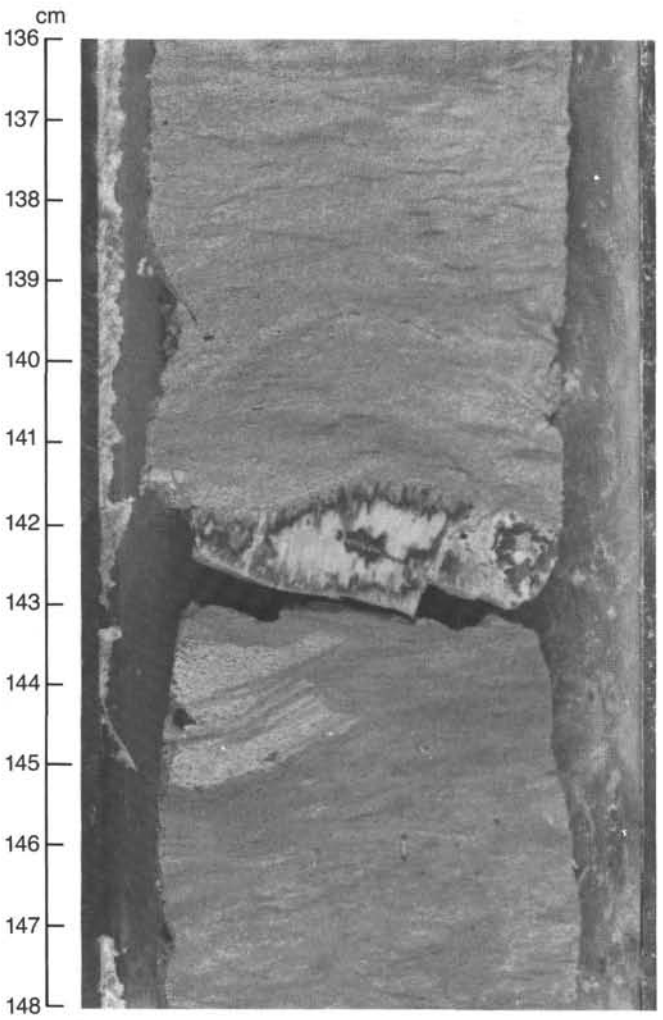


Figure 24. Thick bioturbated interval with *Planolites* (Sample 114-698A-21R-1, 136–148 cm).

Zone. Abundant, well-preserved silicoflagellates were recovered from Sections 114-698A-8R, CC, and 114-698A-10R, CC, including *Corbisema angularis, Corbisema apiculata, Corbisema hastata, Corbisema disymmetrica angulata*, and *Corbisema inermis*, together with *N. contricta* and *Pseudomicromarsupium falklandensis*; this assemblage confirms assigment of the *N. constricta* Zone of late Paleocene age (Busen and Wise, 1977).

### Ebridians

Ebridians occur sporadically in samples from Hole 698A; they were observed only in Sections 114-698A-3R, CC, 114-698A-10R, CC, and 114-698A-11R, CC. Most belong to *Ammodochium rectangulare* sens. lato., and further investigation is needed to refine the species assignments. A few, apparently new ebridians were also identified in these samples.

## GEOCHEMISTRY

Interstitial-water chemistry, headspace gas chemistry, inorganic carbon (% $CaCO_3$), and summaries of X-ray diffraction (XRD) and X-ray fluorescence (XRF) analyses of sediments and rocks are presented for Site 698. Poor recovery in Hole 698A precluded detailed geochemical assessment of sediments, and pore-water chemistry displayed little direct evidence of diagenetic reactions within the sediment column or within the basement because of sparse data coverage. Headspace gases (methane/ethane) were very low, characteristic of organic-carbon-poor sediments. The major sediment lithology is demonstrated by the uniformly high carbonate contents (over 80%). Dolomite is absent. The bottom of the hole contains a series of interbedded altered and unaltered basalts and iron-rich sediments.

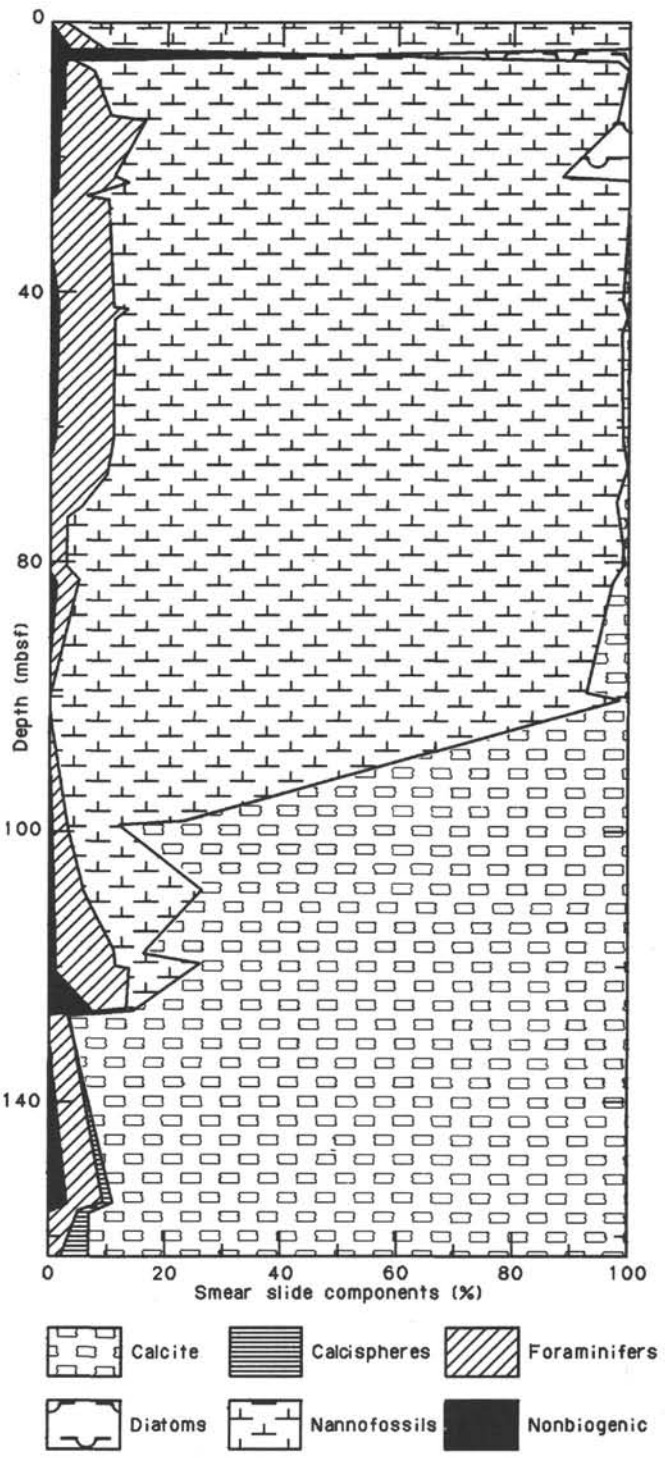


Figure 25. Composition of the pelagic column at Site 698 from smear slide data. Nonbiogenic = quartz, feldspar, clay, mica, volcanic glass, and accessory minerals (opaques, zeolites, and pyroxene).

### Interstitial-Water Chemistry

Pore waters were squeezed from five 5-$cm^3$ whole rounds taken at about 30-m intervals. The results of the pore-water chemistry are summarized in Table 5 and in Figure 28. In gen-

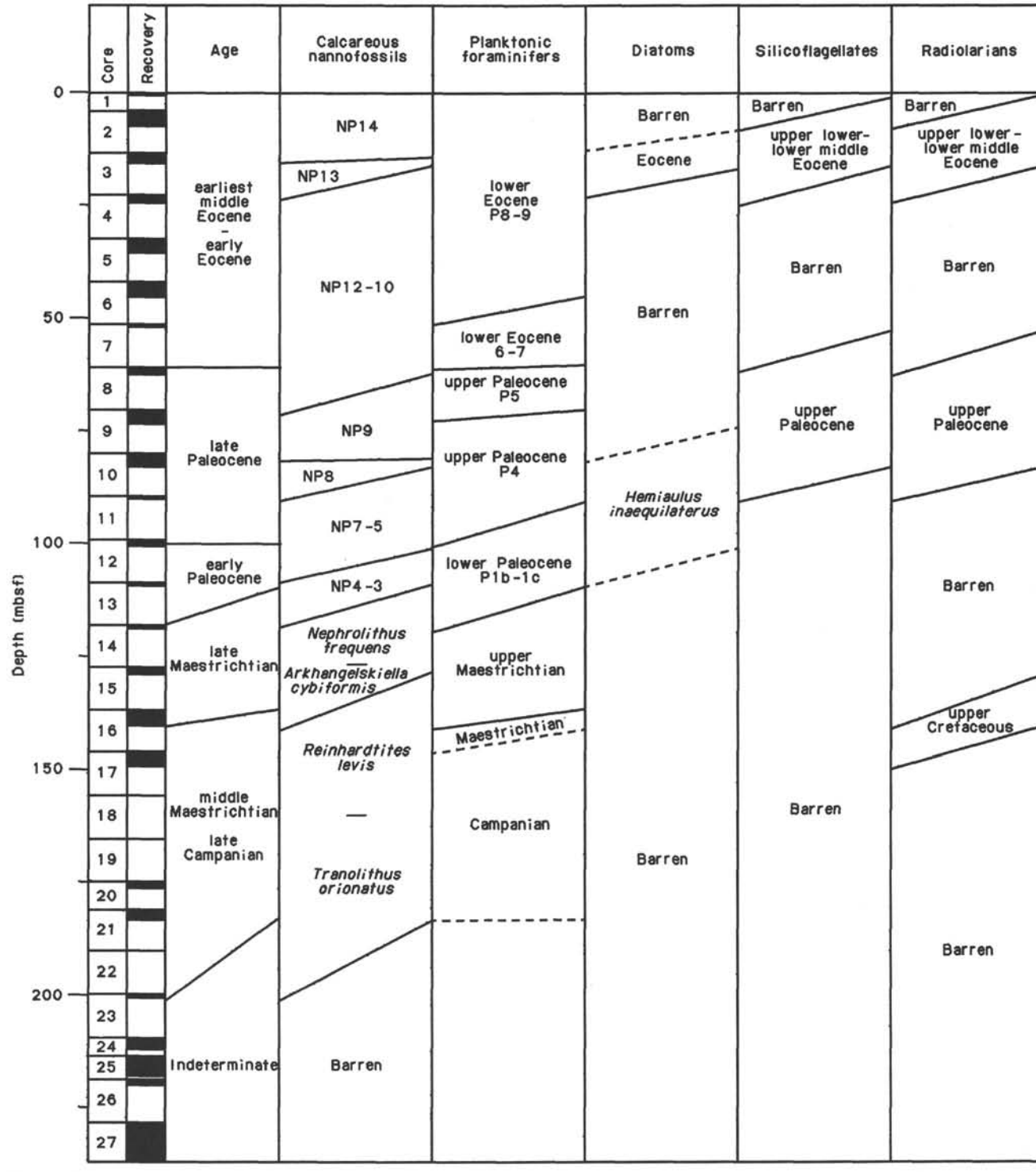


Figure 26. Summary of planktonic microfossil data from Site 698.

eral, alkalinity and magnesium decrease downhole from bottom-water concentrations (about 2.5 and 55 mmol/L, respectively), whereas calcium increases downhole from bottom-water concentrations of 28 mmol/L. These gradients suggest basement reactions consuming alkalinity and magnesium while releasing calcium by low-temperature alteration of basalts. Sulfate decreases gradually downhole but never approaches zero, indicating that anoxic conditions do not occur in this hole. Slight sulfate reduction may be occurring near basement, perhaps in a basal section that was not recovered. Dissolved silica concentrations are fairly constant at 500 μmol/L and do not appear to vary significantly with depth. Fluoride concentrations are systematically higher than seawater (70 μmol/L), but we suspect that this is an artifact. Salinities and chloride concentrations are similar to the values of seawater at the site.

## Volatile Hydrocarbon Gases

Concentrations of hydrocarbons extracted from headspace samples were very low, similar to ambient air. The results of the

**Table 4. Microfossil datums identified at Site 698.**

| Microfossil and paleomagnetic datums[a] | Age (Ma) | Reference[b] | Bracketing samples of datums | Depth range[c] (mbsf) | Mean position (mbsf) |
|---|---|---|---|---|---|
| Mixed assemblage of early Pliocene to Quaternary | | | | 0–4.00 | |
| Hiatus ~52.0–<5.0 Ma | | | In unrecovered interval above 1R, CC | 0–4.00 | |
| 1. Top P9 Zone, *Morozovella crater* (F) | 52.0 | 4, 6 | 1R, CC/1R-1, 0 cm | 0–4.00 | |
| 2. Base NP14 Zone (N) | 52.6 | 4 | 3R-1, 21 cm/3R, CC | 13.70–23.00 | 18.45 |
| 3. Top NP12 Zone (N) | 53.7 | 4 | 4R, CC/3R, CC | 23.00–32.50 | 27.75 |
| 4. Base P9 Zone, *M. crater* (F) | 53.4 | 4, 6 | 5R-2, 107 cm/5R, CC | 35.05–42.00 | 38.53 |
| *5. Base P8 Zone, FAD *Acarinina pentacamerata* (F) | 55.2 | 4 | 6R, CC/7R, CC | 51.50–61.00 | 56.25 |
| Possible hiatus Maximum range = ~57.8–53.4 Ma Minimum range = ~57.8–55.2 Ma | | | 6R, CC/8R-1, 16 cm | 51.50–61.16 | |
| 6. Base P6 Zone, FAD *Pseudohastigerina wilcoxensis* (F) | 57.8 | 4 | 8R-1, 16 cm/8R-2, 91 cm | 61.16–63.41 | 62.29 |
| 7. LAD *Fasciculithus* (N) | 57.6 | 4 | 9R-1, 52 cm/8R, CC | 70.50–71.02 | 70.76 |
| 8. Base P5, LAD *Subbotina pseudobulloides* (F) | 58.8 | 4 | 8R, CC/9R-2, 20 cm | 70.50–72.20 | 71.35 |
| 9. Base NP9 Zone (N) | 59.2 | 4 | 10R-1, 67 cm/10R-2, 35 cm | 80.67–81.85 | 81.26 |
| 10. Base NP8 Zone (N) | 60.0 | 4 | 10R, CC/11R, CC | 89.50–99.00 | 94.25 |
| 11. Base P4 Zone (F) | 61.0 | 4 | 11R, CC/12R-1, 115 cm | 99.5–100.15 | 99.58 |
| 12. Base NP5 Zone (N) | 62.0 | 4 | 12R, CC/13R, CC | 108.50–118.00 | 113.25 |
| *13. Base P1b Zone, FAD *S. pseudobulloides* (F) | 66.1 | 4 | 13R, CC | 118.0 | |
| Hiatus Maximum range = ~64.4–67.5 Ma Minimum range = ~66.1–66.4 Ma | | | 14R-1, 1–2 cm/13R, CC | ~118.05 | |
| *14. Top *Nephrolithus frequens* (N) | 66.4 | 5 | 14R-1, 1 cm/13R, CC | 118.00–118.10 | 118.05 |
| 15. Top *Reinhardtites levis* (N) | 71.5 | 5 | 16R, CC/15R, CC | 137.00–146.50 | 141.75 |
| 16. Base *Abathomphalus mayaroensis* Zone (F) | 68.0 | 5 | 16R-2, 109 cm/16R, CC | 139.60–146.50 | 143.05 |
| 17. Maestrichtian/Campanian (F) | 74.5 | 5 | 16R, CC/17R-1, 110 cm | 146.50–147.60 | 147.05 |
| 18. Base Campanian (F) | 84.0 | 5 | 21R, CC | >190.5 | |

[a] + = direct correlation to paleomagnetic stratigraphy; # = absolute age data; * = probable truncation of range by hiatus; D = diatom; F = planktonic foraminifer; N = calcareous nannofossil.
[b] 4. Berggren et al. (1985); 5. Kent and Gradstein (1985); 6. Jenkins (1985).
[c] Core-catcher depths in this table were calculated by assuming the core-catcher sample was obtained from the bottom of the cored interval.

headspace analyses for methane ($C_1$) and ethane ($C_2$) are reported in Table 6.

## Sedimentary Organic and Inorganic Carbon

Sediment residues from physical-properties samples were analyzed for inorganic carbon and tabulated as percent calcium carbonate (Table 7).

## Sedimentary and Basement Mineralogy and Elemental Composition

The following mineral assemblages were identified in samples from Hole 698A by XRD. No dolomite peaks were present in the limestone units.

Top of Cretaceous limestone—Subunit IIC

| | |
|---|---|
| 17R-1, 50–52 cm | Calcite |
| 17R-2, 50–52 cm | Calcite |

Top of upper basalt—Subunit IIIB

| | |
|---|---|
| 24R-1, 3-05 cm | Hematite, clay, quartz, plagioclase |
| 25R-2, 91–93 cm | Na-plagioclase, diopside, enstatite, fayalite, and hematite(?) |

Lower iron oxide-rich altered basalt—Subunit IIIC

| | |
|---|---|
| 26R-1, 31–33 cm | Hematite, magnetite, clay (chlorite?) |
| 26R-1, 72–74 cm | Hematite, magnetite, clay (chlorite?), and quartz |
| 27R-1, 45–47 cm | Hematite, magnetite, clay (palygorskite?) |
| 27R-3, 78–80 cm | Hematite, magnetite, clay (palygorskite?) |
| 27R-4, 102–104 cm | Quartz, plagioclase, clay; plus minor calcite, magnetite, and hematite |
| 27R-5, 100–102 cm | Quartz, plagioclase, clay; plus minor calcite, magnetite, and hematite |
| 27R-6, 30–32 cm | Quartz, plagioclase, clay; plus minor calcite, magnetite, and hematite |
| 27R, CC (10–12 cm) | Quartz, plagioclase, clay, hematite, and magnetite |

The results of XRF analyses for major elements (wt%) of selected samples from Hole 698A are as follows:

| | 26R-1, 29–33 cm | 17R-1, 55–57 cm | 17R-1, 69–71 cm | 17R-2, 126–128 cm |
|---|---|---|---|---|
| $SiO_2$ | 34.81 | 7.01 | 18.75 | 24.39 |
| $TiO_2$ | 6.16 | 0.01 | 0.03 | 0.21 |
| $Al_2O_3$ | 23.03 | 1.32 | 2.09 | 5.76 |
| $Fe_2O_3$ | 30.29 | 0.63 | 0.72 | 2.25 |
| MnO | 0.19 | 0.04 | 0.04 | 2.25 |
| MgO | 1.12 | 0.00 | 0.00 | 0.00 |
| CaO | 0.99 | 89.79 | 75.72 | 58.42 |
| $Na_2O$ | 1.16 | 0.00 | 0.12 | 0.79 |
| $K_2O$ | 0.27 | 0.07 | 0.15 | 0.92 |
| $P_2O_5$ | 0.22 | 0.13 | 0.14 | 0.28 |
| Total | 98.24 | 99.00 | 97.76 | 93.04 |

Samples from Sections 114-698A-17R-1 and 114-698A-17R-2 are from various horizons in the intercalated limestone and chert stringers. The relative proportions of CaO and $SiO_2$ are indirectly related in these three samples, reflecting mixtures of

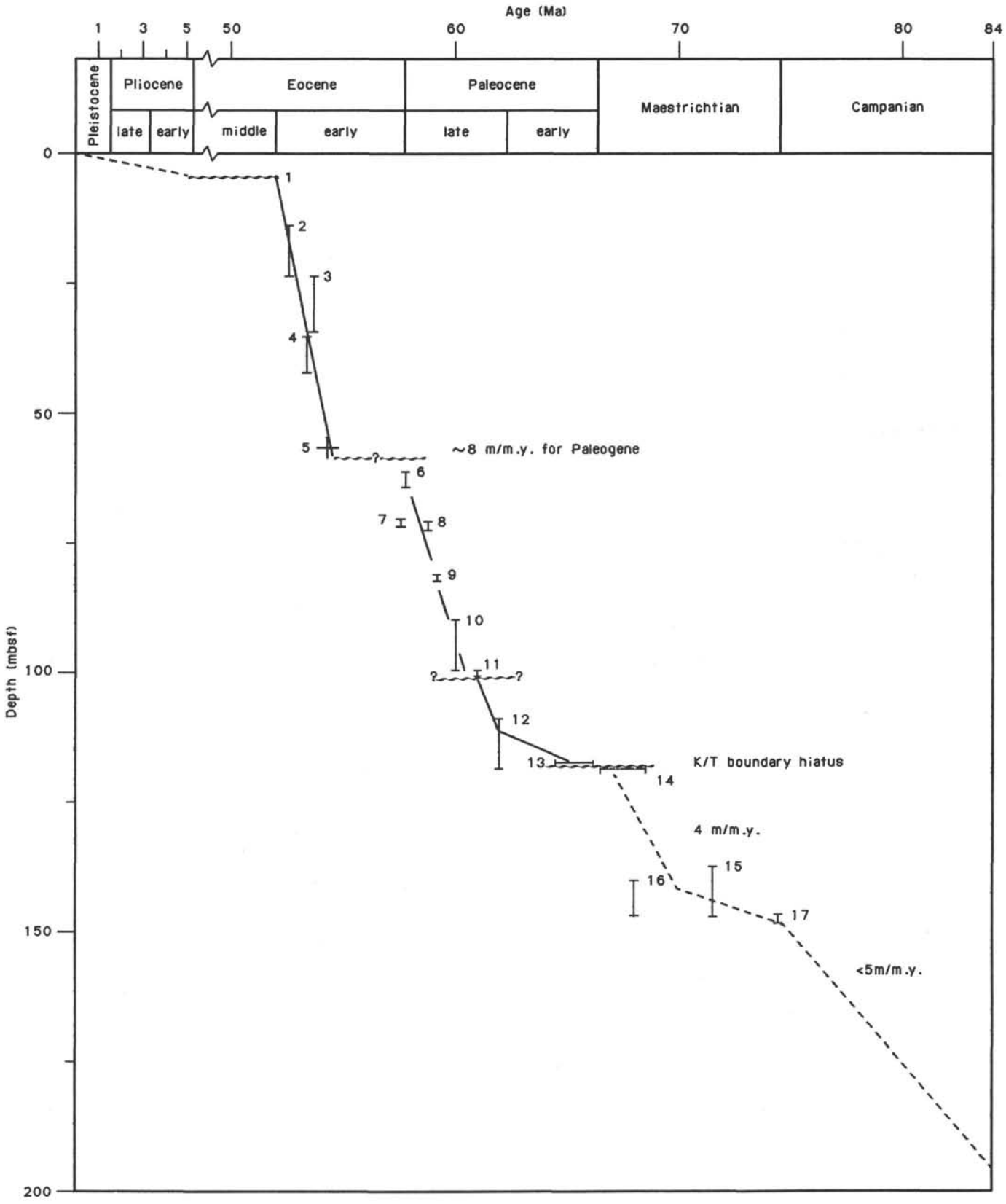


Figure 27. Age vs. depth relationship for Site 698 with sedimentation rate estimates.

**Table 5. Interstitial-water chemistry from Hole 698A.**

| Sample (core, section, cm) | Depth (mbsf) | Volume (mL) | pH | Alkalinity (mmol/L) | Salinity (g/kg) | Magnesium (mmol/L) | Calcium (mmol/L) | Chloride (mmol/L) | Sulfate (mmol/L) | Fluoride (μmol/L) | Silica (μmol/L) | Mg/Ca |
|---|---|---|---|---|---|---|---|---|---|---|---|---|
| 2R-2, 145–150 | 6.95 | 30 | 7.49 | 2.91 | 34.8 | 37.53 | 11.37 | 558.12 | 28.60 | 83.00 | 513 | 3.30 |
| 3R-1, 145–150 | 14.95 | 60 | 7.65 | 2.81 | 35.0 | 52.66 | 11.47 | 564.90 | 28.80 | 83.00 | 539 | 4.59 |
| 6R-2, 125–130 | 44.75 | 25 | 7.70 | 2.51 | 35.2 | 51.22 | 14.05 | 561.95 | 27.70 | 86.00 | 411 | 3.65 |
| 9R-1, 145–150 | 71.95 | 34 | 7.61 | 2.41 | 35.0 | 49.89 | 15.58 | 569.83 | 27.90 | 91.00 | 456 | 3.20 |
| 16R-2, 145–150 | 139.95 | 30 | 7.60 | 1.70 | 35.0 | 41.25 | 28.48 | 568.84 | 26.30 | 72.00 | 474 | 1.45 |

almost pure opal (chert) and calcite. The pure calcite end-member (Sample 114-698A-17R-1, 55–57 cm) contains very little aluminum and iron (clays) and is almost devoid of magnesium, demonstrating the absence of dolomite or high-magnesium calcite. The cherty samples (114-698A-17-2, 126–128 cm, and 114-698A-17-1, 69–71 cm) contain high silica and some calcite. Sample 114-698A-26R-1, 29–33 cm, is from the hematite-rich altered basalt. The elemental analysis reported here is consistent with the previous mineralogical assignments (hematite, magnetite, and clays).

## PALEOMAGNETICS

The principal objectives of ODP drilling at Site 698 concern the age of the basement and the paleodepth/paleoenvironment of the sediments that immediately overlie it. Because of the limited time available for drilling at this site (approximately 1.5 days) it was not feasible to use the APC or XCB systems. The hole was rotary cored and consequently, much of the recovered sediment is too highly deformed to be suitable for paleomagnetic investigations. Furthermore, sediment recovery was discontinuous, with only 52.3 m of recovery from a total cored interval of 237 m. For these reasons, magnetostratigraphic data from this site are of limited use and the paleomagnetic investigations instead focused on the following objectives:

1. To obtain information on the typical intensities of natural remanent magnetization (NRM) of the recovered sediment
2. To perform preliminary alternating field (AF) demagnetization analyses on representative specimens in order to investigate the stability of their remanent magnetization
3. To perform whole-core magnetic susceptibility measurements as an aid to identifying lithological changes and possibly also cyclic phenomena in the recovered sediments from this site.

### NRM Intensities and Directions

The NRM intensities and directions were determined for 23 sediment samples from this site, using a Minispin discrete-sample magnetometer. No shipboard remanence measurements were made on the basalts recovered from basement. These will be the subject of a shore-based study.

The NRM determinations for the sediments are listed in Table 8. Only 30% of these samples have well-defined magnetic intensities, that is, intensities more than three times the noise level of the Minispin magnetometer. The majority of the NRM intensity values lie within the range 0.1 to 0.5 mA/m, which appears to be typical for both the carbonate- and silica-rich sediments. However, significantly higher values occur in Samples 114-698A-5R-2, 99–101 cm, 114-698A-6R-1, 9–11 cm, and 114-698A-21R-1, 43–45 cm. These may indicate a higher terrigenous content or the presence of small amounts of disseminated pyroclastic material at these particular levels.

### Whole-Core Susceptibility Data

Whole-core susceptibility measurements were performed on 17 core sections from Hole 698A. Most of the susceptibility values are within the range $1.0 \times 10^{-12}$ to $50.0 \times 10^{-12}$ SI units. Anomalously high values, ranging up to $10^{-9}$ SI units, were observed at certain levels, but subsequent splitting of the cores revealed that these values were caused by dropstones of igneous material (mainly basalts) that had been incorporated in the cores during drilling. Quasicyclical fluctuations with a wavelength of ~20 to 30 cm were identified in a number of sections and may represent subtle variations in lithology. However, the amplitudes of the fluctuations are very small, only just above the instrument noise level.

The log-mean susceptibility value was calculated for each of the sections measured, and these values are listed, together with their Gaussian standard deviations, in Table 9. Separate mean values are shown for the parts of the sections that contain dropstones. Duplicate measurements were made for a number of sections, and the agreement is generally very good.

In addition to the 14 sections of nannofossil ooze measured from Cores 114-698A-2R to 114-698A-17R, four sections through the basalts and underlying regolith of Cores 114-698A-25R to 114-698A-27R were also measured. The values for these units are three orders of magnitude greater than those typical of the nannofossil oozes. Furthermore, the values for the basalts are indistinguishable from those for the underlying regolith. This suggests that the magnetic mineral content of the regolith is likely to be very similar to that of the basalt.

## PHYSICAL PROPERTIES

The objectives of physical-property measurements at Site 698 were to investigate the link between changes in physical properties and seismic-reflector sequences of pelagic deep-sea sediment lithologies in the Atlantic sector of the Southern Ocean.

The techniques used for shipboard physical-property measurements at Site 698 are outlined in the "Explanatory Notes" chapter. Four sets of measurements were obtained: (1) index properties, which consist of gravimetric determinations of bulk density, porosity, water content, and grain density; (2) vane shear strength; (3) compressional-wave (*P*-wave) velocity; and (4) thermal conductivity. The carbonate content (see "Geochemistry" section, this chapter) is shown for comparison with the physical-property data. All the data presented in this section are unscreened for bad data points, except for one obviously anomalous result.

Index properties measured on selected samples from undisturbed sections of rotary-cored sediments are listed in Table 10. Downhole profiles of wet-bulk density, porosity, water content, and grain density are illustrated in Figure 29. These parameters show changes that correlate with two major lithostratigraphic units (see "Lithostratigraphy" section, this chapter).

Lithostratigraphic Unit II is divided into Subunits IIA (4.25–42.0 mbsf), IIB (42.0–146.5 mbsf), and IIC (146.5–190.5 mbsf). Index properties characterize the lithostratigraphic units as follows:

Subunit IIA (4.25–42.0 mbsf, Eocene)

| | | Mean | Minimum | Maximum |
|---|---|---|---|---|
| Wet-bulk density | (g/cm$^3$) | 1.76 | 1.69 | 1.80 |
| Grain density | (g/cm$^3$) | 2.74 | 2.66 | 2.84 |
| Porosity | (%) | 59.82 | 56.04 | 65.35 |
| Water content | (%) | 34.99 | 32.16 | 38.37 |

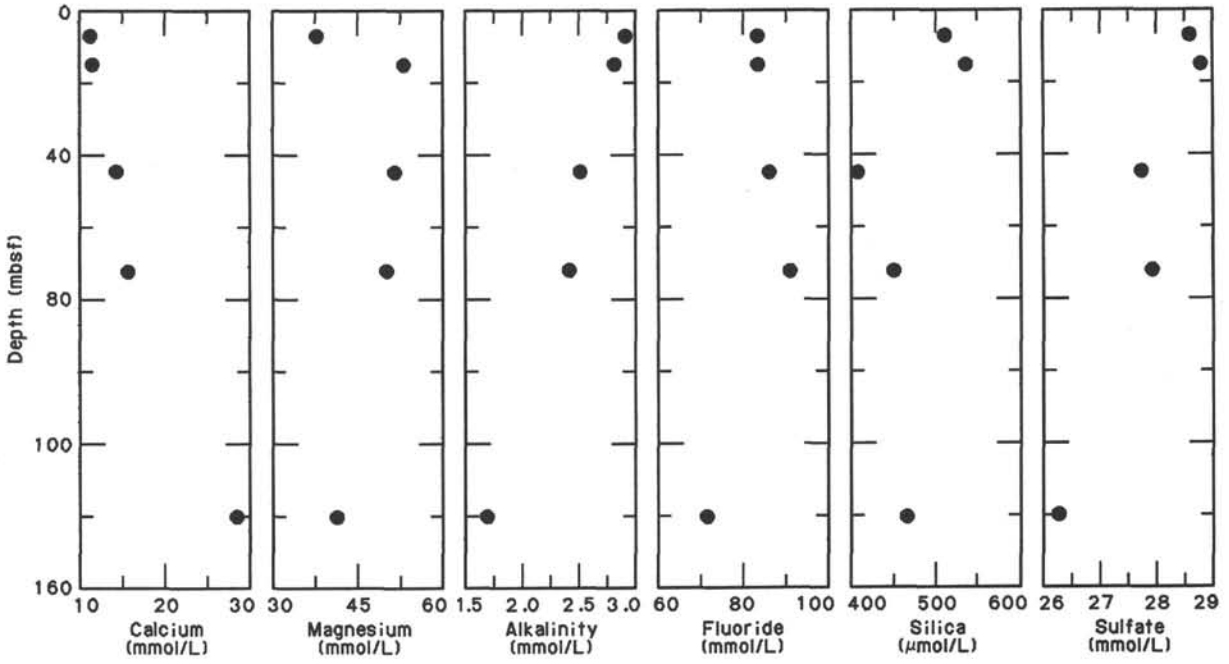


Figure 28. Pore-water calcium, magnesium, alkalinity, fluoride, sulfate, and dissolved silica profiles, Hole 698A.

Subunit IIB (42.0–146.5 mbsf, Eocene–Upper Cretaceous)

| | | Mean | Minimum | Maximum |
|---|---|---|---|---|
| Wet-bulk density | (g/cm$^3$) | 1.87 | 1.69 | 2.06 |
| Grain density | (g/cm$^3$) | 2.71 | 2.66 | 2.75 |
| Porosity | (%) | 52.83 | 43.10 | 61.54 |
| Water content | (%) | 29.09 | 20.90 | 34.87 |

Subunit IIC (146.5-190.5 mbsf, Upper Cretaceous)

| | | Mean | Minimum | Maximum |
|---|---|---|---|---|
| Wet-bulk density | (g/cm$^3$) | 2.09 | 1.97 | 2.20 |
| Grain density | (g/cm$^3$) | 2.68 | 2.67 | 2.71 |
| Porosity | (%) | 42.63 | 39.00 | 49.40 |
| Water content | (%) | 21.03 | 18.20 | 25.70 |

Lithostratigraphic Unit III consists of Subunits IIIA (200–200.15 mbsf), IIIB (209.5–219.28 mbsf), and IIIC (219.28–237 mbsf). The lithology changes from a plagioclase-phyric basalt through hematite-rich clay sediments (Subunit IIIB) to strongly weathered basalt (Subunit IIIC). These subunits represent the most dramatic changes in index properties at Site 698.

Subunit IIIB (209.5–219.28 mbsf)

| | | Mean | Minimum | Maximum |
|---|---|---|---|---|
| Wet-bulk density | (g/cm$^3$) | 2.96 | 2.83 | 3.32 |
| Grain density | (g/cm$^3$) | 3.08 | 2.93 | 3.29 |
| Porosity | (%) | 13.82 | 6.60 | 23.10 |
| Water content | (%) | 4.82 | 2.30 | 8.50 |

Subunit IIIC (219.28 mbsf)

| | | Mean | Minimum | Maximum |
|---|---|---|---|---|
| Wet-bulk density | (g/cm$^3$) | 1.90 | 1.86 | 1.94 |
| Grain density | (g/cm$^3$) | 3.41 | 3.36 | 3.47 |
| Porosity | (%) | 66.15 | 63.10 | 69.20 |
| Water content | (%) | 35.70 | 33.40 | 38.00 |

Subunit IIIC (237 mbsf)

| | | Mean | Minimum | Maximum |
|---|---|---|---|---|
| Wet-bulk density | (g/cm$^3$) | 1.87 | 1.40 | 2.03 |
| Grain density | (g/cm$^3$) | 3.00 | 2.80 | 3.14 |
| Porosity | (%) | 59.67 | 46.80 | 80.00 |
| Water content | (%) | 33.85 | 27.50 | 58.70 |

The results of carbonate content measurements (see "Geochemistry" section) from lithostratigraphic Unit II are listed in Table 11. Carbonate content is high and varies between 76% and 96% (Fig. 29), which indicates that dilution of carbonate sediments by terrigenous and siliceous material was low throughout the Eocene and Late Cretaceous.

The results of shear-strength measurements are listed in Table 12. Measurements in soft to stiff sediments of the upper 35 mbsf show a steady increase in shear strength from 16 (5 mbsf) to 37 kPa (35.1 mbsf) (Fig. 29). This may indicate an increase in consolidation and diagenetic alteration of the sediments with depth. Below 35 mbsf, the sediments were too stiff to properly measure shear strength.

The results of the *P*-wave velocity measurements are listed in Table 13. In the upper 75 mbsf, *P*-wave velocities were determined by using the P-Wave Logger (PWL). To obtain reliable results with the PWL, the core liner must be filled completely and no gaps should exist between the sediments and the liner. Furthermore, the core should contain relatively unbroken material. At Site 698, the recovered sediment was often broken, often with significant gaps occurring between the sediment and the liner. Poor PWL results made it necessary to measure *P*-wave velocity on individual samples removed from the liner. Below 75 mbsf, measurements were made on individual samples by using the Hamilton Frame Velocimeter (Fig. 29). In spite of the sample quality, however, distinct changes in *P*-wave velocity clearly correspond to lithologic changes that are characterized by increasing lithification with depth of the nannofossil-bearing sediments. The measured velocities increase from 1.58 to 1.68 km/s

**Table 6. Volatile hydrocarbon gases (methane and ethane) from Hole 698A.**

| Sample (core, section, cm) | Depth (mbsf) | $C_1$ (ppm) | $C_2$ (ppm) |
|---|---|---|---|
| 2R-2, 140–145 | 6.90 | 2.4 | 0.7 |
| 3R-2, 0–5 | 15.00 | 2.5 | 0.8 |
| 8R-1, 128–130 | 62.28 | 2.7 | 1.9 |
| 9R-1, 123–125 | 71.73 | 4.4 | 1.1 |
| 10R-1, 148–150 | 81.48 | 3.9 | 0.9 |
| 12R-1, 149–150 | 100.49 | 3.0 | 0.6 |
| 14R-1, 60–61 | 118.60 | 4.4 | 0.3 |
| 15R-1, 149–150 | 128.99 | 2.4 | 0.7 |
| 16R-2, 119–120 | 139.69 | 2.7 | 0.7 |

**Table 7. Sedimentary calcium carbonate in Hole 698A.**

| Sample (core, section, cm) | Depth (mbsf) | $CaCO_3$ (%) |
|---|---|---|
| 2R-1, 100–102 | 5.00 | 95.08 |
| 2R-2, 100–102 | 6.50 | 95.66 |
| 3R-1, 70–72 | 14.20 | 87.49 |
| 4R-1, 130–132 | 24.30 | 94.33 |
| 5R-1, 100–102 | 33.50 | 93.57 |
| 5R-2, 110–112 | 35.10 | 90.74 |
| 6R-1, 100–102 | 43.00 | 90.99 |
| 6R-2, 80–82 | 44.30 | 89.49 |
| 6R-3, 10–12 | 44.90 | 96.24 |
| 8R-1, 70–72 | 61.70 | 95.91 |
| 8R-2, 20–22 | 62.50 | 93.66 |
| 9R-1, 100–102 | 71.50 | 88.92 |
| 9R-2, 100–102 | 73.00 | 93.24 |
| 10R-1, 100–102 | 81.00 | 92.74 |
| 12R-1, 100–102 | 100.00 | 88.07 |
| 14R-1, 55–57 | 118.55 | 91.24 |
| 15R-1, 60–62 | 128.10 | 90.49 |
| 16R-1, 96–98 | 137.96 | 93.41 |
| 16R-2, 103–105 | 139.53 | 89.32 |
| 17R-1, 103–105 | 147.53 | 76.31 |
| 17R-2, 100–102 | 149.00 | 94.41 |
| 20R-1, 76–78 | 175.76 | 79.90 |
| 21R-1, 41–43 | 181.41 | 84.73 |

in the nannofossil ooze (5–46.6 mbsf), from 1.68 to 2.23 km/s in the chalk (42–146.5 mbsf), and from 2.28 to 2.38 km/s in the limestone (146.5–190.5 mbsf). *P*-wave velocity in the underlying basalts ranges from 4.2 to 5.3 km/s, which is similar to measurements in Layer 2B of the oceanic crust. A velocity of 1.8 km/s is observed in the intercalated hematite-rich clay.

The results of thermal-conductivity measurements are listed in Table 14. Thermal conductivity shows highly variable values between 0.6 and 2.3 W/m/K (Fig. 29). Because of the brittle and broken nature of the rotary-cored material, good contact between the needle probe and the sediment was not always possible. Thus, some measurements yielded erroneous values, (e.g., at 40 mbsf), which may only indicate changes in the disturbance of sediments. For this reason, we attempted no further detailed interpretation.

## SEISMIC STRATIGRAPHY

The seismic data aquisition system was streamed on approach of the *JOIDES Resolution* about 7 nmi from the site (Fig. 30). The location of Site 698 was chosen from a single-channel seismic profile (*Islas Orcadas* cruise 0775; 2200 hr, 25 November 1975) acquired with an air gun source (Fig. 31). On the first pass the beacon was dropped 3 nmi from the eastern perimeter of the main ridge of the Northeast Georgia Rise, where the estimated sediment thickness was 200 m (Fig. 30). The hull-mounted, 3.5-kHz high-resolution echo-sounder gave no penetration in the vicinity of the site. A 14-nmi tie-line to seismic lines collected by *Polar Duke* was recorded during departure from the site.

At Site 698, two seismic reflectors of regional extent are observed above acoustic basement, and there is clear evidence of internal acoustic layering below the basement interface (Figs. 31 and 32). In the upper sediments, a 5%–10% increase in porosity within the nannofossil ooze at 35 mbsf is associated with a reflection. The seismic velocity of the nannofossil ooze is nearly constant in the upper 75 mbsf and increases at the level where the lithification gradient is at its highest (100–125 mbsf). This occurs at the transition from nannofossil chalk to micrite, rather than at the chalk/limestone boundary (146.5 mbsf) defined by the lithostratigraphy of this site. A reflection event is associated with this velocity increase (Fig. 31). *P*-wave velocities show a linear increase in the limestone, but we have no representative value in the lowest part of the section where thin chert layers become abundant.

The deepest continuous reflection at Site 698 is close to acoustic basement, but diverges from basement toward the southwest and south (Fig. 31). Intervening reflection events show conformity with this reflector and no clear indication of progradational events above basement. We therefore consider the deepest continuous reflection to be related to an increase in the occurrence of chert layers in the limestone, as seen in Core 114-698A-21R, rather than to the interface between the limestone and basal sandy mud (Fig. 32). This implies that the sandy mud is most likely only a few meters thick. The transition between the limestone and the sandy mud would be associated with a wave-phase polarity reversal that cannot be properly evaluated because of the data quality. The TWTs of an assumed 25-m-thick chert-rich limestone layer (181–204 mbsf) and a 5-m-thick sandy mud (204–209 mbsf) would be 13 ms.

The highest velocities (4.2–5.3 km/s) are found in the basalt and are comparable to that of Layer 2B of the oceanic crust. The recovery of a low-velocity (1.8 km/s) regolith of weathered basalt and hematite-rich sediments below an approximately 10-m-thick layer of flow basalt verifies the acoustic layering of basement. Basement below Site 698 shows acoustic layering in the upper 500 m, and a southwest-dipping deep reflector is observed at a depth of ~1.5 km (assuming v = 4.0 km/s) below the southwest end of the line in Figure 30. Intrabasement reflectors with slight north and westward components of dip are observed over most parts of the ridge where basement is smooth except at basement culminations. An easterly dip would be expected from progressive loading of the volcanic layers at a spreading center migrating eastward with respect to the rise. The abundance of heavily oxidized iron minerals and presence of clay are a strong argument for subaerial exposure of the ridge sometime in the pre-Campanian.

The data collected by *JOIDES Resolution* upon leaving the site enables an unambiguous seismic tie between the drill site and the thickest stratigraphic section on the western ridge (Figs. 30 and 31). The seismic stratigraphy of the section above the level sampled at Site 698 on the western ridge of the Northeast Georgia Rise shows acoustically well-bedded sequences with two significant unconformities. By correlation with neighboring sites on Maurice Ewing Bank (Site 329) and Sites 513 and 514 to the northeast, we tentatively relate these to earliest Miocene–late Miocene and late Miocene events, respectively. Enhanced bottom circulation resulting from opening of the Drake Passage created an early Miocene to late Miocene hiatus at Site 513 (Ciesielski and Weaver, 1983). The late Miocene unconformity is related to a more vigorous Antarctic Circumpolar Current connected with steepening of the latitudinal thermal gradient with the expansion of the East and West Antarctic ice sheets.

In the post-Campanian, the topography of the rise was draped by deposition of pelagic sediments until sometime before the

**Table 8. Hole 698A NRM directions and intensities.**

| Interval (core, section, cm) | Depth (mbsf) | Size ($cm^3$) | Size Type | NRM Declination | NRM Inclination | Intensity (mA/m) | Circular standard deviation |
|---|---|---|---|---|---|---|---|
| 5R-2, 22-24 | 34.23 | 7 | Box | 263 | -31 | 0.249 | 15.8 |
| 5R-2, 99-101 | 35.00 | 10 | Plug | 348 | -72 | 2.234 | 2.2 |
| 6R-1, 9-11 | 42.10 | 10 | Plug | 39 | 58 | 1.30 | 8.0 |
| 6R-1, 81-83 | 42.82 | 10 | Plug | 243 | 18 | 0.234 | 18.2 |
| 6R-2, 74-76 | 44.25 | 10 | Plug | 155 | -61 | 0.106 | 20.0 |
| 8R-1, 114-116 | 62.15 | 10 | Plug | 5 | -71 | 0.023 | 43.1 |
| 8R-2, 28-30 | 62.79 | 10 | Plug | 91 | -71 | 0.258 | — |
| 9R-1, 23-25 | 70.74 | 10 | Plug | 132 | -42 | 0.387 | 6.3 |
| 9R-1, 65-67 | 71.16 | 10 | Plug | 7 | -72 | 0.426 | 6.3 |
| 9R-2, 51-53 | 72.52 | 10 | Plug | 163 | 41 | 0.176 | 16.3 |
| 9R-2, 117-119 | 73.18 | 7 | Box | 220 | -18 | 0.113 | 21.6 |
| 10R-1, 40-42 | 80.41 | 10 | Plug | 232 | 58 | 0.112 | 16.8 |
| 10R-1, 137-139 | 81.38 | 10 | Plug | 3 | 71 | 0.060 | 13.7 |
| 10R-2, 8-10 | 81.59 | 10 | Plug | 106 | 40 | 0.318 | 20.1 |
| 10R-2, 132-134 | 82.83 | 7 | Box | 160 | -20 | 0.088 | 52.1 |
| 12R-1, 54-56 | 99.55 | 7 | Box | 165 | 58 | 0.186 | 38.4 |
| 12R-1, 145-147 | 100.46 | 7 | Box | 249 | -57 | 0.459 | 17.2 |
| 14R-1, 11-13 | 118.12 | 7 | Box | 145 | -54 | 0.357 | 10.5 |
| 15R-1, 98-100 | 128.49 | 7 | Box | 88 | 0 | 0.046 | 67.5 |
| 16R-1, 98-100 | 137.99 | 7 | Box | 341 | 62 | 0.213 | 20.6 |
| 16R-2, 16-18 | 138.67 | 7 | Box | 189 | 75 | 0.272 | 19 |
| 17R-1, 106-108 | 147.57 | 7 | Box | 127 | -55 | 0.184 | 22 |
| 21R-1, 43-45 | 181.44 | 7 | Box | 322 | -53 | 0.961 | 4.3 |

**Table 9. Hole 698A mean susceptibility values.**

| Interval (core, section, cm) | Mean susceptibility ($\times 10^{-12}$ SI units) | Standard deviation on on arithmetic mean | Number of samples | Notes |
|---|---|---|---|---|
| 2R-1, 20-40 | 551.7 | 236.3 | 3 | Dropstones |
| 2R-1, 50-170 | 28.9 | 20.1 | 13 | |
| 3R-1, 10-140 | 2.5 | 1.2 | 14 | |
| 4R-1, 10 | 46.5 | - | 1 | Dropstones |
| 4R-1, 12-140 | 1.3 | 3.8 | 13 | |
| 9R-1, 10-110 | 36.5 | 10.0 | 11 | |
| 9R-2, 10-140 | 31.4 | 15.1 | 14 | |
| [a]9R-2, 10-140 | 28.9 | 15.1 | 14 | |
| 10R-1, 10-140 | 10.0 | 33.9 | 14 | |
| [a]10R-1, 10-140 | 6.3 | 32.7 | 27 | |
| 10R-2, 10-130 | 1.3 | 2.5 | 25 | |
| 12R-1, 20-40 | 658.6 | 604.5 | 3 | |
| 12R-1, 50-140 | 22.6 | 7.5 | 10 | |
| [a]12R-1, 15-40 | 747.8 | 585.7 | 6 | |
| [a]12R-1, 45-135 | 25.1 | 10.0 | 19 | |
| 15R-1, 10-145 | 2.5 | 3.8 | 28 | |
| [a]15R-1, 5-145 | 2.5 | 3.8 | 29 | |
| 16R-1, 10-140 | 6.3 | 8.8 | 27 | |
| [a]16R-1, 10-140 | 3.8 | 10.0 | 27 | |
| 16R-2, 10-115 | 2.5 | 3.8 | 22 | |
| 16R-3, 10-35 | 6.3 | 2.5 | 6 | |
| 17R-1, 30-140 | 6.3 | 20.1 | 23 | |
| 17R-2, 10-145 | 3.8 | 3.8 | 28 | |
| 25R-3, 10-140 | 17343.8 | 3493.9 | 27 | Basalt |
| 26R-1, 10-25 | 12679.5 | 705.0 | 4 | Basalt |
| 26R-1, 30-105 | 14991.7 | 4210.0 | 16 | Regolith |
| 27R-4, 10-145 | 15921.6 | 1843.7 | 28 | |
| 27R-5, 10-145 | 17982.5 | 1998.0 | 28 | |

[a] Repeat measurement.

**Table 10. Index properties, Hole 698A.**

| Sample (core, section, cm) | Depth (mbsf) | Water content (%) | Porosity (%) | Wet-bulk density ($g/cm^3$) | Grain density ($g/cm^3$) |
|---|---|---|---|---|---|
| 2R-1, 100 | 5.0 | 34.67 | 59.40 | 1.76 | 2.69 |
| 2R-2, 100 | 6.5 | 34.20 | 58.50 | 1.75 | 2.70 |
| 3R-1, 70 | 14.2 | 38.37 | 65.35 | 1.74 | 2.84 |
| 4R-1, 130 | 24.3 | 32.16 | 56.04 | 1.79 | 2.76 |
| 5R-1, 100 | 33.5 | 32.26 | 56.54 | 1.80 | 2.66 |
| 5R-2, 110 | 35.1 | 38.30 | 63.09 | 1.69 | 2.76 |
| 6R-1, 100 | 43.0 | 34.87 | 60.90 | 1.79 | 2.81 |
| 6R-2, 80 | 44.3 | 29.68 | 53.72 | 1.85 | 2.70 |
| 6R-3, 10 | 46.5 | 30.73 | 54.88 | 1.83 | 2.68 |
| 8R-1, 70 | 61.7 | 29.79 | 53.81 | 1.85 | 2.72 |
| 8R-2, 20 | 62.7 | 30.92 | 55.61 | 1.84 | 2.73 |
| 9R-1, 100 | 71.5 | 27.18 | 50.00 | 1.88 | 2.71 |
| 9R-2, 100 | 73.0 | 28.29 | 51.66 | 1.87 | 2.69 |
| 10R-1, 100 | 81.0 | 27.82 | 51.07 | 1.88 | 2.66 |
| 10R-2, 100 | 82.5 | 37.35 | 61.54 | 1.69 | 2.68 |
| 12R-1, 100 | 100.0 | 27.91 | 51.86 | 1.90 | 2.69 |
| 14R-1, 55 | 118.5 | 27.25 | 51.14 | 1.92 | 2.71 |
| 16R-1, 96 | 137.9 | 22.33 | 44.79 | 2.06 | 2.75 |
| 16R-2, 103 | 139.5 | 24.05 | 45.77 | 1.95 | 2.64 |
| 17R-1, 103 | 147.5 | 20.89 | 43.12 | 2.12 | 2.66 |
| 17R-2, 100 | 149.0 | 25.69 | 49.38 | 1.97 | 2.68 |
| 20R-1, 76 | 175.7 | 18.19 | 39.04 | 2.20 | 2.71 |
| 21R-1, 41 | 181.4 | 19.22 | 39.53 | 2.11 | 2.67 |
| 24R-1, 93 | 210.4 | 4.45 | 12.26 | 2.83 | 3.10 |
| 24R-2, 90 | 211.9 | 8.47 | 23.09 | 2.79 | 3.00 |
| 25R-2, 90 | 215.9 | 2.31 | 6.58 | 2.92 | 2.93 |
| 25R-3, 22 | 218.2 | 4.11 | 13.29 | 3.32 | 3.29 |
| 26R-1, 70 | 219.7 | 33.39 | 63.15 | 1.94 | 3.47 |
| 26R-1, 72 | 219.8 | 38.02 | 69.19 | 1.86 | 3.36 |
| 27R-1, 45 | 228.9 | 31.29 | 60.38 | 1.98 | 3.14 |
| 27R-3, 78 | 232.2 | 27.28 | 53.72 | 2.02 | 3.11 |
| 27R-4, 100 | 234.0 | 27.48 | 53.15 | 1.98 | 2.92 |
| 27R-5, 100 | 235.5 | 43.83 | 69.17 | 1.62 | 2.99 |
| 27R-6, 30 | 236.3 | 58.70 | 80.04 | 1.40 | 2.82 |
| 27R, CC (10) | 236.9 | 23.60 | 46.76 | 2.03 | 2.80 |

early Miocene, for which syntectonic deposition is clearly evidenced. The entire sedimentary section has been downfaulted into a half-graben (Fig. 2) by a major north-trending fault and a parallel minor fault cutting obliquely across the western perimeter of the Northeast Georgia Rise. Vertical displacement on the main fault is over 1 km.

## SUMMARY AND CONCLUSIONS

Site 698 lies near the eastern edge of the shallowest portion of the Northeast Georgia Rise, at 51°27.51′S, 33°05.96′W, in a water depth of 2128 mbsl. The morphology of the rise is characterized by a 400-km-long and 100-km-wide north-northwest-trending arcuate main ridge (shallowest water depth 1538 m) in the west, separated by a saddle from a smaller 150-km-long north-striking ridge (minimum water depth 2540 m) that confines the rise to the east.

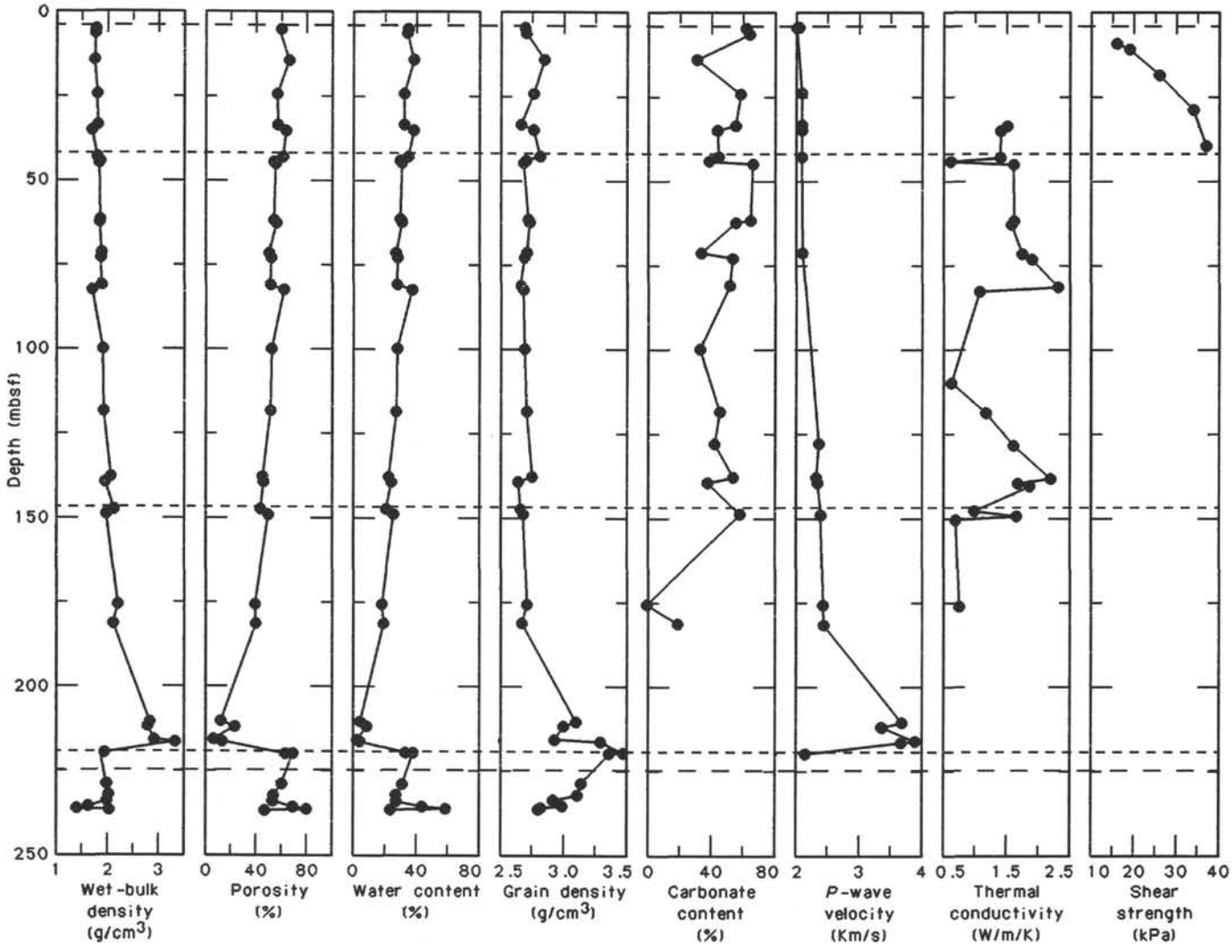


Figure 29. Wet-bulk density, porosity, water content, grain density, carbonate content, *P*-wave velocity (solid dots = *P*-wave logger), thermal conductivity, and shear strength profiles, Hole 698A.

The primary objectives of this site focused on the origin and tectonic history of the rise, that is, the nature, age, and subsidence history of basement, in order to establish

1. The possible role of Northeast Georgia Rise as a Late Cretaceous–early Tertiary convergent boundary between the Malvinas plate and the South American plate
2. Any temporal relationship between subduction at the Northeast Georgia Rise and the southern Andean Orogeny.

These objectives are also important for evaluating the influence of the Northeast Georgia Rise, other regional plateaus, and ridges as Late Cretaceous–Paleogene obstructions to deep-water interchange between the Weddell and South Atlantic basins.

Seismic-reflection data show that the main (western) ridge of the Northeast Georgia Rise is capped by sediments up to 1 s (TWT) thick, with largely conformable internal layering cut by erosional truncation at the ridge perimeter. The sedimentary section on the western side of the ridge has been subjected to a major tectonic event with vertical displacement on the order of 1 km.

Early departure from port and rapid transit resulted in net gain of 2.3 days of operational time, which permitted drilling of this lower priority site. A single hole was rotary drilled (to ensure basement penetration in the time available) in 2 days and 9 hr, from 17 to 19 March 1987. Hole 698A consists of 27 cores to a depth of 237 mbsf with 22% recovery. Low recovery was often related to the occurrence of stringers of chert. Drilling conditions were excellent. Drilling terminated 27.6 m into basement because of time limitations.

Site 698 consists of a surficial, residual lag deposit of ice-rafted detritus above a thick, pelagic carbonate sequence of nannofossil ooze of early Eocene age, overlying nannofossil chalk and a basal limestone of early Eocene to Campanian-Maestrichtian age. Frequent chert stringers and nodules occur throughout the carbonate section. A sandy mud, separated from the underlying basement by a 9.4-m recovery gap and from the overlying limestone by a 16.4-m recovery gap, may represent a transgressive sand incorporating some eroded weathered basalt. Sparse nannofossils in the sandy mud, if *in situ*, suggest a Campanian age. Basement consists of a sparsely phyric, holocrystalline basalt, trachytic to subtrachytic basalt, and ferro(?)basalt overlying a hematite-rich regolith.

**Table 11. Carbonate content, Hole 698A.**

| Sample (core, section, cm) | Depth (mbsf) | Carbonate content (%) |
|---|---|---|
| 2R-1, 100–102 | 5.0 | 95.08 |
| 2R-2, 100–102 | 6.5 | 95.66 |
| 3R-1, 70–72 | 14.2 | 87.49 |
| 4R-1, 130–132 | 24.3 | 94.33 |
| 5R-1, 100–102 | 33.5 | 93.57 |
| 5R-2, 110–112 | 35.1 | 90.74 |
| 6R-1, 100–102 | 43.0 | 90.99 |
| 6R-2, 80–82 | 44.3 | 89.49 |
| 6R-3, 10–12 | 45.1 | 96.24 |
| 8R-1, 70–72 | 61.7 | 95.91 |
| 8R-2, 20–22 | 62.7 | 93.66 |
| 9R-1, 100–102 | 71.5 | 88.32 |
| 9R-2, 100–102 | 73.0 | 93.24 |
| 10R-1, 100–102 | 81.0 | 92.74 |
| 12R-1, 100–102 | 100.0 | 88.07 |
| 14R-1, 55–57 | 118.5 | 91.24 |
| 15R-1, 60–62 | 128.1 | 90.49 |
| 16R-1, 96–98 | 137.9 | 93.41 |
| 16R-2, 103–105 | 139.5 | 89.32 |
| 17R-2, 100–102 | 149.0 | 94.41 |
| 20R-1, 76–78 | 175.7 | 79.90 |
| 21R-1, 41–43 | 181.4 | 84.73 |

**Table 12. Shear strength, Hole 698A.**

| Sample (core, section, cm) | Depth (mbsf) | Shear strength (kPa) |
|---|---|---|
| 2R-1, 100 | 5.0 | 16.0 |
| 2R-2, 100 | 6.5 | 19.0 |
| 3R-1, 70 | 14.2 | 26.0 |
| 4R-1, 130 | 24.3 | 34.0 |
| 5R-2, 110 | 35.1 | 37.0 |

**Table 13. *P*-wave velocity, Hole 698A.**

| Sample (core, section, cm) | Depth (mbsf) | *P*-wave velocity (m/s) | Lithology |
|---|---|---|---|
| 2R-1, 50 | 4.5 | 1580.00 | |
| 2R-1, 100 | 5.0 | 1520.00 | |
| 4R-1, 100 | 24.0 | 1680.00 | Ooze |
| 5R-1, 100 | 33.5 | 1680.00 | |
| 5R-2, 100 | 35.0 | 1680.00 | |
| 6R-1, 100 | 43.0 | 1680.00 | |
| 9R-1, 100 | 71.5 | 1700.0 | |
| 15R-1, 60 | 128.1 | 2223.04 | Chalk |
| 16R-1, 96 | 137.9 | 2143.28 | |
| 16R-2, 103 | 139.5 | 2187.21 | |
| 17R-2, 100 | 149.0 | 2280.04 | |
| 20R-1, 76 | 175.7 | 2347.76 | Limestone |
| 21R-1, 41 | 181.4 | 2377.63 | |
| 24R-1, 93 | 210.4 | 4845.43 | |
| 24R-2, 90 | 211.5 | 4198.00 | |
| 24R-2, 90 | 211.5 | 4220.00 | Basalt |
| 25R-2, 90 | 214.4 | 5275.00 | |
| 25R-3, 22 | 216.7 | 4822.22 | |
| 26R-1, 72 | 219.7 | 1797.50 | Hematite clay |

The sequence at Site 698 was divided into three units based upon compositional differences and diagenetic maturity.

Unit I consists of a 35-cm residual-lag gravel deposit recovered between the seafloor and 25 mbsf. It is interpreted as winnowed ice-rafted detritus of mixed rock types (predominantly sandstone and gneiss) and is inferred to be of early Pliocene–Quaternary age. The unit also contains cherts fragments from the underlying unit, which are imbedded in it.

Unit II extends from 4.25 to 190.5 mbsf and is composed of a sequence of pelagic carbonate that exhibits progressive diagenetic maturity with depth. The calcareous component consists almost entirely of calcareous nannofossils; foraminifers are consistently present as a minor component. Subunits were defined on the basis of diagenetic maturity. Subunit IIA (4.25–42.0 mbsf) is a foraminifer-bearing nannofossil ooze of late early Eocene to possibly earliest middle Eocene age. Foraminifer-bearing chalk, of Maestrichtian to early Eocene age, comprises Subunit IIB (42.0–146.5 mbsf). The lower part of Unit II (Subunit IIC, 146.5–190.5 mbsf) is a very-fine-grained limestone of Campanian age.

Unit III extends from 200 mbsf to the base of the hole at 237 mbsf and is separated from Unit II by a 16.4-m gap in core recovery. Unit III includes basement and two other subunits that are partially or totally derived from basement. Subunit IIIA (200–200.15 mbsf) is a sandy mud with clasts of highly weathered basalt that is no younger than Campanian. A 9.4-m unrecovered interval separates Subunit IIIA from the basalt of Subunit IIIB (209.5–219.28 mbsf). This subunit consists of sparsely phyric, holocrystalline basalt (Core 114-698A-24R), trachytic to subtrachytic basalt, ferro(?)basalt (Core 114-698A-25R), and variable amounts of alteration products. At the base of Hole 698A is Subunit IIIC (219.28–237 mbsf), a reddish brown, extremely weathered basalt (regolith) in which the Fe-Mg minerals have been completely altered to hematite.

Units I and III are barren of microfossils, except for the presence of diatoms and radiolarians in Unit I and sparse calcareous nannofossils within the sandy mud of Subunit IIIA. Within the Upper Cretaceous–lower Paleogene sequence of Unit II, calcareous nannofossils are the dominant microfossil constituents. Planktonic and benthic foraminifers consistently occur as the most common minor constituents. Calcispherulids occur throughout the Upper Cretaceous, occasionally becoming common to abundant. Siliceous microfossils are a significant component of the overall microfossil assemblage only in portions of the lower Paleogene, most notably in the upper Paleocene. Calcareous nannofossils are poorly to moderately well preserved. Planktonic and benthic foraminifers are abundant throughout Unit II, with moderate to good preservation of planktonics and good preservation of benthics. Little evidence of downhole contamination or sediment redeposition was noted from the foraminifer and calcareous nannofossil assemblages. The occurrence of radiolarians is sporadic; however, in the Paleocene they are common to abundant and preservation is good. Occurrences of diatoms in the Paleocene and Eocene are sparse and reveal signs of intensive dissolution. Common to abundant and moderately well-preserved diatoms do occur, however, in the upper Paleocene. Other siliceous microfossil groups, the silicoflagellates and ebridians, also exhibit their best preservation and greatest abundance in the upper Paleocene.

## Seismic and Tectonic Interpretation

A major part of the western ridge of Northeast Georgia Rise has generally smooth basement with indication of sub-basement acoustic layering, except at and in the vicinity of basement culminations. At Site 698 the acoustic layering results from the large impedance contrast between partially altered basalt flows, which have a minimum thickness of 8.8 m, overlying a more than 17.7-m-thick low-velocity layer of highly weathered (subaerially?) basalt regolith. Acoustic layering is observed to at least 500 m below the sediment/basement interface at Site 698, extending to a depth of 1.5 km about 14 nmi southwest of the

**Table 14. Thermal conductivity data, Hole 698A.**

| Sample (core section, cm) | Depth (mbsf) | Thermal conductivity (W/m/K) |
|---|---|---|
| 5R-1, 100 | 33.5 | 1.503 |
| 5R-2, 100 | 35.0 | 1.400 |
| 6R-1, 100 | 43.0 | 1.395 |
| 6R-2, 80 | 44.3 | 0.615 |
| 6R-3, 12 | 45.1 | 1.610 |
| 8R-1, 70 | 61.7 | 1.614 |
| 8R-2, 20 | 62.7 | 1.578 |
| 9R-1, 100 | 71.5 | 1.748 |
| 9R-2, 100 | 73.0 | 1.902 |
| 10R-1, 100 | 81.0 | 2.314 |
| 10R-2, 100 | 82.5 | 1.069 |
| 12R-1, 100 | 109.5 | 0.626 |
| 14R-1, 55 | 118.5 | 1.169 |
| 15R-1, 60 | 128.1 | 1.610 |
| 16R-1, 100 | 138.0 | 2.196 |
| 16R-2, 100 | 139.5 | 1.673 |
| 16R-3, 20 | 140.2 | 1.865 |
| 17R-1, 100 | 147.5 | 0.989 |
| 17R-2, 100 | 149.0 | 1.653 |
| 17R-3, 8 | 150.3 | 0.696 |
| 20R-1, 70 | 175.7 | 0.751 |

site. Intrabasement reflectors show small components of westward and northward dip, whereas an easterly dip would be expected from progressive loading of the volcanic layers at a spreading center migrating eastward with respect to the rise.

Correlation of lithology and physical properties with the seismic stratigraphy shows the physical significance of the following regional seismic marker horizons (Fig. 33):

1. The deepest continuous reflection above basement is probably related to a dramatic increase in the abundance of thin chert layers within the deepest part of the limestone (mid-Maestrichtian to Campanian), as seen in Core 114-698A-21R.
2. A velocity increase associated with increasing micrite within the lower Paleocene nannofossil chalk gives rise to a distinct reflection.
3. The ooze/chalk transition within the lower Eocene is associated with a 10% excursion in wet-bulk density and a seismic-reflection event.

The section below the deepest seismic stratigraphic marker, related to an increased abundance of chert (at the base of the limestone), thickens slightly to the southwest from Site 698 and pinches out toward the basement high south of the site. The Northeast Georgia Rise may have been completely submerged in less than 10 m.y. following deposition of the Campanian sandy mud at Site 698, assuming an initial subsidence rate similar to that of oceanic crust generated at a spreading center. By the Paleocene, lower bathyal depths (1500 mbsl ± 500 m) had developed at Site 698. In post-mid-Maestrichtian to Campanian time, the topography of the rise was draped by deposition of pelagic sediments until sometime during the late Miocene, after which there is clear evidence in the seismic records of syntectonic sedimentation. The entire sedimentary section has been downfaulted into a half-graben by a major north-trending fault, and a parallel minor fault, cutting obliquely across the western perimeter of the Northeast Georgia Rise. Displacement on the westernmost major fault is over 1 km.

LaBrecque and Hayes (1979) proposed that the Northeast Georgia Rise originated as a locus of intraplate deformation during the Campanian through Paleocene by clockwise rotation of the Malvinas plate with respect to the Falkland block. The Late Cretaceous and Paleogene depositional environment at Site 698 was that of a quiet pelagic realm with purely biogenic input. Any major tectonic event related to incipient subduction must therefore be pre-Campanian in age. Faulting along the western perimeter of Northeast Georgia Rise is tentatively assigned a late Miocene age and is likely to be related to interaction with the advance of the South Georgia block in response to seafloor spreading in the Scotia Sea. This deformational event may be responsible for the post-eruptive veining and mineralization of the basalt in Subunit IIIB.

## Environmental History of Site 698

Basement, lithostratigraphic, and faunal and floral characteristics of Hole 698A document a varied history of the Northeast Georgia Rise, including Late Cretaceous subaerial exposure and subsidence into an open-ocean pelagic environment. The continuity of Campanian-early Paleogene pelagic carbonate sedimentation at Site 698 contrasts greatly with contemporaneous deep-water terrigenous sedimentation at Site 328 in the West Georgia Basin and reflects the mode of terrigenous sediment transport into basinal areas adjacent to the South American margin.

Portions of the Northeast Georgia Rise, particularly the western basement high, apparently were above sea level during implacement of part of the upper volcanic sequence. The basalts of Subunit IIIB are not typical submarine eruptives and appear more like subaerial flows (M. Perfit, pers. comm., 1988). Further evidence is found in Subunit IIIC, an extremely weathered basalt regolith (>17 m thick) underlying the basalt of Subunit IIIB. XRD analyses of five samples from this regolith reveal it to be almost entirely hematite. The hematite was probably produced by total oxidation of the Fe-Mg minerals of the original basalt, which survives as rare altered clasts within the hematite. A similar composition for the weathered basalt and the regolith is also indicated by their similar magnetic susceptibilities. The intensive chemical weathering, and other characteristics exhibited by this unit, suggest formation in a tropical climate on a surface of low relief favoring the retention of local weathering products.

The age for the initial subsidence of the Northeast Georgia Rise is problematic because of a 9.4-m gap in recovery above the basalt of Subunit IIIB. A sandy mud (Subunit IIIA) between 200.0 and 200.15 mbsf is the oldest sediment above basement and may represent the only recovered portion of a transgressive facies formed during the initial subsidence of the Northeast Georgia Rise. Rare calcareous nannofossils in this unit suggest an age no older than Campanian; however, the nannofossils occur in chalk fragments that may represent downhole contamination.

Benthic foraminifers found in the base of the Upper Cretaceous-lower Paleogene pelagic carbonate sequence of Unit II (16.4 m above the sandy mud of Subunit IIIA) are indicative of lower bathyal depths (1500 mbsl ± 500 m). By the Maestrichtian, the Northeast Georgia Rise probably had subsided to at least half its present water depth. Major subsidence of the Falkland Plateau and Maurice Ewing Bank occurred during the late Albian-Cenomanian. Site 700 contains a more complete Cretaceous sedimentary record for comparison of the subsidence histories of these regional bathymetric highs (see "Site 700" chapter, this volume) (Sliter, 1977; Ludwig, Krasheninikov, et al., 1983).

A relatively uninterrupted sequence of pelagic carbonate accumulated on the Northeast Georgia Rise during the Campanian/Maestrichtian though early Eocene. Accumulation of nannofossil ooze may have been nearly continuous across the Cretaceous/Tertiary boundary. Unfortunately, the Cretaceous/Tertiary boundary occurs in an unrecovered interval between Section 114-698A-13R, CC, and Sample 114-698A-14R, 1 cm (108.6–

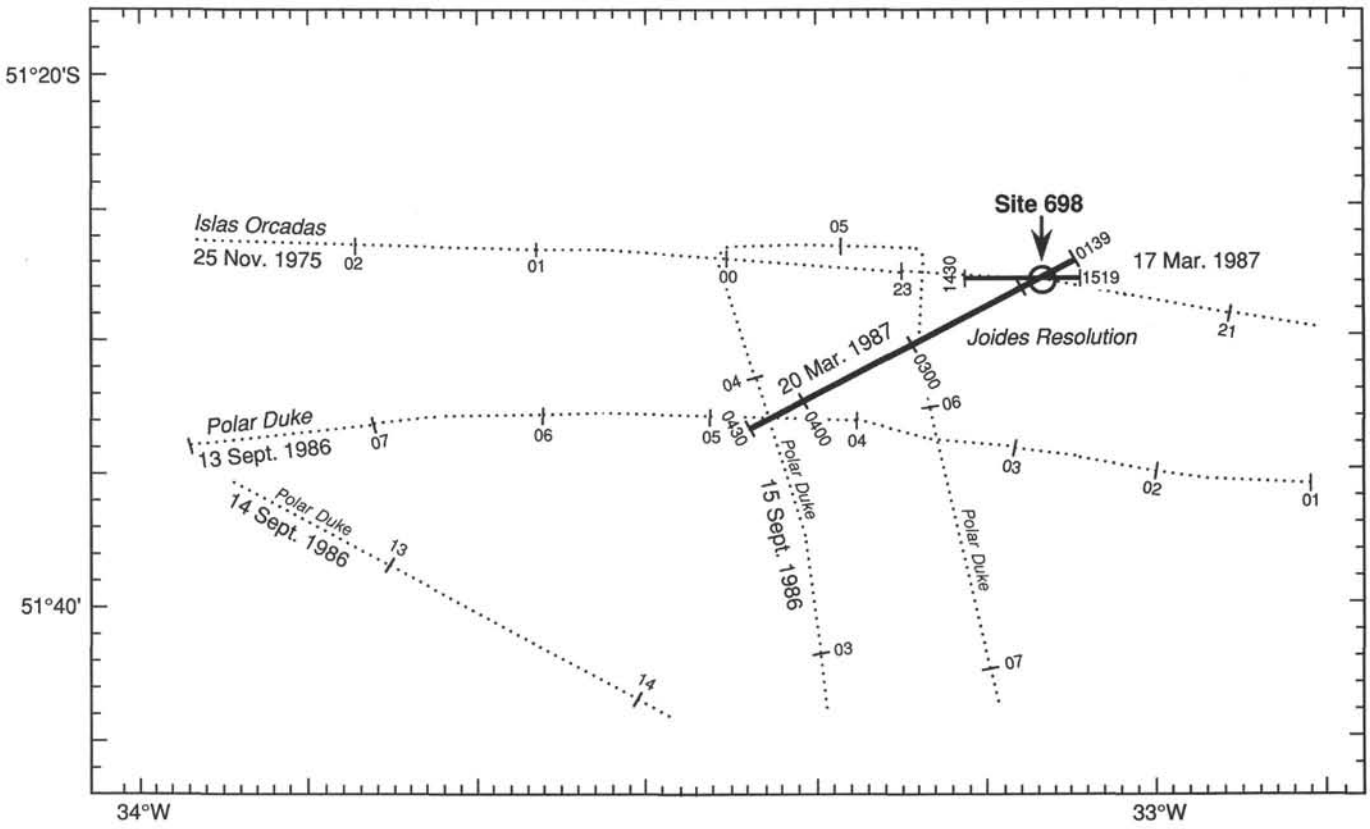


Figure 30. Location of single-channel seismic lines in the vicinity of Site 698 on the western ridge of Northeast Georgia Rise. *JOIDES Resolution* track shown by heavy line.

118 mbsf); however, planktonic foraminifers and calcareous nannofossils bracketing the recovery gap are late Maestrichtian and Danian (planktonic foraminifer P16 Zone) in age. The consistent presence of foraminifers and calcareous nannofossils and their state of preservation indicate that Site 698 remained above the lysocline throughout the Late Cretaceous and early Paleogene.

Site 698 was characterized by a relatively stable depositional and oceanographic environment from the Late Cretaceous to early Paleogene. Surface waters were well oxygenated, allowing for a steady but modest rain of calcareous microfossils to a seafloor removed from terrigenous sedimentary influence (< 10%). Sedimentation rates appear low (4–5 m/m.y.) for the Late Cretaceous and average 8 m/m.y. during the Paleogene–early Eocene, suggesting relatively low surface-water productivity.

Sediment characteristics and the ichnological community therein reveal a low-energy Late Cretaceous to early Paleogene benthic environment that periodically experienced oxygen-reduced conditions. Weak benthic circulation is indicated by the lack of current-produced structures, little to no microfossil reworking, and a varied and consistently present ichnological community. Suboxic conditions occurred episodically, leading to well-developed ichnological communities of *Planolites, Cylindrichnus, Zoophycos*, and *Chrondrites*. Greatly reduced oxygen levels are not indicated for this interval by interstitial-water sulfur content.

Late Cretaceous planktonic foraminifers in Hole 698A are extratropical in character. Strong similarities exist between Northeast Georgia Rise assemblages and those from the Falkland Plateau and New Zealand, and they are are indicative of the austral province of Sliter (1977). Low- to midlatitude globotruncanids were not observed in the upper Maestrichtian; however, *Globotruncana, Rosita*, and other representatives of warm-water provinces were present prior to late Maestrichtian deposition. This mixture of warm-water and austral assemblages in the high latitudes of the southwest Atlantic suggests an influence of Pacific and lower latitude surface waters. Although the Drake Passage was not yet open, an influx of Pacific (austral assemblage) surface waters would be expected through the unglaciated basins of West Antarctica, which was probably an archipelego with a shallow seaway during the Late Cretaceous (Ciesielski et al., 1982). Warmer water constituents of the Late Cretaceous age assemblage were probably associated with the southern limb of a large South Atlantic gyre that mixed with the cooler waters from the Pacific.

Small and smooth planktonic foraminifers occur in Danian sediments of Hole 698A. Such assemblages are widespread in the lower Paleocene and are inferred to represent stressed faunas. Cooler water planktonic foraminifers (e.g., *Catapsydrax*) occur in the lower Eocene; however, the presence of discoasters and sphenoliths suggests that surface waters at Site 698 remained relatively warm through the early Paleogene.

The only significant occurrence of siliceous microfossils in Hole 698A is in the upper Paleocene (NP5–9). Abundant and diverse assemblages of diatoms, silicoflagellates, radiolarians, and ebridians are found in the nannofossil chalk of this age. Elsewhere in the South Atlantic rich siliceous microfossil assemblages are also known from the Paleocene of the Falkland Plateau (Gombos, 1977), Cape Basin (Gombos, 1984), southeastern Indian Ocean (Murkhina, 1976), and Central Pacific (Leinen, 1979). With the exception of the North Atlantic, the upper Paleocene represents the first known widespread siliceous productivity and may represent increased local upwelling resulting from strong vertical mixing of surface-water masses. Late Pa-

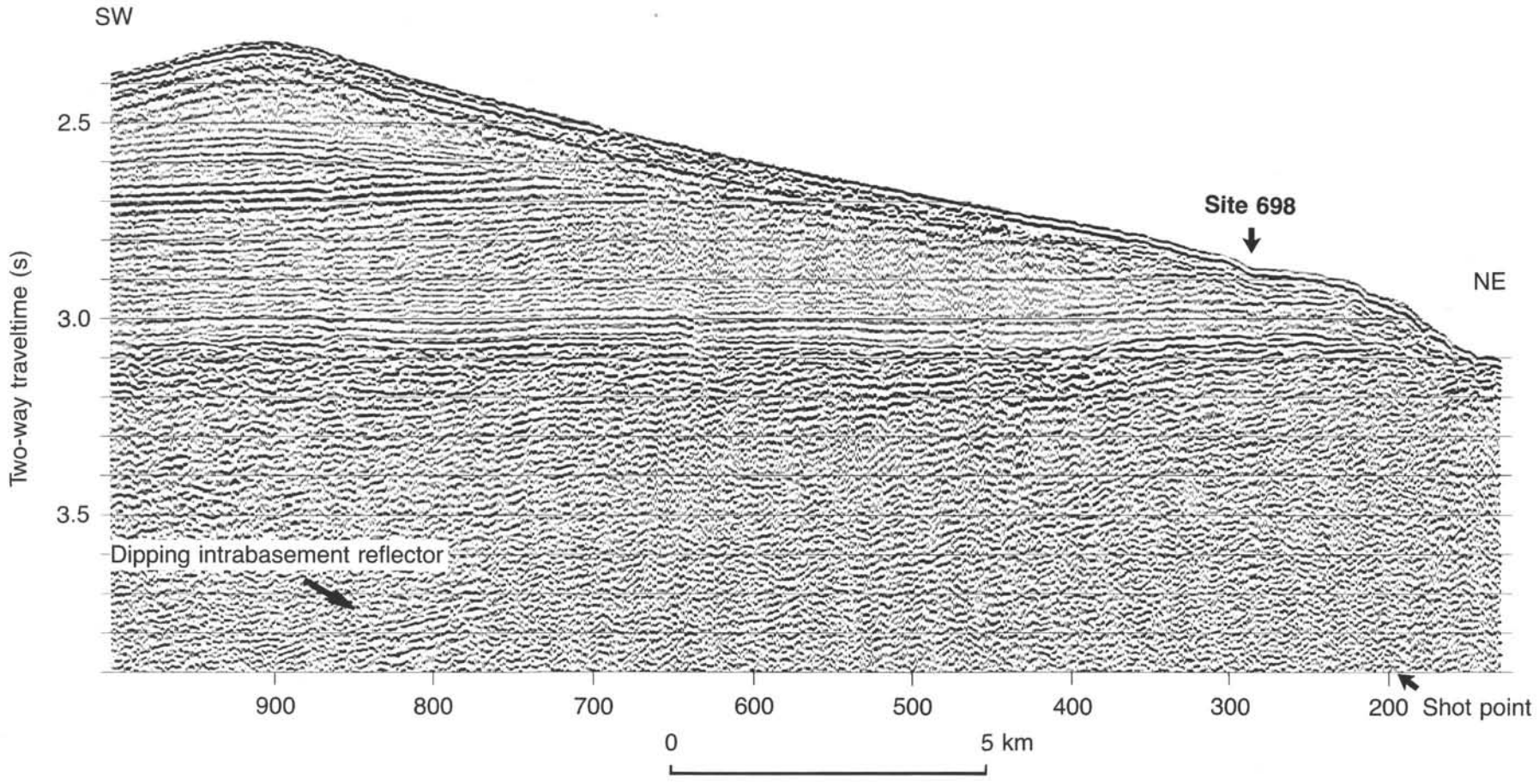


Figure 31. *JOIDES Resolution* single-channel seismic profile (northeast-southwest) recorded as tie-line through Site 698 on the Northeast Georgia Rise. Profile location shown in Figure 31. The signal-to-noise ratio of the data has been improved by trace mixing for cancellation of random noise, filtering, and pulse shaping by deconvolution.

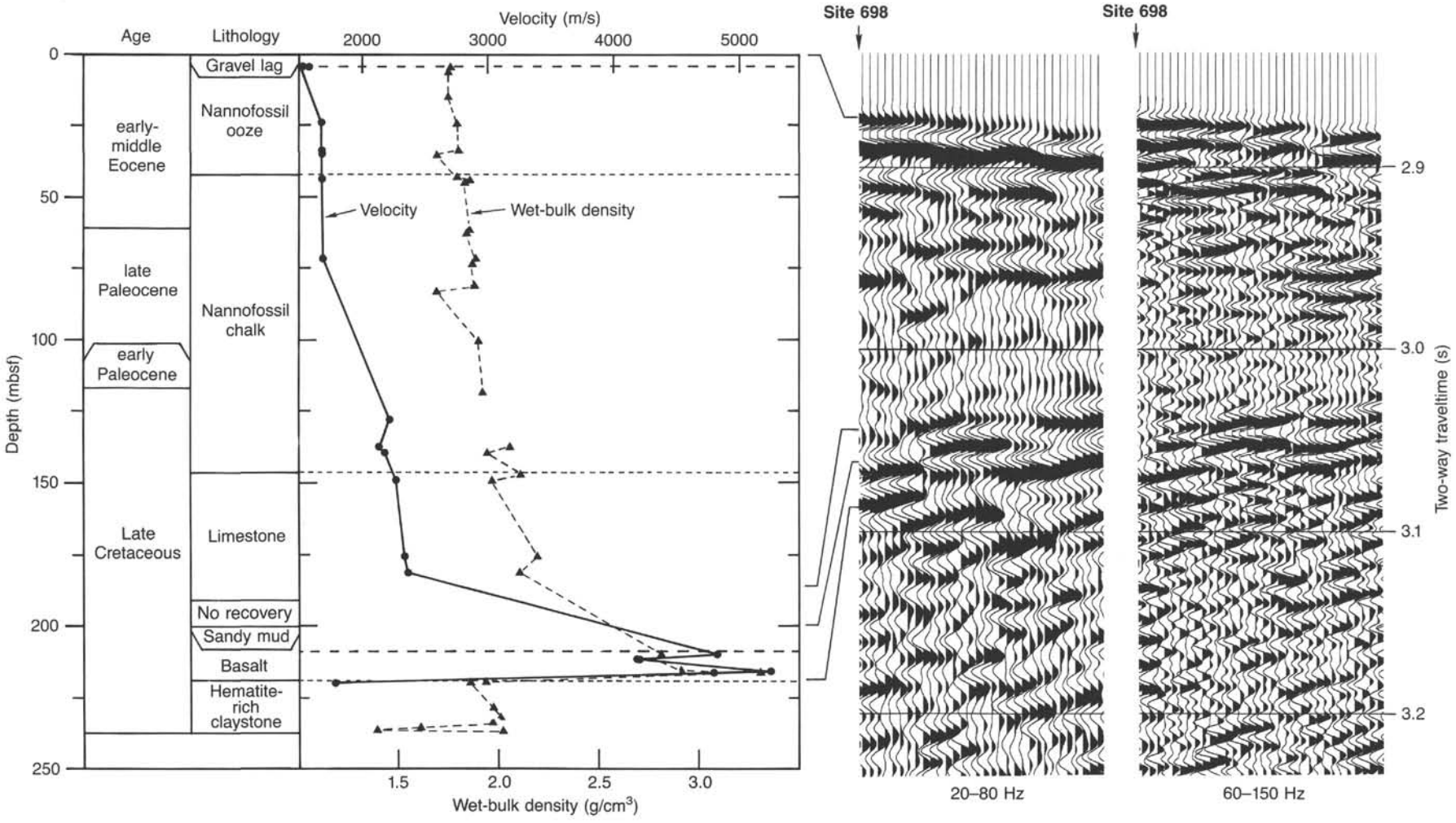


Figure 32. Summary of age (from "Biostratigraphy" section), lithology (from "Lithostratigraphy" section), and physical properties (from "Physical Properties" section) of Site 698 correlated with seismic-reflection profile (west-east) obtained by *JOIDES Resolution* on approach to the site. Profile location shown in Figure 31.

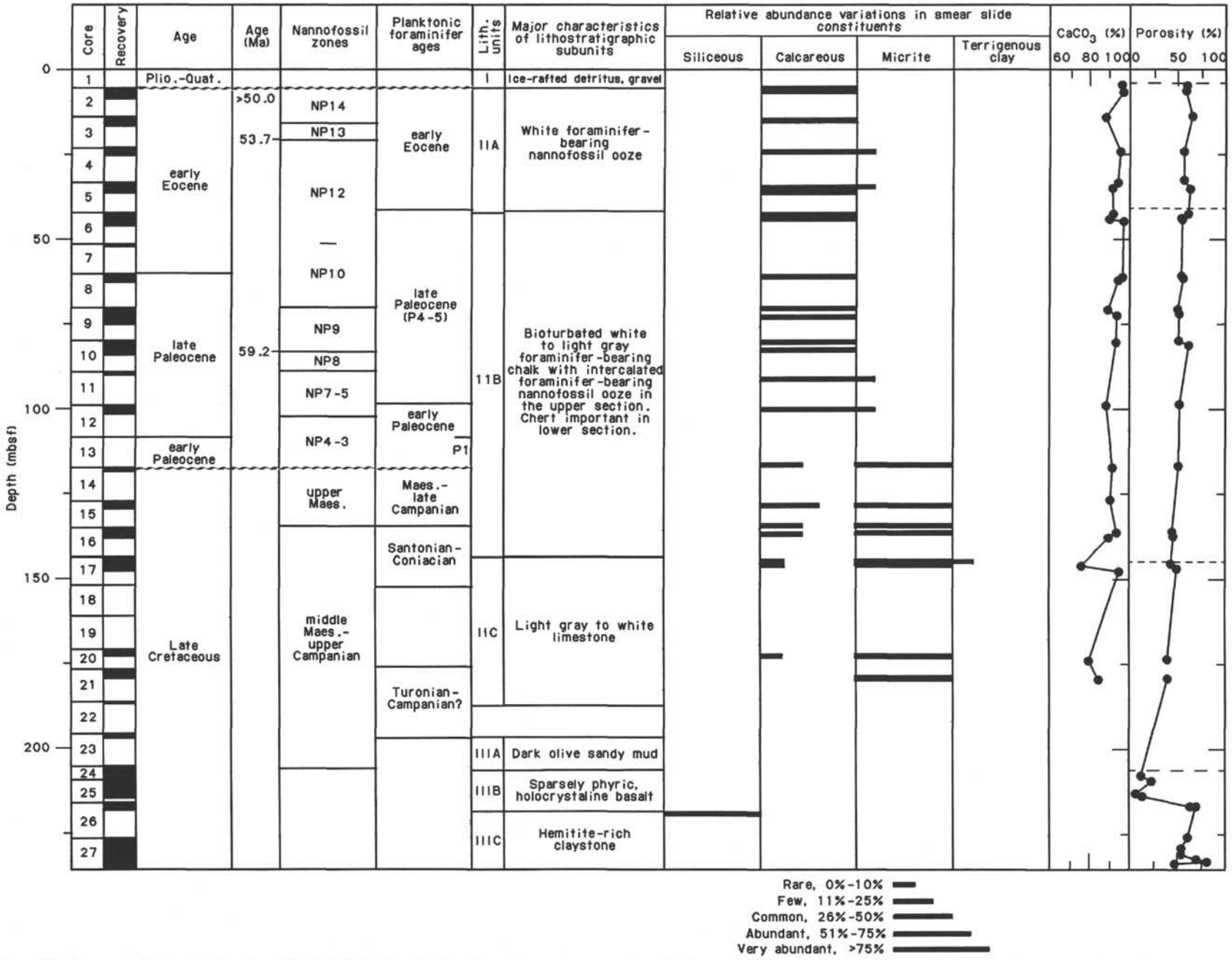


Figure 33. Summary of selected data from Site 698, including depth, sediment recovery, age, selected paleontological zones or ages, lithostratigraphic units and subunits and a description of their major characteristics, variation in smear slide constituents, % $CaCO_3$, and porosity.

leocene siliceous productivity on the Northeast Georgia Rise suggests a possible continuous zone of siliceous productivity extending across the South Atlantic from the Falkland Plateau to the Cape Basin. Such a belt of siliceous productivity is evidence for stronger latitudinal thermal contrast and surface-water mixing than is evident from the Upper Cretaceous and lower Paleocene.

The Late Cretaceous to early Paleogene depositional environment at Site 698 (2128 mbsl, present depth) differed greatly from contemporaneous sedimentation at DSDP Site 328 (5103 mbsl, present depth) in the West Georgia Basin. The Upper Cretaceous to upper Eocene sequence at Site 328, near the northwest margin of the Northeast Georgia Rise, consists entirely of zeolitic clay and zeolitic claystone almost completely devoid of biogenic constituents. What could be the possible explanation for this striking contrast between terrigenous sedimentation at Site 328 and biogenic sedimentation at Site 698, which are only 265 km from one another? A probable answer to this question can be gleaned from a comparison of contemporaneous sedimentary records of regional basins and rises with the tectonic history of the continental margins.

The Andean Cordillera and adjacent Deseado Massif, the West Antarctic Cordillera, and the African craton are possible sources for terrigenous input into southwest Atlantic basins during the Late Cretaceous and early Paleogene. Of these, an African source seems least likely because the Falkland-Agulhas Fracture Zone forms a significant barrier to transport to the site from this source (Barker, Dalziel, et al., 1977; Shipboard Scientific Party, 1977). A more likely source would be the young southern Andean Cordillera, which underwent its main deformation and initial uplift during the late Albian–Cenomanian (Dalziel et al., 1974). A further extension of this highland source would have continued eastward from the southern Andean Cordillera along the western North Scotia Ridge (prior to ridge extension), where the South Georgia block was positioned at that time (Dalziel et al., 1975).

Terrigenous sediment derived from the high Late Cretaceous borderland had easy access to the basin to the east through the deepened Magallanes Basin (>1500 m; Natland et al., 1974) and contiguous Falkland Trough (Fig. 34). Thick accumulations of Upper Cretaceous terrigenous sediments that occur in the Magallanes Basin and in the Falkland Basin (Ludwig, 1983) are without doubt from an Andean Cordillera source. The thick zeolitic clays and claystones at West Georgia Basin Site 328 were probably also derived from this highland and transported to the basin through the Falkland Trough.

Upper Cretaceous sediment on the Northeast Georgia Rise and on the Maurice Ewing Bank is much more pelagic than in the surrounding basins where terrigenous sedimentation predominates. Cretaceous claystones thin from the Falkland Basin onto the Maurice Ewing Bank, where they grade updip into mixed facies of clay and biosiliceous-calcareous pelagic sediments of Late Cretaceous to Eocene age (Shipboard Scientific Party, 1977). On the shallow part of the Northeast Georgia Rise (Site 698) the terrigenous component in Campanian–lower Paleogene sediments is negligible (<10%). These regional differences in facies between basins and rises suggest that the probable mode of terrigenous transport was within a nepheloid layer that was confined to basinal environments and the lower flanks of adjacent rises. During the Late Cretaceous–early Paleogene, Site 698 remained above the zone of nepheloid transport, accumulating nannofossil-rich pelagic sediments.

Because of the low vertical temperature gradient (3°–4°C) and the apparent absence of significant antarctic ice at sea level during this period, strong thermohaline-driven benthic circulation was unlikely. Bottom currents dispersing clays from the adjacent cordillera were most likely driven by density gradients provided by the large volume of terrigenous sediment.

A thick sedimentary sequence upslope from Site 698 was not drilled because of time limitations for drilling at this site. Seismic correlation of the top of the Eocene nannofossil ooze at Site 698 to thicker sections on the Northeast Georgia Rise indicates up to 600 m of post-lower middle Eocene sediments. Several major erosional events are noted in this sequence, which may represent major paleoceanographic events (Figs. 2 and 3). The age of erosional episodes may be inferred in the future by comparisons of the seismic records of the Northeast Georgia Rise with those of Maurice Ewing Bank, Site 699, and other Leg 114 sites on the Islas Orcadas Rise and Meteor Rise.

Unit I consists of 10 cm of gravel derived from the upper 4 m of sediment. This unit overlies the lower Paleogene nannofossil ooze and probably represents a surface sediment residual lag of ice-rafted detritus. Numerous piston cores taken on the Northeast Georgia Rise by Ciesielski and Weaver (1983) (Figs. 3 and 4) all recovered Pliocene to Quaternary age sediment rich in ice-rafted detritus. The condensed Pliocene-Quaternary section of these piston cores (<6 m) and the abundance of coarse ice-rafted detritus within the cores suggest that the Northeast Georgia Rise is covered by a winnowed lag of ice-rafted detritus similar to that found on the Maurice Ewing Bank (Ciesielski and Wise, 1977; Ciesielski et al., 1982). By the late Pliocene, the lag of ice-rafted detritus on the Northeast Georgia Rise, as on the Maurice Ewing Bank, had probably produced a clastic veneer over the pelagic sediment cover, "armoring" the pelagic drape from subsequent erosion. The formation of this residual ice-rafted detrital lag deposit is a testimony to the late Neogene increase in circum-Antarctic circulation.

## REFERENCES


Barker, P., Dalziel, I.W.D., et al., 1977. *Init. Repts. DSDP*, 36: Washington (U.S. Govt. Printing Offfice).

Barker, P. F., Kennett, J. P., et al., 1988. *Proc. ODP, Init. Repts.*, 113: College Station, TX (Ocean Drilling Program).

Barron, J. A., Keller, G., and Dunn, D. A., 1985. A multiple microfossil biochronology for the Miocene. *Geol. Soc. Am. Mem.*, 163:21–36.

Berggren, W. A., Kent, D. V., and Flynn, J. J., 1985. Jurassic to Paleogene: Part 2. Paleogene geochronology and chronostratigraphy. *In* Snelling, N. J. (Ed.), *The Chronology of the Geological Record*: Geol. Soc. London Mem., 10:141–195.

Blow, W. H. 1979. *The Cainozoic Globigerinida*: Leiden (E. J. Brill).

Bromley, R. G., and Ekdale, A. A., 1984. *Chondrites*: a trace fossil indicator of anoxia in sediments. *Science*, 224:872–874.

Busen, K. E., and Wise, S. W., Jr., 1977. Silicoflagellate stratigraphy, Deep Sea Drilling Project, Leg 36. *In* Barker, P., Dalziel, I.W.D., et al., *Init. Repts. DSDP*, 36: Washington (U.S. Govt. Printing Office), 697–743.

Caron, M., 1985. Cretaceous planktic foraminifera. *In* Bolli, H. M., Saunders, J. B., and Perch-Nielsen, K. (Eds.), *Plankton Stratigraphy*: Cambridge (Cambridge Univ. Press), 17–86.

Ciesielski, P. F., 1985. Middle Pliocene to Quaternary diatom biostratigraphy of Deep Sea Drilling Project Site 594, Chatham Rise, Southwest Pacific. *In* Kennett, J. P., von der Burch, C. C., et al., *Init. Repts., DSDP*, 90: Washington (U.S. Govt Printing Office), 863–885.

Ciesielski, P. F., Ledbetter, M. T., and Brooks, B. B., 1982. The development of Antarctic glaciation and the Neogene paleoenvironment of the Maurice Ewing Bank. *Mar. Geol.*, 46:1–51.

Ciesielski, P. F., and Weaver, F. M., 1983. Neogene and Quaternary paleoenvironmental history of Deep Sea Drilling Project Leg 71 sediments, southwest Atlantic Ocean. *In* Ludwig, W. J., Krasheninnikov, V. A., et al., *Init. Repts. DSDP*, 71: Washington (U.S. Govt. Printing Office), 461–477.

Ciesielski, P. F., and Wise, S. W., Jr., 1977. Geologic history of the Maurice Ewing Bank of the Falkland Plateau (southwest Atlantic sector of the Southern Ocean) based on piston and drill cores. *Mar. Geol.*, 25:175–207.

Crux, J. A., 1982. Upper Cretaceous (Cenomanian to Campanian) calcareous nannofossils. *In* Lord, A. R. (Ed.), *A Stratigraphical Index of Calcareous Nannofossils*: Chichester (Ellis Horwood), 81–135.

Dalziel, I.W.D., Caminos, R., Palmer, K. F., Nullo, F., and Casanova, R., 1974. Southern extremity of the Andes: the geology of Isla de los Estados, Argentine Tierra del Fuego. *AAPG Bull.*, 58:2502–2512.

Dalziel, I.W.D., Dott, R. H., Winn, R. D., and Bruhn, R. L., 1975. Tectonic relations of South Georgia Island to the southernmost Andes. *Geol. Soc. Am. Bull.*, 86:1034–1040.

Dumitrica, P., 1973. Paleogene radiolaria, DSDP Leg 21. *In* Burns, R. E., Andrews, J. E., et al., *Init. Repts. DSDP*, 21: Washington (U.S. Govt. Printing Office), 787–818.

Edwards, A. R., 1973. Calcareous nannofossils from the southwest Pacific. *In* Burns, R. E., Andrews, J. E., et al., *Init. Repts. DSDP*, 21: Washington (U.S. Govt. Printing Office), 641–691.

Gombos, A. M., 1977. Paleogene and Neogene diatoms from the Falkland Plateau and Malvinas Outer Basin: Leg 36 Deep Sea Drilling Project. *In* Barker, P., Dalziel, I.W.D., et al., *Init. Repts. DSDP*, 36: Washington (U.S. Govt. Printing Office), 575–602.

_____, 1984. Late Paleocene diatoms in the Cape Basin. *In* Hsü, K. J., LaBrecque, J. L., et al., *Init. Repts. DSDP*, 73: Washington (U.S. Govt. Printing Office), 495–511.

Gordon, A. L., 1971. Oceanography of Antarctic waters. *Antarct. Res. Ser.*, 15:169–203.

Hallam, A., Hancock, J. M., LaBrecque, J. L., Lowrie, W., and Channell, J.E.T., 1985. Jurassic to Paleogene: Part 1. Jurassic and Cretaceous geochronology and Jurassic to Paleogene magnetostratigraphy. *In* Snelling, N. J. (Ed.), *The Chronology of the Geological Record*: Geol. Soc. London Mem., 10:118–140.

Jenkins, D. G., 1985. Southern mid-latitude Paleocene to Holocene planktic foraminifera. *In* Bolli, H. M., Saunders, J. B., and Perch-Nielsen, K. (Eds.), *Plankton Stratigraphy*: Cambridge (Cambridge Univ. Press), 263–282.

Kennett, J. P., 1978. The development of planktonic biogeography in the Southern Ocean during the Cenozoic. *Mar. Micropaleontol.*, 3: 301–345.

Kent, D. V., and Gradstein, F., 1985. A Creatceous and Jurassic geochronology. *Geol. Soc. Am. Bull.*, 96:1419–1427.

La Brecque, J. L. (Ed.), 1986. *South Atlantic Ocean and Adjacent Continental Margin Atlas 13*: Ocean Margin Drilling Program Reg. Atlas Ser., 13.

LaBrecque, J. L., and Hayes, D. E., 1979. Seafloor spreading in the Agulhas Basin. *Earth Planet. Sci. Lett.*, 45:411–428.

Ladd, J. W., 1974. South Atlantic seafloor spreading and Caribbean tectonics [Ph.D. Thesis]. Columbia Univ., New York.

Leinen, M., 1979. Biogenic silica accumulation in the central Equatorial Pacific and its implications for Cenozoic paleoceanography. *Geol. Soc. Am. Bull.*, 90:1310–1376.

Ludwig, W. J., 1983. Geologic framework of the Falkland Plateau. *In* Ludwig, W. J., Krasheninnikov, V. A., et al., *Init. Repts. DSDP*, 71: Washington (U.S. Govt. Printing Office), 281–303.

Ludwig, W. J., Krasheninnikov, V. A., et al., 1983. *Init. Repts. DSDP*, 71: Washington (U.S. Govt. Printing Office).

Martini, E., 1971. Standard Tertiary and Quaternary calcareous nannoplankton zonation. *In* Farinacci, A. (Ed.), *Proc. Planktonic Conf. II Rome 1970*, Rome (Technoscienza), 2:739–785.

Mead, G. A., 1982. Taxonomy and distribution of deep-sea calcareous benthic foraminifera of the Polar Front region in the southern Southwest Atlantic Ocean [M.S. Thesis]. Univ. of Rhode Island.

Mukhina, V. V., 1976. Species composition of the late Paleocene diatoms and silicoflagellates in the Indian Ocean. *Micropaleontology*, 22:151–158.

Natland, M. L., Gonzalez, E., Canon, A., and Ernst, M., 1974. A system of stages for correlation of Magallanes Basin sediments. *Geol. Soc. Am. Mem.*, 139:1–126

Perch-Nielsen, K., 1985. Cenozoic calcareous nannofossils. *In* Bolli, H. M., Saunders, J. B., and Perch-Nielsen, K. (Eds.), *Plankton Stratigraphy*: Cambridge (Cambridge Univ. Press), 427–554.

Sanfilippo, A., Westberg-Smith, M. J., and Riedel, W. R., 1985. Cenozoic radiolaria. *In* Bolli, H. M., Saunders, J. B., and Perch-Nielsen, K. (Eds.), *Plankton Stratigraphy*: Cambridge (Cambridge Univ. Press), 631–712.

Shipboard Scientific Party, 1977. Evolution of the southwestern Atlantic Ocean Basin: results of Leg 36, Deep Sea Drilling Project. *In* Barker, P., Dalziel, I.W.D., et al., *Init. Repts. DSDP*, 36: Washington (U.S. Govt. Printing Office), 993–1014.

Sissingh, W., 1977. Biostratigraphy of Cretaceous calcareous nannoplankton. *Geol. Mijnbouw*, 56:37–65.

Sliter, W. V., 1977. Cretaceous foraminifers from the southwestern Atlantic Ocean, Leg 36, Deep Sea Drilling Project. *In* Barker, P., Dalziel, I.W.D., et al., *Init. Repts. DSDP*, 36: Washington (U.S. Govt. Printing Office), 519–573.

Westberg-Smith, M. J., and Riedel, W. R., 1984. Radiolarians from the western margin of the Rockall Plateau: Deep Sea Drilling Project Leg 81. *In* Roberts, D. G., Schnitker, D., et al., *Init. Repts. DSDP*, 81: Washington (U.S. Govt. Printing Office), 479–501.

Wise, S. W., Jr., and Weaver, F. M., 1974. Chertification of oceanic sediments. *In* Hsü, K. J., and Jenkyns, H. C. (Eds.), *Pelagic Sediments: on Land and under the Sea*: Spec. Publ. Int. Assoc. Sedimentol., 1: 301–326.

Wise, S. W., and Wind, F. H., 1977. Mesozoic and Cenozoic calcareous nannofossils recovered by DSDP Leg 36 drilling on the Falkland Plateau, southwest Atlantic Ocean. *In* Barker, P., Dalziel, I.W.D., et al., *Init. Repts. DSDP*, 36: Washington (U.S. Govt. Printing Office), 269–492.

Worsley, T., and Martini, E., 1970. Late Maestrichtian nannoplankton provinces. *Nature*, 225:1242–1243.

**Ms 114A-105**

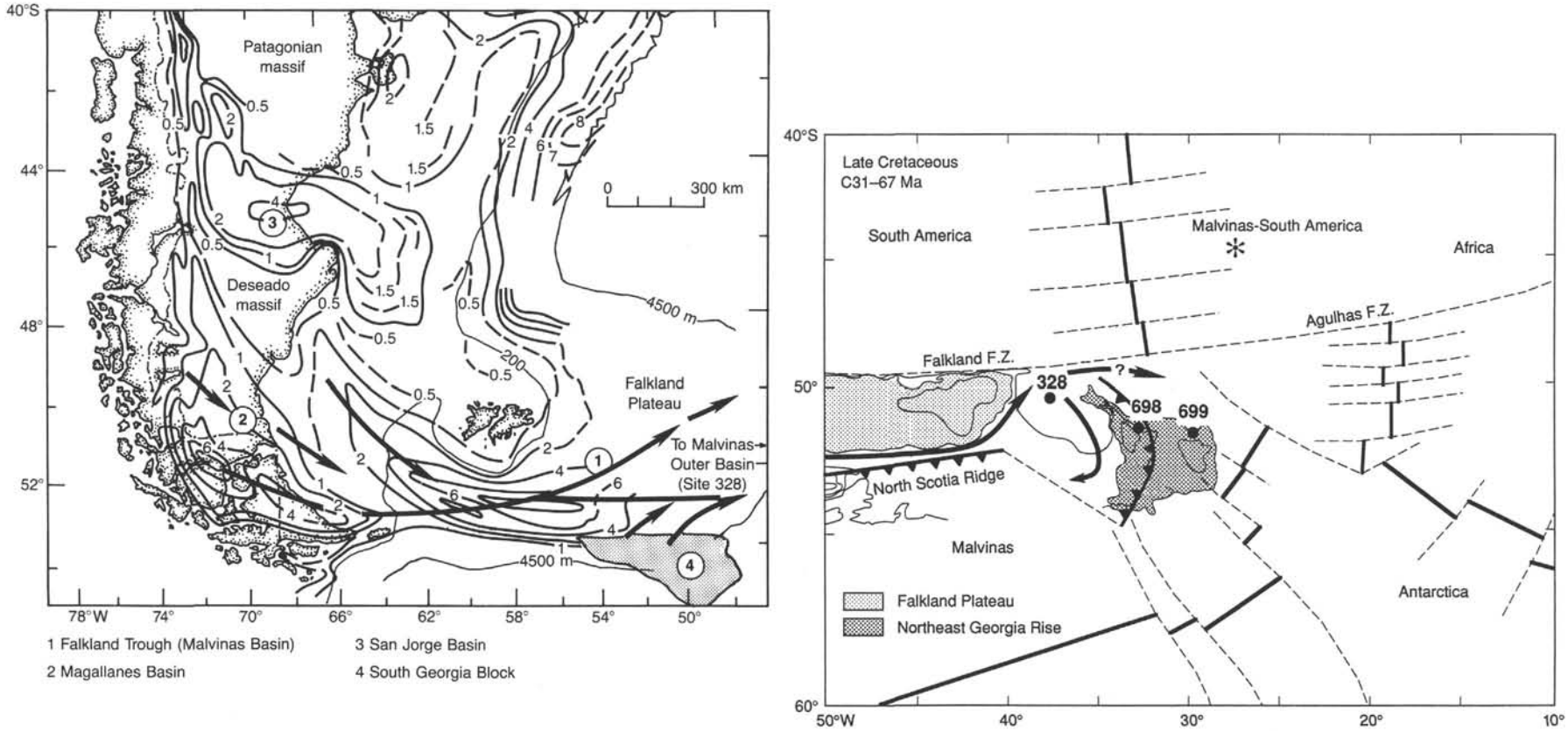


Figure 34. Dispersal routes (arrows) for terrigenous sediment supply to the Magallanes, Falkland Plateau, and West Georgia basins during the Late Cretaceous to early Paleogene. Sediment supply is mainly from the Deseado Massif, southern Andes, and South Georgia block. Isopachs in left map represent kilometers of Upper Mesozoic and Cenozoic sedimentary cover over Middle to Upper Jurassic volcanic or Paleozoic-Lower Mesozoic metamorphic-plutonic basement. Base map from Barker, Dalziel, et al., 1977.

SITE 698 HOLE A CORE 1R CORED INTERVAL 2127.5-2131.5 mbsl; 0.0-4.0 mbsf

| TIME-ROCK UNIT | BIOSTRAT. ZONE/ FOSSIL CHARACTER: FORAMINIFERS | NANNOFOSSILS | RADIOLARIANS | DIATOMS | SILICOFLAGELLATES | PALEOMAGNETICS | PHYS. PROPERTIES | CHEMISTRY | SECTION | METERS | GRAPHIC LITHOLOGY | DRILLING DISTURB. | SED. STRUCTURES | SAMPLES | LITHOLOGIC DESCRIPTION |
|---|---|---|---|---|---|---|---|---|---|---|---|---|---|---|---|
| LOWER-MIDDLE EOCENE | *M. crater* Zone (LOWER EOCENE) P9 | NP 14 | Barren | Barren | Barren | | | | CC | | | | | * | FORAMINIFER-BEARING NANNOFOSSIL OOZE |

Drilling disturbed.

Major lithology: Foraminifer-bearing nannofossil ooze, white (2.5Y N/8), disseminated within the CC.

Minor lithology: Gravel, dropstones (sandstone, gneiss), one manganese nodule, and several chert pieces.

SMEAR SLIDE SUMMARY (%):

| | CC, 10 M |
|---|---|
| COMPOSITION: | |
| Quartz | Tr |
| Mica | Tr |
| Accessory minerals | Tr |
| Zeolites | Tr |
| Foraminifers | 10 |
| Nannofossils | 89 |
| Diatoms | Tr |
| Radiolarians | Tr |
| Sponge spicules | Tr |

SITE 698 HOLE A CORE 2R CORED INTERVAL 2131.5-2140.5 mbsl; 4.0-13.5 mbsf

| TIME-ROCK UNIT | BIOSTRAT. ZONE/ FOSSIL CHARACTER: FORAMINIFERS | NANNOFOSSILS | RADIOLARIANS | DIATOMS | SILICOFLAGELLATES | PALEOMAGNETICS | PHYS. PROPERTIES | CHEMISTRY | SECTION | METERS | GRAPHIC LITHOLOGY | DRILLING DISTURB. | SED. STRUCTURES | SAMPLES | LITHOLOGIC DESCRIPTION |
|---|---|---|---|---|---|---|---|---|---|---|---|---|---|---|---|
| LOWER-MIDDLE EOCENE | *M. crater* Zone (LOWER EOCENE) P9 | NP 14 | Barren | Barren | Barren | $\phi$=58.5 $\rho_g$=2.70 | $\phi$=59.4 $\rho_g$=2.63 | | 1 | 0.5 | | | | * | NANNOFOSSIL OOZE |
| | | | | | | | | | | 1.0 | | | | * | |
| | | | | | | | | | 2 | | | | | * | |
| | | | | | | | | | 3 | | | | | IW | |
| | | | | | | | | | CC | | | | | | |

Major lithology: Nannofossil ooze, white (no color code).

Minor lithology: "Gravel" (downcore slump) in a "matrix" of ash-bearing muddy diatom ooze.

SMEAR SLIDE SUMMARY (%):

| | 1, 10 M | 1, 100 D | 2, 100 D |
|---|---|---|---|
| COMPOSITION: | | | |
| Quartz | 3 | — | — |
| Feldspar | 3 | — | Tr |
| Mica | 3 | — | — |
| Clay | 36 | — | — |
| Volcanic glass | 5 | — | — |
| Accessory minerals | 1 | — | — |
| Zeolites | — | — | Tr |
| Foraminifers | — | 5 | 5 |
| Nannofossils | — | 94 | 94 |
| Diatoms | 50 | Tr | — |
| Sponge spicules | 2 | Tr | — |

Information on Core Description Forms, for ALL sites, represents field notes taken aboard ship. Some of this information has been refined in accord with post-cruise findings, but production schedules prohibit definitive correlation of these forms with subsequent findings. Thus the reader should be alerted to the occasional ambiguity or discrepancy.

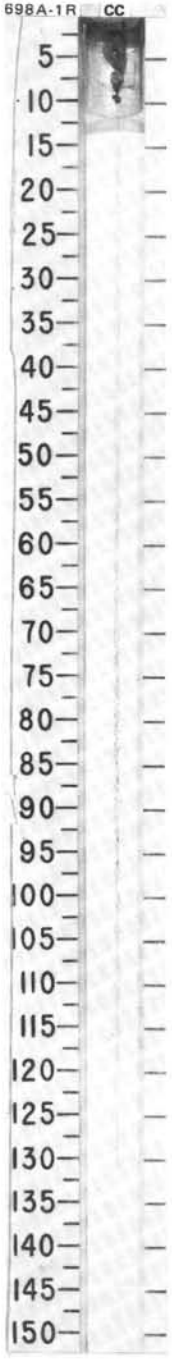


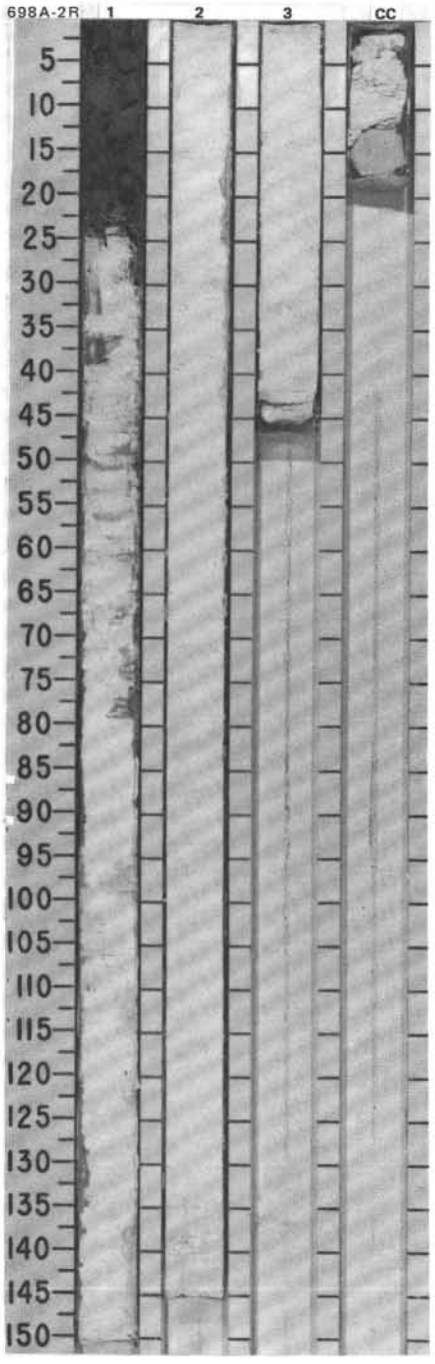

SITE 698 HOLE A CORE 3R CORED INTERVAL 2140.5-2150.5 mbsl; 13.5-23.0 mbsf

| TIME-ROCK UNIT | BIOSTRAT. ZONE/ FOSSIL CHARACTER: FORAMINIFERS | NANNOFOSSILS | RADIOLARIANS | DIATOMS | SILICOFLAGELLATES | PALEOMAGNETICS | PHYS. PROPERTIES | CHEMISTRY | SECTION | METERS | GRAPHIC LITHOLOGY | DRILLING DISTURB. | SED. STRUCTURES | SAMPLES |
|---|---|---|---|---|---|---|---|---|---|---|---|---|---|---|
| LOWER EOCENE | LOWER EOCENE P9 | NP 14 | LOWER MIDDLE EOCENE to LOWER EOCENE | LOWER MIDDLE EOCENE to LOWER EOCENE | LOWER MIDDLE EOCENE to LOWER EOCENE | [~65.35] [~2.84] | $\phi$ $\rho_g$ | | 1 | 0.5 1.0 | VOID | | | ** |
| | *M. crater* Zone (LOWER EOCENE) | NP 13 not examined | | | | | | | 2 | | | | | * |
| | | | | | | | | | CC | | | | | |

LITHOLOGIC DESCRIPTION

FORAMINIFER-BEARING NANNOFOSSIL OOZE

Major lithology: Foraminifer-bearing nannofossil ooze, white (no color code).

Minor lithology: Radiolarian- and foraminifer-bearing nannofossil ooze, light gray (5Y 7/1), in lower half of CC. Color boundary with overlying (in CC) foraminifer-bearing nannofossil ooze; sharp but uneven.

SMEAR SLIDE SUMMARY (%):

| | 1, 71 D | 1, 88 D | CC, 10 M |
|---|---|---|---|
| COMPOSITION: | | | |
| Accessory minerals | — | — | Tr |
| Foraminifers | 10 | 15 | 10 |
| Nannofossils | 90 | 85 | 80 |
| Diatoms | Tr | Tr | — |
| Radiolarians | — | Tr | 10 |
| Sponge spicules | Tr | — | Tr |
| Silicoflagellates | — | — | Tr |

SITE 698 HOLE A CORE 4R CORED INTERVAL 2150.5-2160.0 mbsl; 23.0-32.5 mbsf

| TIME-ROCK UNIT | BIOSTRAT. ZONE/ FOSSIL CHARACTER: FORAMINIFERS | NANNOFOSSILS | RADIOLARIANS | DIATOMS | SILICOFLAGELLATES | PALEOMAGNETICS | PHYS. PROPERTIES | CHEMISTRY | SECTION | METERS | GRAPHIC LITHOLOGY | DRILLING DISTURB. | SED. STRUCTURES | SAMPLES |
|---|---|---|---|---|---|---|---|---|---|---|---|---|---|---|
| LOWER EOCENE | LOWER EOCENE P9 | NP 10-12 ; not examined | Barren | Barren | Barren | [~56.04] [~2.76] | $\phi$ $\rho_g$ | | 1 | 0.5 1.0 | VOID | | | * |

LITHOLOGIC DESCRIPTION

FORAMINIFER-BEARING NANNOFOSSIL OOZE

Major lithology: Foraminifer-bearing nannofossil ooze, white (no color code) above Section 1, 87 cm. Below 87 cm, white (10YR 8/2).

Minor lithology: Chert, very pale brown (10Y 8/3) with brown spots (10YR 4/3), at 18-30 and 48 cm.

SMEAR SLIDE SUMMARY (%):

| | 1, 70 D |
|---|---|
| COMPOSITION: | |
| Feldspar | Tr |
| Foraminifers | 12 |
| Nannofossils | 88 |

SITE 698 HOLE A CORE 5R CORED INTERVAL 2160.0-2169.5 mbsl; 32.5-42.0 mbsf

| TIME-ROCK UNIT | BIOSTRAT. ZONE/ FOSSIL CHARACTER: FORAMINIFERS | NANNOFOSSILS | RADIOLARIANS | DIATOMS | SILICOFLAGELLATES | PALEOMAGNETICS | PHYS. PROPERTIES | CHEMISTRY | SECTION | METERS | GRAPHIC LITHOLOGY | DRILLING DISTURB. | SED. STRUCTURES | SAMPLES | LITHOLOGIC DESCRIPTION |
|---|---|---|---|---|---|---|---|---|---|---|---|---|---|---|---|
| LOWER EOCENE | LOWER EOCENE P9 | NP 10-12 | Barren | Barren | Barren | | $\phi$=63.09 $\rho_g$=2.76 $\phi$=56.54 $\rho_g$=2.66 | | 1 2 | 0.5 1.0 | | | | * ** | FORAMINIFER-BEARING NANNOFOSSIL OOZE |

Major lithology: Foraminifer-bearing nannofossil ooze, white (no color code).

Minor lithology: Chert, pale yellow (2.5Y 7/4). Mottled and bioturbated with *Planolites* burrows, Section 2, 51-61 and 84-101 cm.

SMEAR SLIDE SUMMARY (%):

| | 1, 80 D | 2, 92 M | 2, 95 D |
|---|---|---|---|
| COMPOSITION: | | | |
| Accessory minerals | — | Tr | — |
| Foraminifers | 10 | 5 | 10 |
| Nannofossils | 90 | 95 | 90 |

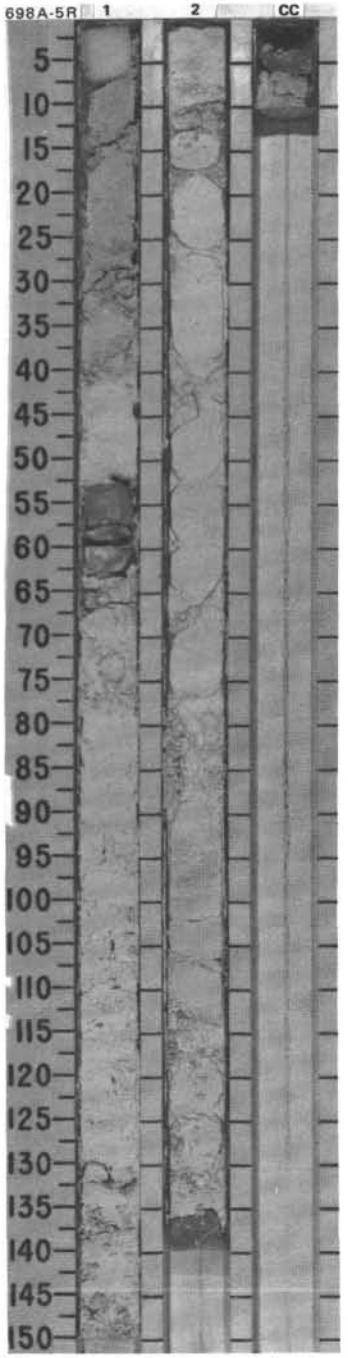

SITE 698 HOLE A CORE 6R CORED INTERVAL 2169.5-2179.0 mbsl; 42.0-51.5 mbsf

TIME-ROCK UNIT: LOWER EOCENE (LOWER EOCENE) P8 *Pseudohastigerina wilcoxensis* Zone

BIOSTRAT. ZONE/FOSSIL CHARACTER: FORAMINIFERS; NANNOFOSSILS: NP 10-12; RADIOLARIANS: Barren; DIATOMS: Barren; SILICOFLAGELLATES: Barren

PALEOMAGNETICS

PHYS. PROPERTIES: $\phi$=54.88 $\rho_g$=2.68; $\phi$=53.72 $\rho_g$=2.70; $\phi$=60.90 $\rho_g$=2.81

CHEMISTRY

SECTION: 1, 2, 3, CC

METERS: 0.5, 1.0

GRAPHIC LITHOLOGY: VOID

DRILLING DISTURB.

SED. STRUCTURES

SAMPLES

LITHOLOGIC DESCRIPTION

FORAMINIFER-BEARING NANNOFOSSIL OOZE/CHALK

Major lithology: Foraminifer-bearing nannofossil chalk, white (no color code), and ooze. Bioturbated in several thin layers.

SMEAR SLIDE SUMMARY (%):

| | 1, 51 D | 1, 52 D | 2, 82 D | 3, 10 D |
|---|---|---|---|---|
| COMPOSITION: | | | | |
| Quartz | — | — | Tr | Tr |
| Accessory minerals | Tr | Tr | — | — |
| Foraminifers | 10 | 12 | 10 | 10 |
| Nannofossils | 90 | 88 | 90 | 90 |
| Radiolarians | Tr | Tr | — | Tr |

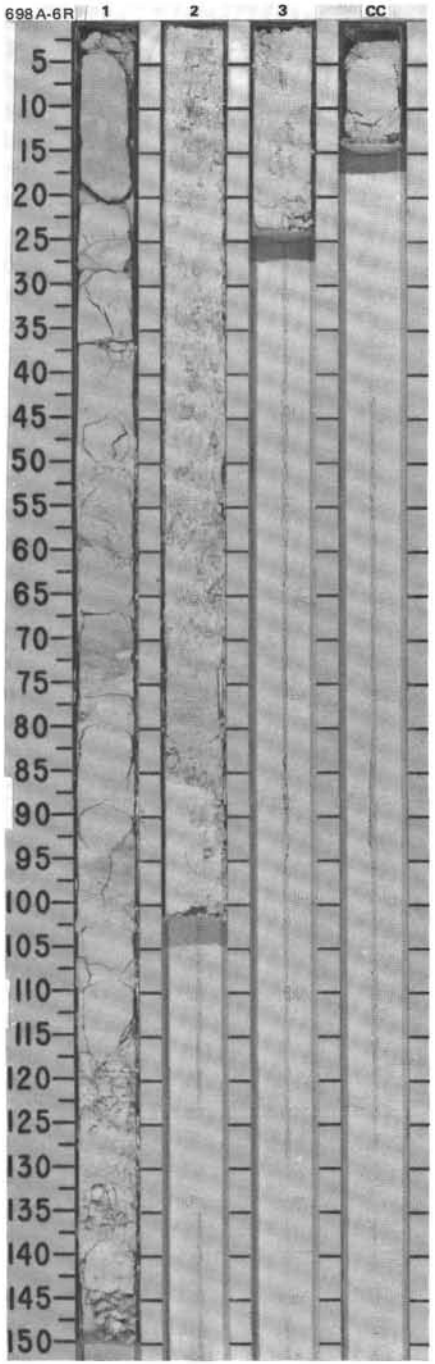

SITE 698 HOLE A CORE 7R CORED INTERVAL 2179.0-2188.5 mbsl; 51.5-61.0 mbsf

| TIME-ROCK UNIT | BIOSTRAT. ZONE/ FOSSIL CHARACTER: FORAMINIFERS | NANNOFOSSILS | RADIOLARIANS | DIATOMS | SILICOFLAGELLATES | PALEOMAGNETICS | PHYS. PROPERTIES | CHEMISTRY | SECTION | METERS | GRAPHIC LITHOLOGY | DRILLING DISTURB. | SED. STRUCTURES | SAMPLES | LITHOLOGIC DESCRIPTION |
|---|---|---|---|---|---|---|---|---|---|---|---|---|---|---|---|
| LOWER EOCENE | *P. wilcoxensis* Zone (LOWER EOCENE) P6 - P7 | NP10-12 | | Barren | Barren | | | | CC | | | | | | GRAVEL with CHERT and NANNOFOSSIL CHALK FRAGMENTS<br>Drilling disturbed.<br>Major lithology: Gravel with chert and nannofossil chalk fragments. |

SITE 698 HOLE A CORE 8R CORED INTERVAL 2188.5-2198.0 mbsl; 61.0-70.5 mbsf

| TIME-ROCK UNIT | BIOSTRAT. ZONE/ FOSSIL CHARACTER: FORAMINIFERS | NANNOFOSSILS | RADIOLARIANS | DIATOMS | PALEOMAGNETICS | PHYS. PROPERTIES | CHEMISTRY | SECTION | METERS | GRAPHIC LITHOLOGY | DRILLING DISTURB. | SED. STRUCTURES | SAMPLES | LITHOLOGIC DESCRIPTION |
|---|---|---|---|---|---|---|---|---|---|---|---|---|---|---|
| UPPER PALEOCENE / LOWER EOCENE | UPPER PALEOCENE (P5 - P6a) P6 - P7 | NP 10-12 (LOWER EOCENE) | Barren | Barren | Barren | $\phi$=55.61 $\rho_g$=2.73 $\phi$=53.81 $\rho_g$=2.72 | | 1<br>2<br>CC | 0.5<br>1.0 | VOID<br>VOID | | ≈ | * | FORAMINIFER-BEARING NANNOFOSSIL CHALK<br>Drilling disturbance: Section 1, 0-10 cm, downhole contamination.<br>Major lithology: Foraminifer-bearing nannofossil chalk, white (no color code), moderately bioturbated (mottled).<br>Minor lithology: Chert clast, Section 1, 26-30 cm (probably not *in situ*).<br>SMEAR SLIDE SUMMARY (%):<br>1, 62 D; 2, 15 D<br>COMPOSITION:<br>Mica Tr —<br>Foraminifers 10 10<br>Nannofossils 90 90<br>Radiolarians Tr — |

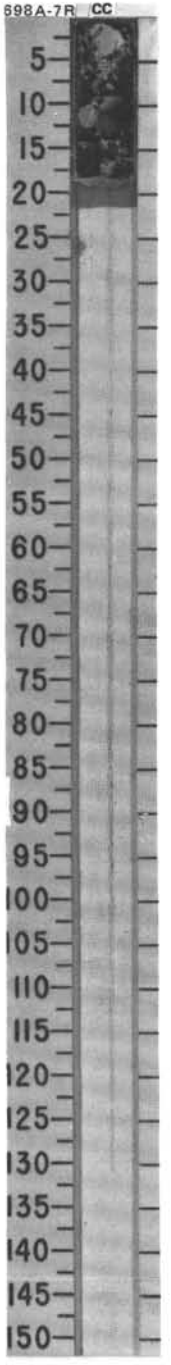


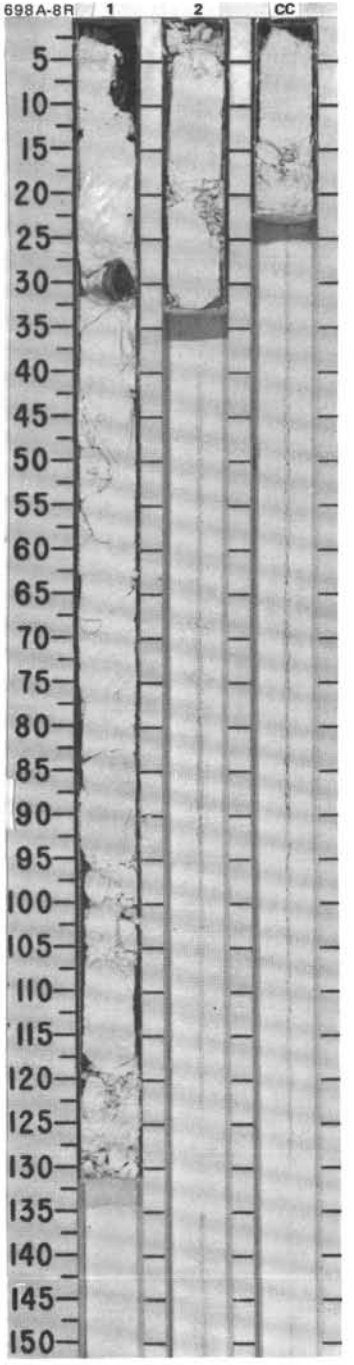

SITE 698 HOLE A CORE 9R CORED INTERVAL 2198.0-2207.5 mbsl; 70.5-80.0 mbsf

| TIME-ROCK UNIT | BIOSTRAT. ZONE/ FOSSIL CHARACTER: FORAMINIFERS | NANNOFOSSILS | RADIOLARIANS | DIATOMS | PALEOMAGNETICS | PHYS. PROPERTIES | CHEMISTRY | SECTION | METERS | GRAPHIC LITHOLOGY | DRILLING DISTURB. | SED. STRUCTURES | SAMPLES |
|---|---|---|---|---|---|---|---|---|---|---|---|---|---|
| UPPER PALEOCENE | P4 (UPPER PALEOCENE) | NP 9 | Barren | Barren | | $\phi$=51.86 $\rho_g$=2.69 $\phi$=50.00 $\rho_g$=2.71 | | 1 | 0.5 1.0 | | | | * |
| | | | | Barren | | | | 2 | | | | | IW OG |
| | | | | | | | | CC | | | | | * |

LITHOLOGIC DESCRIPTION

NANNOFOSSIL CHALK

Drilling disturbance: Minor drilling slurry and fracturing at Section 1, 82-86 and 109-113 cm; and Section 2, 0-8 and 101-141 cm.

Major lithology: Nannofossil chalk, white (no color code), moderately to strongly bioturbated.

Minor lithology: Chert nodules, Section 1, 5-17 cm; and Section 2, 71-76 cm.

SMEAR SLIDE SUMMARY (%):

| | 1, 77 D | 2, 85 D |
|---|---|---|
| COMPOSITION: | | |
| Calcite/dolomite | Tr | 1 |
| Foraminifers | 5 | 3 |
| Nannofossils | 95 | 96 |
| Radiolarians | Tr | Tr |

SITE 698 HOLE A CORE 10R CORED INTERVAL 2207.5-2217.0 mbsl; 80.0-89.5 mbsf

| TIME-ROCK UNIT | BIOSTRAT. ZONE/ FOSSIL CHARACTER: FORAMINIFERS | NANNOFOSSILS | RADIOLARIANS | DIATOMS | PALEOMAGNETICS | PHYS. PROPERTIES | CHEMISTRY | SECTION | METERS | GRAPHIC LITHOLOGY | DRILLING DISTURB. | SED. STRUCTURES | SAMPLES |
|---|---|---|---|---|---|---|---|---|---|---|---|---|---|
| UPPER PALEOCENE | P4-P5 (UPPER PALEOCENE) | NP 8 - NP 9 | UPPER PALEOCENE | *H. inequilaterus* | UPPER PALEOCENE | | | 1 | 0.5 1.0 | | | | |
| | | | | | | | | 2 | | | | | |
| | | | | | | | | CC | | | | | |

LITHOLOGIC DESCRIPTION

NANNOFOSSIL CHALK

Major lithology: Nannofossil chalk, white (no color code), slightly to moderately bioturbated.

Minor lithology: Gray (5Y 7/2) chert, downhole contaminants (chert), in Section 1, 0-20 cm.

SMEAR SLIDE SUMMARY (%):

| | 1, 60 D | 2, 100 D |
|---|---|---|
| COMPOSITION: | | |
| Mica | — | Tr |
| Calcite/dolomite | 1 | 1 |
| Foraminifers | 3 | 4 |
| Nannofossils | 96 | 95 |
| Radiolarians | — | Tr |

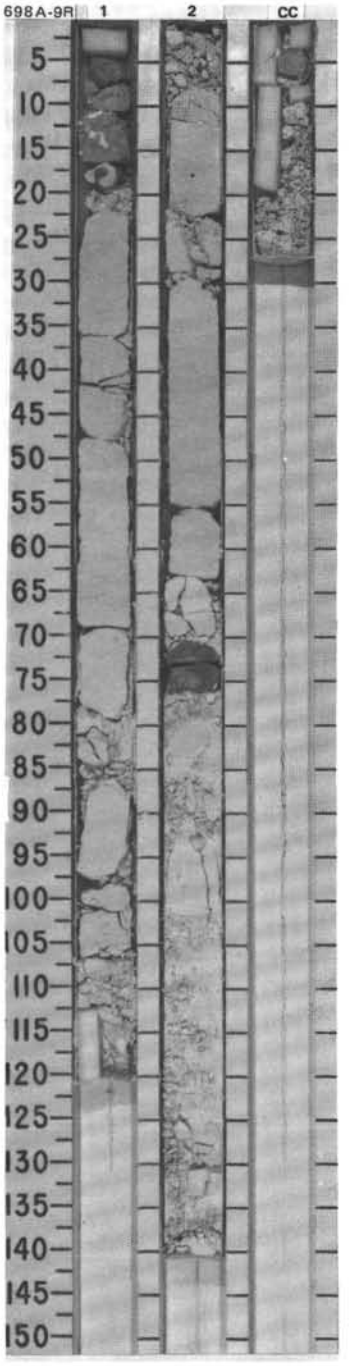


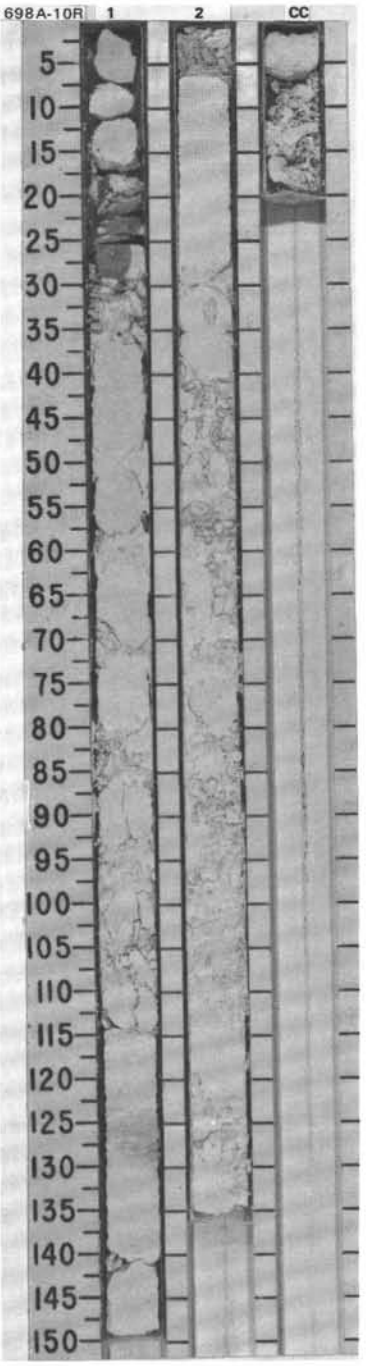

SITE 698 HOLE A CORE 11R CORED INTERVAL 2217.0-2226.5 mbsl; 89.5-99.0 mbsf

| TIME-ROCK UNIT | BIOSTRAT. ZONE/ FOSSIL CHARACTER: FORAMINIFERS | NANNOFOSSILS | RADIOLARIANS | DIATOMS | PALEOMAGNETICS | PHYS. PROPERTIES | CHEMISTRY | SECTION | METERS | GRAPHIC LITHOLOGY | DRILLING DISTURB. | SED. STRUCTURES | SAMPLES | LITHOLOGIC DESCRIPTION |
|---|---|---|---|---|---|---|---|---|---|---|---|---|---|---|
| UPPER PALEOCENE | (UPPER PALEOCENE) P4 | NP 5-7 | UPPER PALEOCENE | *H. inaequilaterus* | UPPER PALEOCENE | | | CC | | | | | | NANNOFOSSIL CHALK, CHERT, and GRAVEL FRAGMENTS<br>Drilling disturbance: Highly fractured. |

SITE 698 HOLE A CORE 12R CORED INTERVAL 2226.5-2236.0 mbsl; 99.0-108.5 mbsf

| TIME-ROCK UNIT | BIOSTRAT. ZONE/ FOSSIL CHARACTER: FORAMINIFERS | NANNOFOSSILS | RADIOLARIANS | DIATOMS | PALEOMAGNETICS | PHYS. PROPERTIES | CHEMISTRY | SECTION | METERS | GRAPHIC LITHOLOGY | DRILLING DISTURB. | SED. STRUCTURES | SAMPLES | LITHOLOGIC DESCRIPTION |
|---|---|---|---|---|---|---|---|---|---|---|---|---|---|---|
| LOWER UPPER PALEOCENE ? | LOWER PALEOCENE P1b - P1c | NP 5-7 | Barren | *H. inaequilaterus* | Barren | $\phi$=51.86 $\rho_g$=2.63 | | 1<br>2<br>CC | 0.5<br>1.0 | | | | * | NANNOFOSSIL CHALK<br>Drilling disturbance: Slightly to highly fractured at Section 1, 60-75 and 90-100 cm, and CC.<br>Major lithology: Nannofossil to nannofossil-bearing chalk, white (no color code), highly bioturbated in Section 1, 80-148 cm, and Section 2, 0-20 cm.<br>Minor lithology: Chert, light gray (5Y 7/1).<br>SMEAR SLIDE SUMMARY (%):<br>1, 40 D — 2, 10 D<br>COMPOSITION:<br>Calcite/dolomite 5 1<br>Foraminifers — 10<br>Nannofossils 95 89<br>Diatoms Tr —<br>Silicoflagellates Tr — |

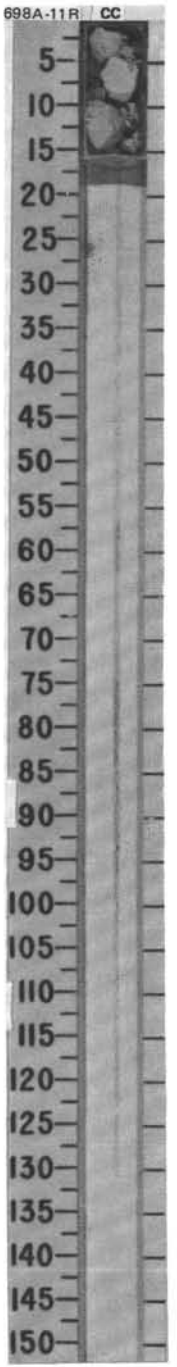


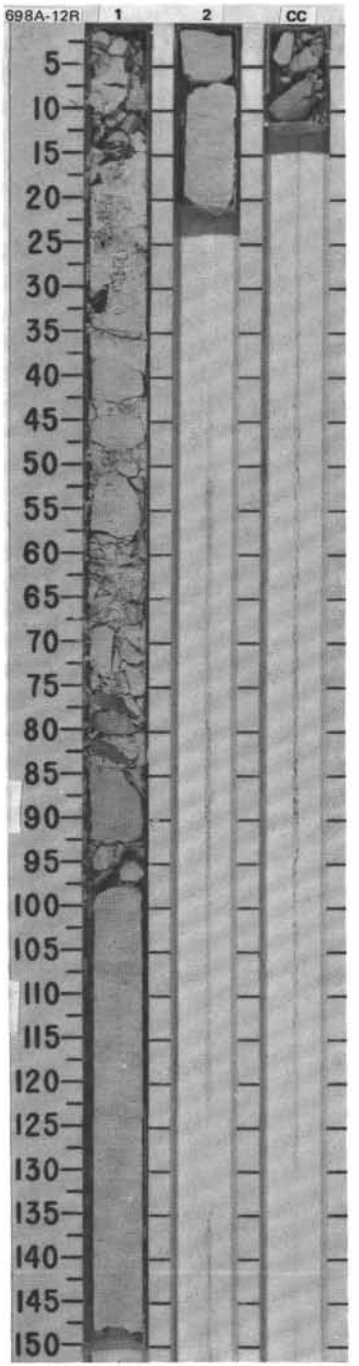

SITE 698 HOLE A CORE 13R CORED INTERVAL 2236.0-2245.5 mbsl; 108.5-118.0 mbsf

| TIME-ROCK UNIT | BIOSTRAT. ZONE/ FOSSIL CHARACTER: FORAMINIFERS | NANNOFOSSILS | RADIOLARIANS | DIATOMS | PALEOMAGNETICS | PHYS. PROPERTIES | CHEMISTRY | SECTION | METERS | GRAPHIC LITHOLOGY | DRILLING DISTURB. | SED. STRUCTURES | SAMPLES | LITHOLOGIC DESCRIPTION |
|---|---|---|---|---|---|---|---|---|---|---|---|---|---|---|
| LOWER PALEOCENE (LOWER PALEOCENE) | P1b | NP 3-4 | Barren | Barren | Barren | | | CC | | | | | | PORCELLANITE<br>Major lithology: Porcellanite, light gray (5Y 8/1). |

SITE 698 HOLE A CORE 14R CORED INTERVAL 2245.5-2255.0 mbsl; 118.0-127.5 mbsf

| TIME-ROCK UNIT | BIOSTRAT. ZONE/ FOSSIL CHARACTER: FORAMINIFERS | NANNOFOSSILS | RADIOLARIANS | DIATOMS | PALEOMAGNETICS | PHYS. PROPERTIES | CHEMISTRY | SECTION | METERS | GRAPHIC LITHOLOGY | DRILLING DISTURB. | SED. STRUCTURES | SAMPLES | LITHOLOGIC DESCRIPTION |
|---|---|---|---|---|---|---|---|---|---|---|---|---|---|---|
| UPPER MAESTRICHTIAN | *Abathomphalus mayaroensis* Zone | *A. cymbiformis* - *N. frequens* Zone | Barren | Barren | Barren | $\phi$=51.14 $\rho_g$=2.71 | | 1<br>CC | 0.5 | | | | ***<br>IW<br>OG | NANNOFOSSIL-BEARING CHALK<br>Drilling disturbance: Moderately fractured throughout; orientation of biscuits preserved.<br>Major lithology: Nannofossil-bearing chalk, very fine-grained calcite (micrite), white (5Y 8/1).<br>Minor lithology: Chert, gray (5Y 7/1); downhole contaminants at Section 1, 0–8 cm.<br>SMEAR SLIDE SUMMARY (%): |

| | 1, 19 D | 1, 22 D | 1, 23 D |
|---|---|---|---|
| COMPOSITION: | | | |
| Mica | Tr | Tr | Tr |
| Calcite/dolomite | 78 | 89 | 88 |
| Foraminifers | 2 | 1 | 2 |
| Nannofossils | 20 | 10 | 10 |
| Radiolarians | Tr | Tr | — |


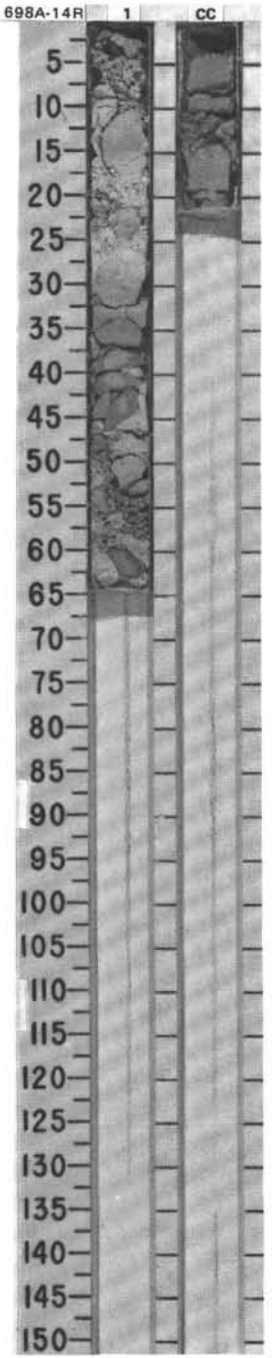

SITE 698 HOLE A CORE 15R CORED INTERVAL 2255.0-2264.5 mbsl; 127.5-137.0 mbsf

TIME-ROCK UNIT: UPPER MAESTRICHTIAN
BIOSTRAT. ZONE/FOSSIL CHARACTER: *Abathomphalus mayaroensis* Zone; *A. cymbiformis* - *N. frequens* Zone
FORAMINIFERS: Barren
NANNOFOSSILS: ?
RADIOLARIANS: Barren
DIATOMS:
PALEOMAGNETICS:
PHYS. PROPERTIES:
CHEMISTRY:
SECTION: 1, CC
METERS: 0.5, 1.0
GRAPHIC LITHOLOGY
DRILLING DISTURB.
SED. STRUCTURES: *
SAMPLES

LITHOLOGIC DESCRIPTION

NANNOFOSSIL-BEARING CHALK

Major lithology: Nannofossil-bearing chalk, white (5Y 8/1) to light gray (5Y 7/1), very fine grained, moderately mottled, with thin, parallel laminated horizons at Section 1, 75, 110, and 130 cm.

Minor lithology: Chert clasts in CC, dark gray (5Y 6/1).

SMEAR SLIDE SUMMARY (%):

| | 1, 87 D |
|---|---|
| COMPOSITION: | |
| Mica | Tr |
| Calcite/dolomite | 75 |
| Foraminifers | 5 |
| Nannofossils | 20 |
| Radiolarians | Tr |

SITE 698 HOLE A CORE 16R CORED INTERVAL 2264.5-2274.0 mbsl; 137.0-146.5 mbsf

TIME-ROCK UNIT: MIDDLE to UPPER MAESTRICHTIAN
BIOSTRAT. ZONE/FOSSIL CHARACTER: MIDDLE MAESTRICHTIAN *A. mayaroensis* Zone; *R. levis* Zone : not examined
FORAMINIFERS: Barren
NANNOFOSSILS: Barren
RADIOLARIANS: Barren
DIATOMS:
PALEOMAGNETICS: $\phi$=45.77 $\rho_g$=2.64 $\phi$=44.79 $\rho_g$=2.75
PHYS. PROPERTIES:
CHEMISTRY:
SECTION: 1, 2, 3, CC
METERS: 0.5, 1.0
GRAPHIC LITHOLOGY
DRILLING DISTURB.
SED. STRUCTURES: *
SAMPLES: IW, OC, *

LITHOLOGIC DESCRIPTION

NANNOFOSSIL-FORAMINIFER-BEARING CHALK

Drilling disturbance: Minor fracturing in Section 1, 20-60, 80-90, 130-135, and 145-150 cm. In CC, major disturbance.

Major lithology: Nannofossil-foraminifer-bearing chalk, light gray (7.5YR N8/1) with green-gray (5G 7/1) laminated horizons, slightly to moderately bioturbated.

Minor lithology: Chert nodules in Section 1, 43-46 cm, and CC; and chert layer, Section 2, 50-60 cm, gray (5Y 6/1).

SMEAR SLIDE SUMMARY (%):

| | 1, 66 | 2, 68 | 3, 20 |
|---|---|---|---|
| | X | X | X |
| COMPOSITION: | | | |
| Mica | Tr | Tr | Tr |
| Calcite/dolomite | 85 | 75 | 78 |
| Foraminifers | 10 | 10 | 12 |
| Nannofossils | 5 | 15 | 10 |

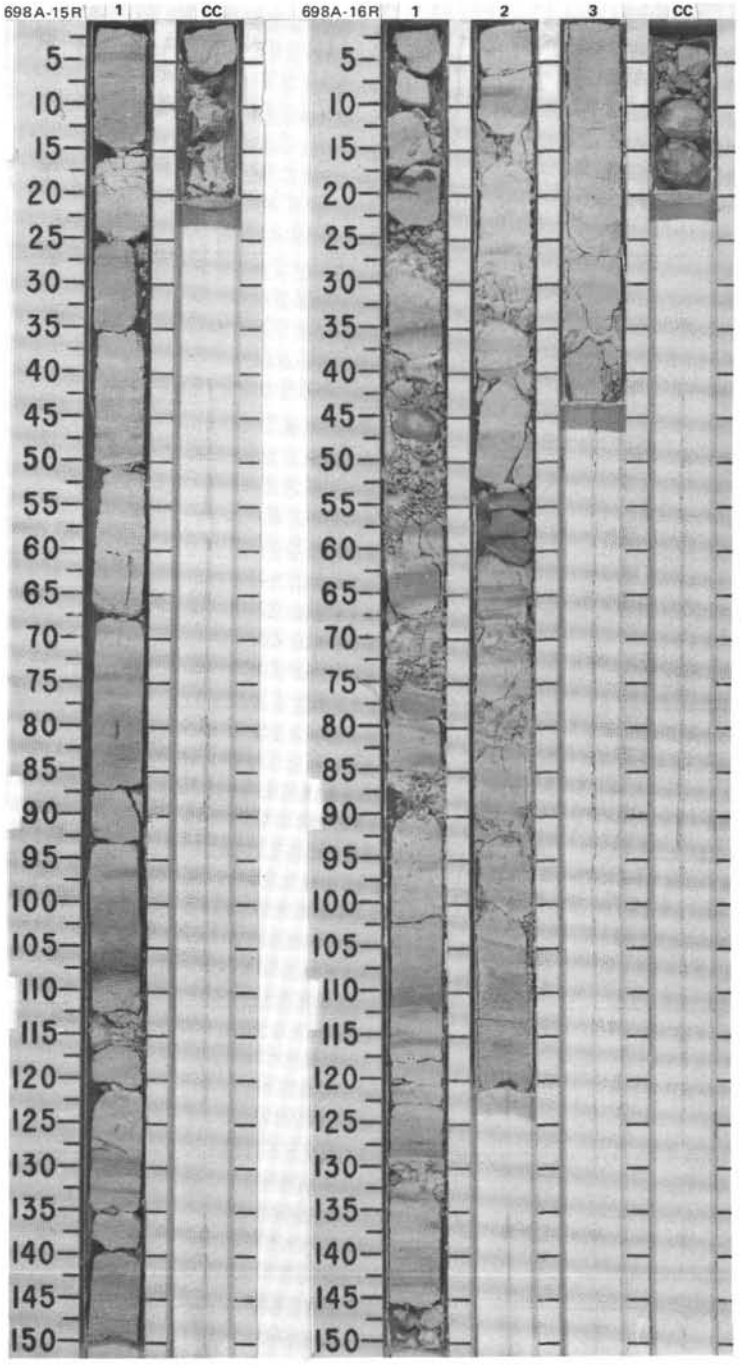

SITE 698 HOLE A CORE 17R CORED INTERVAL 2274.0-2283.5 mbsl; 146.5-156.0 mbsf

| TIME-ROCK UNIT | BIOSTRAT. ZONE/FOSSIL CHARACTER: FORAMINIFERS | NANNOFOSSILS | RADIOLARIANS | DIATOMS | PALEOMAGNETICS | PHYS. PROPERTIES | CHEMISTRY | SECTION | METERS | GRAPHIC LITHOLOGY | DRILLING DISTURB. | SED. STRUCTURES | SAMPLES | LITHOLOGIC DESCRIPTION |
|---|---|---|---|---|---|---|---|---|---|---|---|---|---|---|
| CAMPANIAN-MAESTRICHTIAN | CAMPANIAN - MAESTRICHTIAN | *R. levis* Zone | Barren | Barren | | $\phi$=49.38 $\rho_g$=2.68 $\phi$=43.12 $\rho_g$=1.66 | | 1<br>2<br>CC | 0.5<br>1.0 | | | | | |

LIMESTONE

Drilling disturbance: Highly fragmented in CC.

Major lithology: Limestone, very fine grained, showing rhythmic cycles over 10-20 cm, light gray (5Y 7/1), moderately to highly bioturbated and laminated limestone grading into white (5Y 8/1), faintly to moderately bioturbated limestone. Light gray limestone has < 10% impurities (volcanic ash, radiolarians, diatom fragments, zeolites, and clay). White limestone with no detectable impurities.

Minor lithology: Chert, gray (5Y 6/1).

SMEAR SLIDE SUMMARY (%):

| | 1, 23 D | 1, 49 D |
|---|---|---|
| COMPOSITION: | | |
| Quartz | Tr | — |
| Feldspar | Tr | — |
| Clay | 2 | — |
| Calcite/dolomite | 40 | 97 |
| Foraminifers | 5 | 3 |
| Nannofossils | 1 | — |
| Diatoms | Tr | — |
| Calcispheres | — | Tr |

698A-18R NO RECOVERY

698A-19R NO RECOVERY

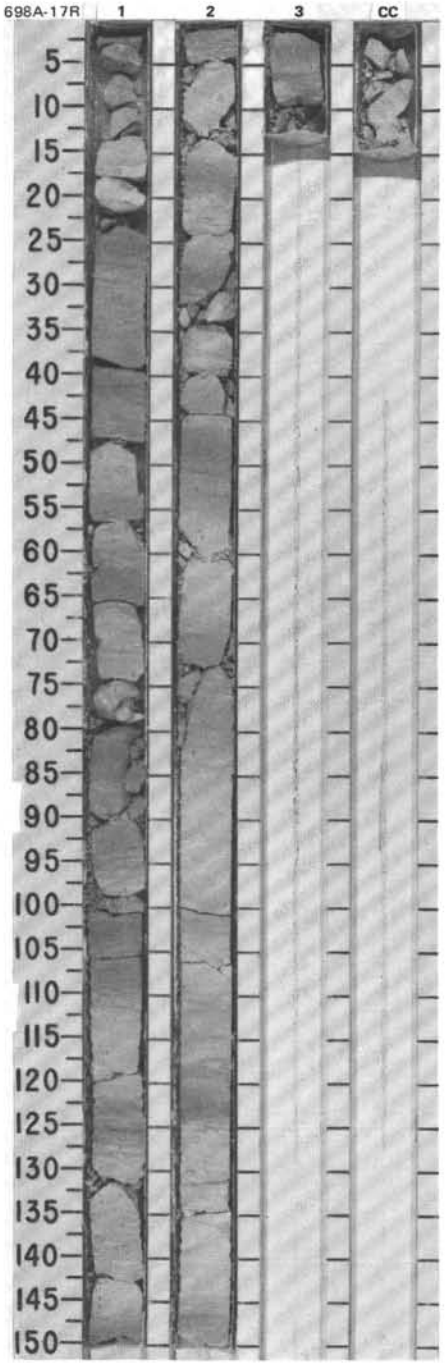

SITE 698 HOLE A CORE 20R CORED INTERVAL 2302.5-2308.5 mbsl; 175.0-181.0 mbsf

| TIME-ROCK UNIT | BIOSTRAT. ZONE/ FOSSIL CHARACTER: FORAMINIFERS | NANNOFOSSILS | RADIOLARIANS | DIATOMS | PALEOMAGNETICS | PHYS. PROPERTIES | CHEMISTRY | SECTION | METERS | GRAPHIC LITHOLOGY | DRILLING DISTURB. | SED. STRUCTURES | SAMPLES | LITHOLOGIC DESCRIPTION |
|---|---|---|---|---|---|---|---|---|---|---|---|---|---|---|
| CAMPANIAN? MAESTRICHTIAN | CAMPANIAN - MAESTRICHTIAN | *R. levis* Zone | Barren | Barren | | $\phi$=39.04 $\rho_g$=2.71 | | 1<br>CC | 0.5<br>1.0 | | | | * | LIMESTONE<br>Drilling disturbance: Moderate throughout.<br>Major lithology: Light gray (5GY 7/1) limestone (dolomite?) with light greenish grey (5GY 6/1) contact horizons with chert.<br>Minor lithology: Light gray (2.5Y 7/0) chert nodules at 0-5, 28-36, 57-62, 81-85, and 90-94 cm. |

SMEAR SLIDE SUMMARY (%):

| | 1, 15<br>D |
|---|---|
| COMPOSITION: | |
| Feldspar | Tr |
| Volcanic glass | Tr |
| Calcite/dolomite | 92 |
| Foraminifers | 7 |
| Calcispheres | Tr |

SITE 698 HOLE A CORE 21R CORED INTERVAL 2308.5-2318.0 mbsl; 181.0-190.5 mbsf

| TIME-ROCK UNIT | BIOSTRAT. ZONE/ FOSSIL CHARACTER: FORAMINIFERS | NANNOFOSSILS | RADIOLARIANS | DIATOMS | PALEOMAGNETICS | PHYS. PROPERTIES | CHEMISTRY | SECTION | METERS | GRAPHIC LITHOLOGY | DRILLING DISTURB. | SED. STRUCTURES | SAMPLES | LITHOLOGIC DESCRIPTION |
|---|---|---|---|---|---|---|---|---|---|---|---|---|---|---|
| CAMPANIAN | LOWER CAMPANIAN? | *T. orionatas* Zone | Barren | Barren | | $\phi$=39.53 $\rho_g$=2.67 | | 1<br>2<br>CC | 0.5<br>1.0 | | | | * | LIMESTONE and CHERT<br>Drilling disturbance throughout.<br>Major lithology: Limestone (and dolomitic limestone?), light gray (5Y 7/1), with horizons of light greenish gray (5GR 6/1).<br>Minor lithology: Chert, light gray (5Y 7/1) to gray (5Y 6/1). |

SMEAR SLIDE SUMMARY (%):

| | 1, 23<br>D | 1, 123<br>D |
|---|---|---|
| COMPOSITION: | | |
| Calcite/dolomite | 93 | 93 |
| Foraminifers | 2 | 2 |
| Calcispheres | 5 | 5 |

698A-22R NO RECOVERY

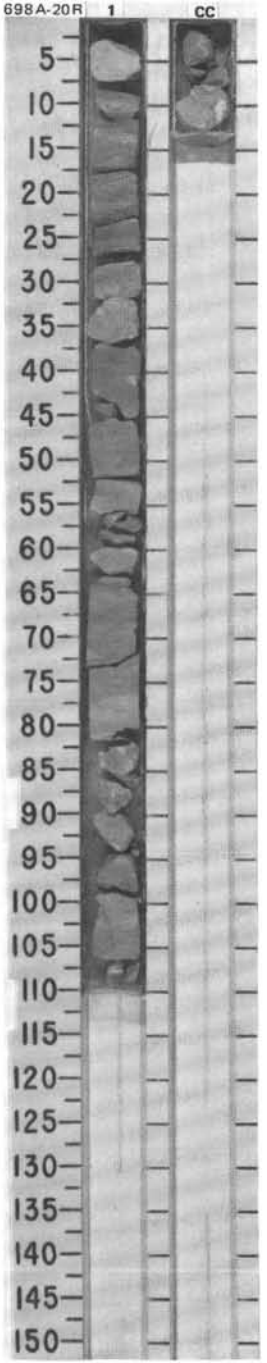


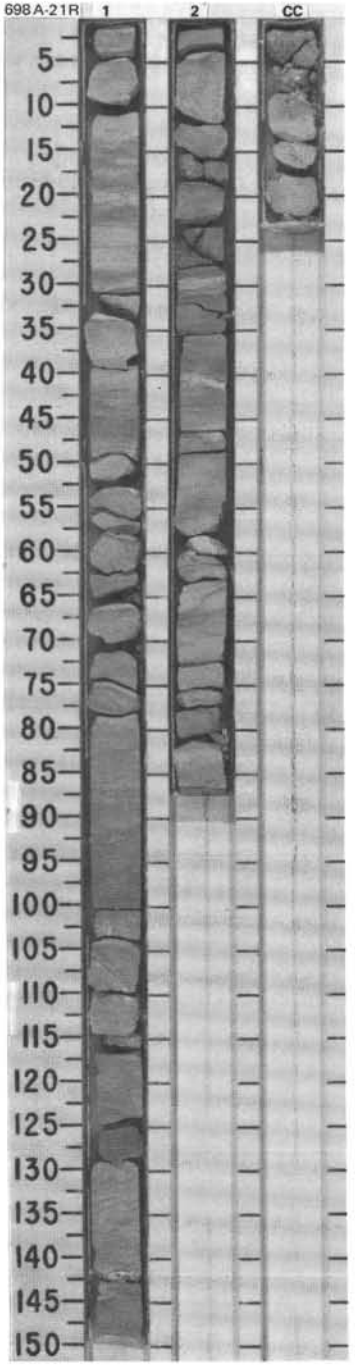

SITE 698 HOLE A CORE 23R CORED INTERVAL 2318.0-2337.0 mbsl; 200-209.5 mbsf

| TIME-ROCK UNIT | BIOSTRAT. ZONE/ FOSSIL CHARACTER: FORAMINIFERS | NANNOFOSSILS | RADIOLARIANS | DIATOMS | | PALEOMAGNETICS | PHYS. PROPERTIES | CHEMISTRY | SECTION | METERS | GRAPHIC LITHOLOGY | DRILLING DISTURB. | SED. STRUCTURES | SAMPLES | LITHOLOGIC DESCRIPTION |
|---|---|---|---|---|---|---|---|---|---|---|---|---|---|---|---|
| | Barren | Barren | Barren | Barren | Barren | | | | 1 | | | O | | • | SANDY MUD<br><br>Drilling disturbed.<br><br>Major lithology: Sandy mud, dark olive gray (5Y 3/2). Contains a few nannofossils and pieces of chalk as drilling contaminants. Material probably derived from basalt. |

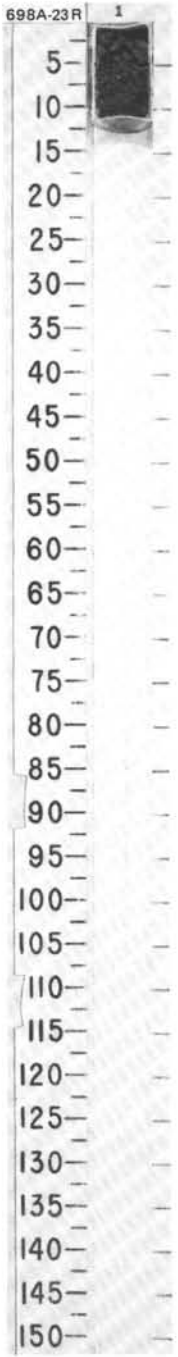

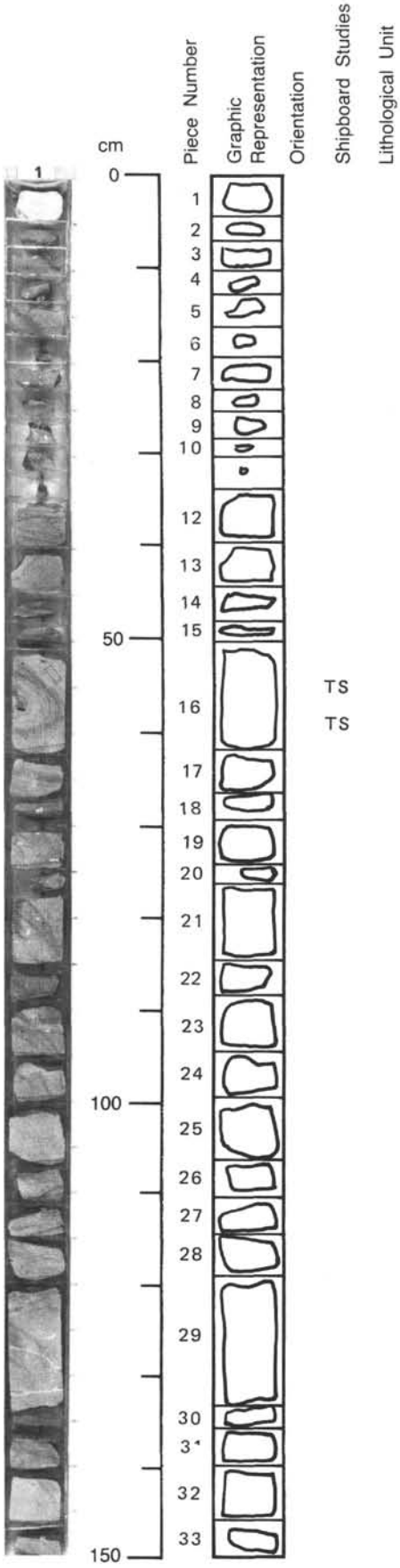


**114-698A-24R-1**

## UNIT 1: CHERT

### Piece 1

**COLOR:** Gray (N7).

## UNIT 2: SPARSELY PLAGIOCLASE(?) PHYRIC (FELDSPATHOID-PHYRIC?) BASALT

### Pieces 2-33

**GROUNDMASS:** Fine-grained plagioclase and augite.
**PHENOCRYSTS:** Feldspar or feldspathoid, 1-3 mm.
**COLOR:** Greenish gray (5BG 6/1).
**VESICLES:** Rare, 2-4 mm, some open, some filled with serpentinite and calcite.
**ALTERATION:** Moderately altered and serpentinized alkali basalt.

**SMEAR SLIDE SUMMARY (%):**

| | 1, 146 (Dominant lithology) |
|---|---|
| COMPOSITION: | |
| Mica | 90 |
| Accessory minerals: | |
| Spinel | Tr |
| Magnetite (opaques) | 10 |

**NOTE:** Smear slide is from material scraped from side of barrel between Pieces 32 and 33.

**PHYSICAL PROPERTIES:**

| | | | 1, 93 |
|---|---|---|---|
| $\phi$ | (%) | = | 12.26 |
| $\rho_g$ | (g/cm$^3$) | = | 3.10 |

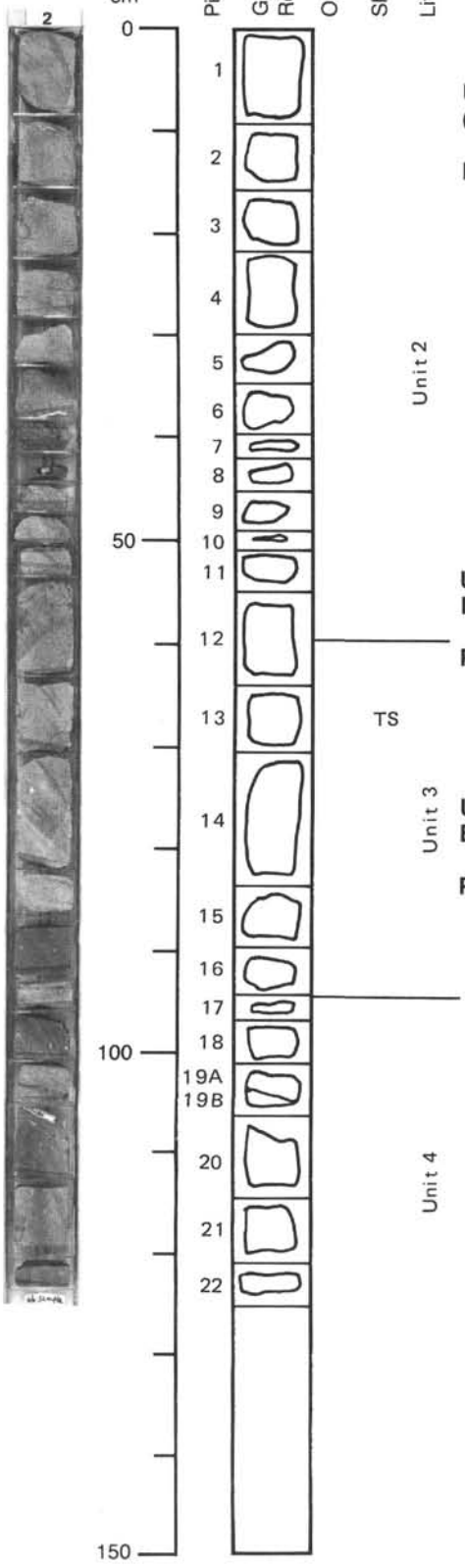


**114-698A-24R-2**

**UNIT 2 (Continued): SPARSELY PLAGIOCLASE-FELDSPATHOID(?) PHYRIC (ALKALI) BASALT**

**Pieces 1-11**

**GROUNDMASS:** Fine-grained plagioclase and augite.
**PHENOCRYSTS:** Feldspar or feldspathoid, 2-4 mm.
**COLOR:** Greenish gray (5BG 6/1).
**VESICLES:** One, 1-2 mm.
**ALTERATION:** Material is serpentinized and slightly oxidized.

**PHYSICAL PROPERTIES:**

| | | | 2, 90 |
|---|---|---|---|
| $\phi$ | (%) | = | 23.09 |
| $\rho_g$ | (g/cm$^3$) | = | 3.00 |

**UNIT 3: SPARSELY PLAGIOCLASE-FELDSPATHOID(?) PHYRIC (ALKALI) BASALT**

**Pieces 12-16, as 114-698A-24R-2, Unit 2, except for alteration**

**ALTERATION:** Fresh, with little or no oxidation.

**UNIT 4: SPARSELY PLAGIOCLASE-FELDSPATHOID(?) PHYRIC (ALKALI) BASALT**

**Pieces 17-22, as 114-698A-24R-2, Unit 2**

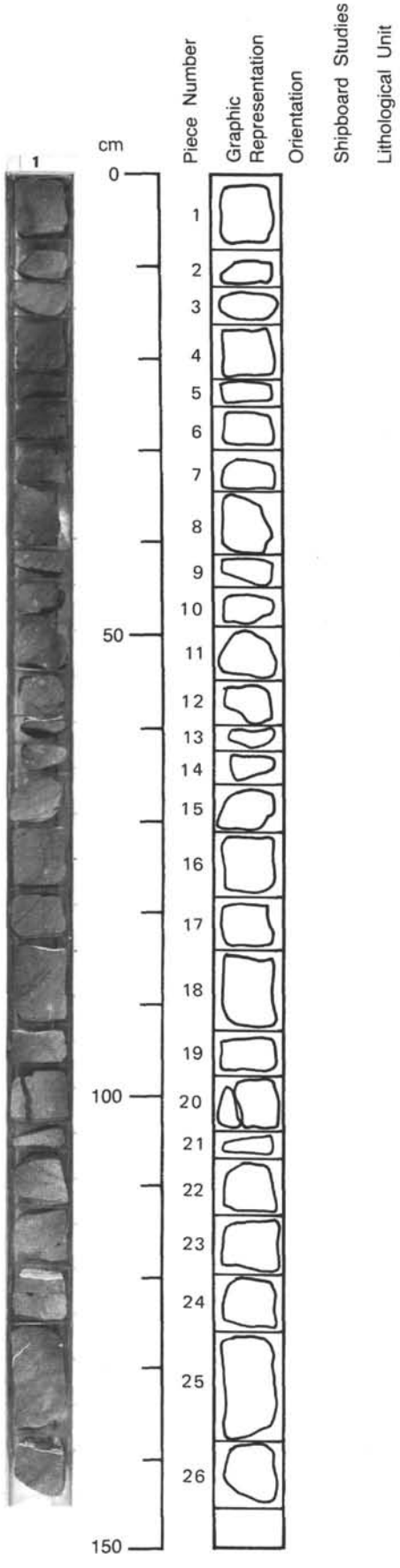


**114-698A-25R-1**

**UNIT 4 (Continued): SPARSELY PHYRIC BASALT**

**Pieces 1-26**

**GROUNDMASS:** Fine grained.
**PHENOCRYSTS:** 1-3 mm.
**COLOR:** Very dark gray (7.5YR to N3).
**ALTERATION:** Moderate. Serpentinized, in part oxidized.
**VEINS/FRACTURES:** Calcite veins common.

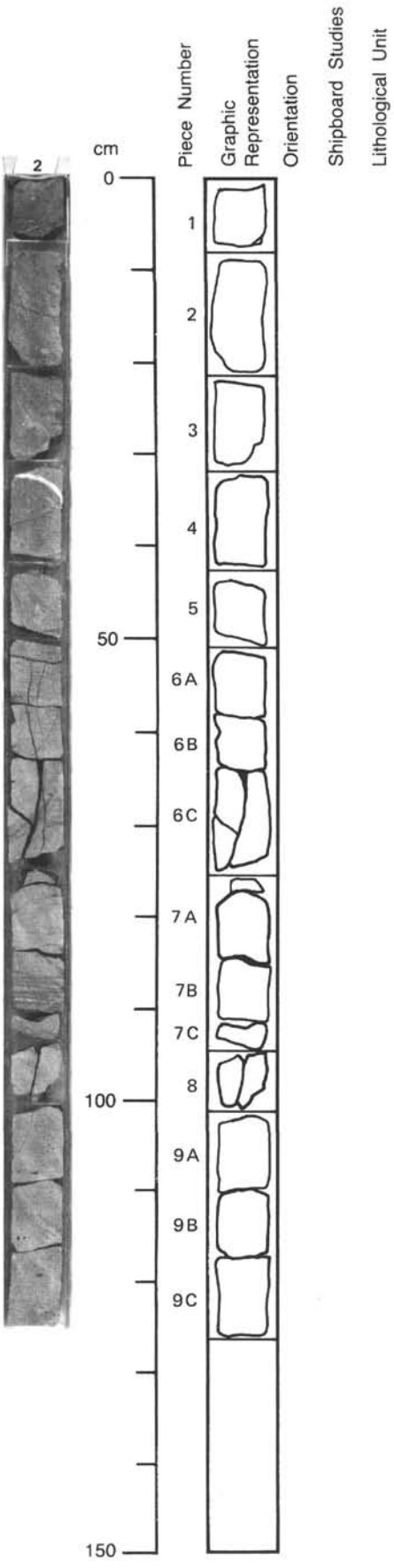


**114-698A-25R-2**

## UNIT 4 (Continued): SLIGHTLY FELDSPAR PHYRIC BASALT

### Pieces 1-9

**GROUNDMASS:** Fine grained.
**PHENOCRYSTS:** 0.9-9.0 mm, feldspar.
**COLOR:** Very dark gray (7.5YR to N3/1).
**STRUCTURE:** Ferromagnesium minerals preferentially oriented, mainly horizontal.
**VEINS/FRACTURES:** In horizontal fractures, weathering and serpentinization. Some fractures are filled with sparry calcite. Some amygdules filled with calcite.

**PHYSICAL PROPERTIES:**

| | | | 2, 90 |
|---|---|---|---|
| $\phi$ | (%) | = | 6.58 |
| $\rho_g$ | ($g/cm^3$) | = | 2.93 |

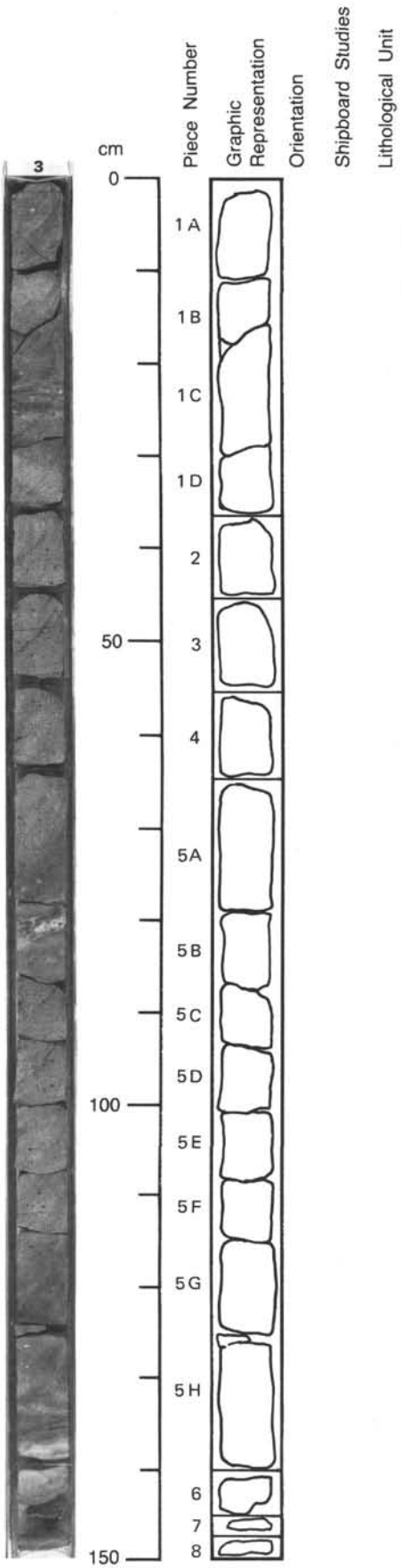


**114-698A-25R-3**

## UNIT 4 (Continued): SLIGHTLY FELDSPAR PHYRIC BASALT

### Pieces 1-8

**GROUNDMASS:** Fine grained.
**COLOR:** Greenish gray (7.5YR to N3/1).
**ALTERATION:** Serpentinization, particularly at 20-22 cm, in Piece 1C.

**PHYSICAL PROPERTIES:**

| | | | 3, 22 |
|---|---|---|---|
| $\phi$ | (%) | = | 13.29 |
| $\rho_g$ | ($g/cm^3$) | = | 3.29 |


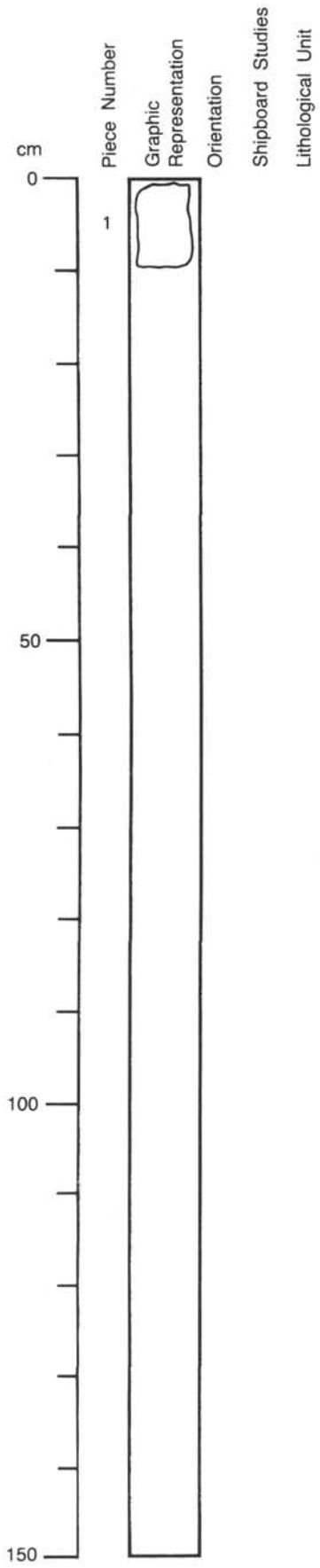


**114-698A-25R-4**

**UNIT 4 (Continued): SLIGHTLY FELDSPAR PHYRIC BASALT**

**Piece 1**

**GROUNDMASS:** Fine grained.
**PHENOCRYSTS:** Up to 3 mm.
**COLOR:** Very dark gray (7.5YR to N3/1).
**ALTERATION:** Serpentinized.

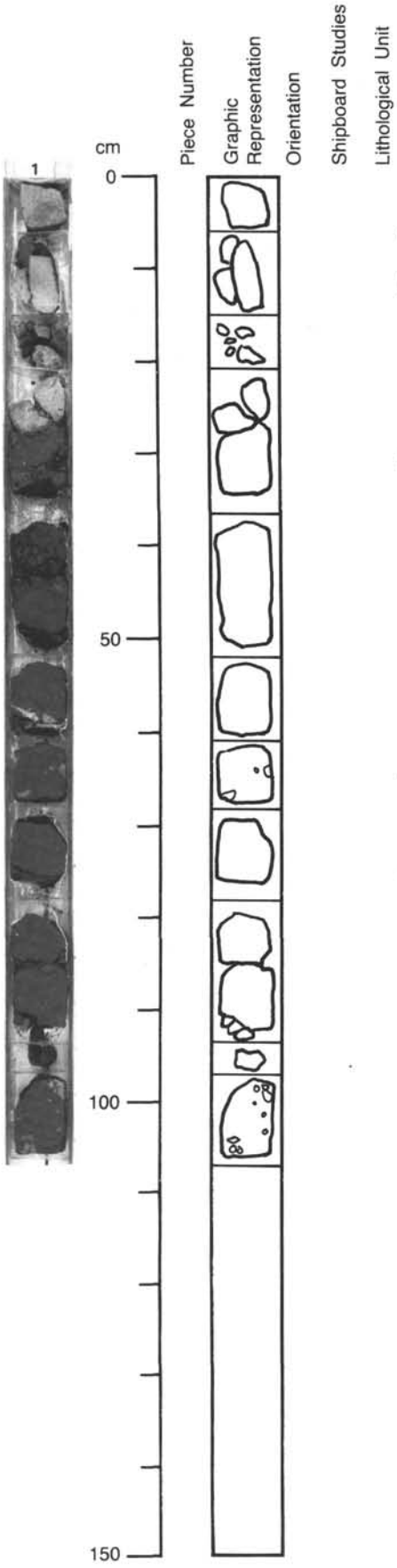


**114-698A-26R-1**

## UNIT 1: DRILLING BRECCIA AND BASALT

### 0-6 cm: POLYGENIC CONGLOMERATE

**STRUCTURE:** Jointing clasts for one half, tangential clasts for the other half where a calcitic white cement has filled the pores. Polygenic clasts are as long as 8-9 mm at long axis. Sphericity: 0.3-0.5. Roundness: 0.1-0.3.

**NOTE:** Possible downhole contamination, but the piece is as large (5 cm × 6 cm) as the core.

### 6-15 cm: PIECES 1-3

**PIECE 1: BASALT**

**GROUNDMASS:** Fine grained.
**COLOR:** Dark gray (7.5YR N4).
**STRUCTURE:** Some black phenocrysts

**PIECE 2: EXTRUSIVE IGNEOUS ROCK (MORE ACIDIC)**

**COLOR:** Gray (7.5YR N5).
**STRUCTURE:** Clear feldspar phenocrysts

**PIECE 3:** MUD (CONTAINS GRAVEL)

**COLOR:** Very dark gray (7.5YR N5).

### 15-21 cm: BASALTIC DRILLING BRECCIA

**COLOR:** Gray (7.5YR N5).

### 21-28 cm: VESICULAR BASALT

**GROUNDMASS:** Fine grained.
**COLOR:** Gray (7.5YR N5).

## UNIT 2: HEMATITIC CLAYSTONE (28-107 cm)

**COLOR:** Dark brown (7.5YR 3/2).
**STRUCTURE:** Includes clasts, some of which are altered. Void: 107-150 cm.
**ALTERATION:** Clast horizons at 62-68 and 98-101 cm.

**SMEAR SLIDE SUMMARY (%):**

| | 1, 99 (Dominant lithology) |
|---|---|
| COMPOSITION: | |
| Clay | 4 |
| Diatoms | 96 |
| Radiolarians | Tr |
| Silicoflagellates | Tr |

**PHYSICAL PROPERTIES:**

| | | | 1, 72 |
|---|---|---|---|
| $\phi$ | (%) | = | 69.19 |
| $G_\gamma$ | (g/cm$^3$) | = | 3.47 |

**NOTE:** Claystone has been divided in parts by drilling disturbance at 37, 52, 62, 68, 79, 94, and 98 cm.

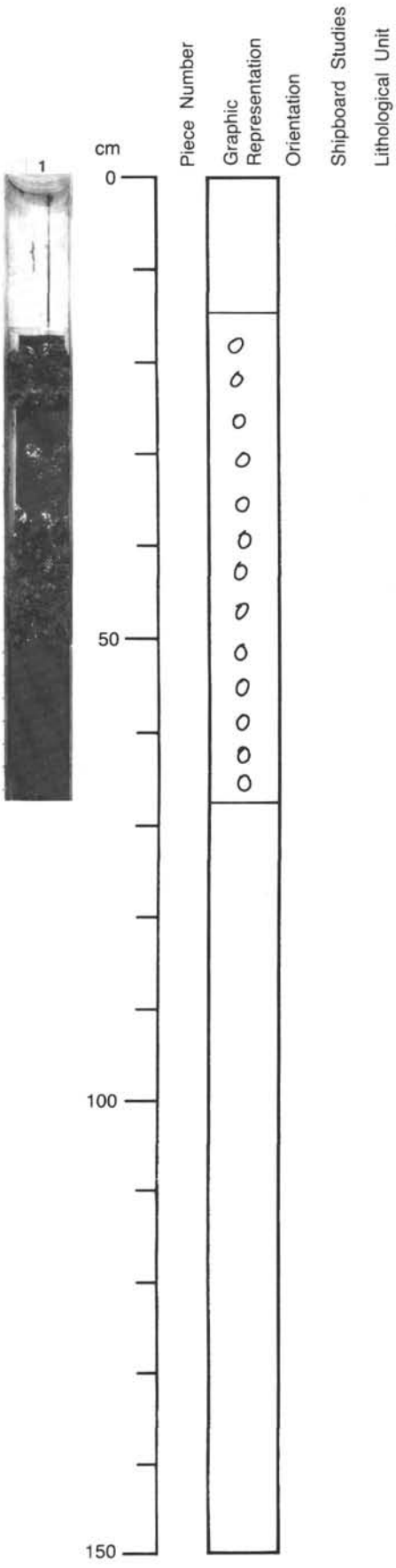


**114-698A-27R-1**

## UNIT 1: REGOLITH OF COMPLETELY WEATHERED BASALT (16-68 cm)

**COLOR:** Dark reddish brown (5YR 2.5/1).

**VESICLES:** Some pieces in the drilling slurry which are less weathered can be recognized as basalt with vesicles, microliths. etc.

**STRUCTURE:** Voids at 0-16 and 68-150 cm.

**PHYSICAL PROPERTIES:**

| | | | 1, 45 |
|---|---|---|---|
| $\phi$ | (%) | = | 60.38 |
| $\rho_g$ | ($g/cm^3$) | = | 3.14 |

**NOTE:** Pieces are in drilling slurry. Slurry contains some pieces of still recognizable basalt.

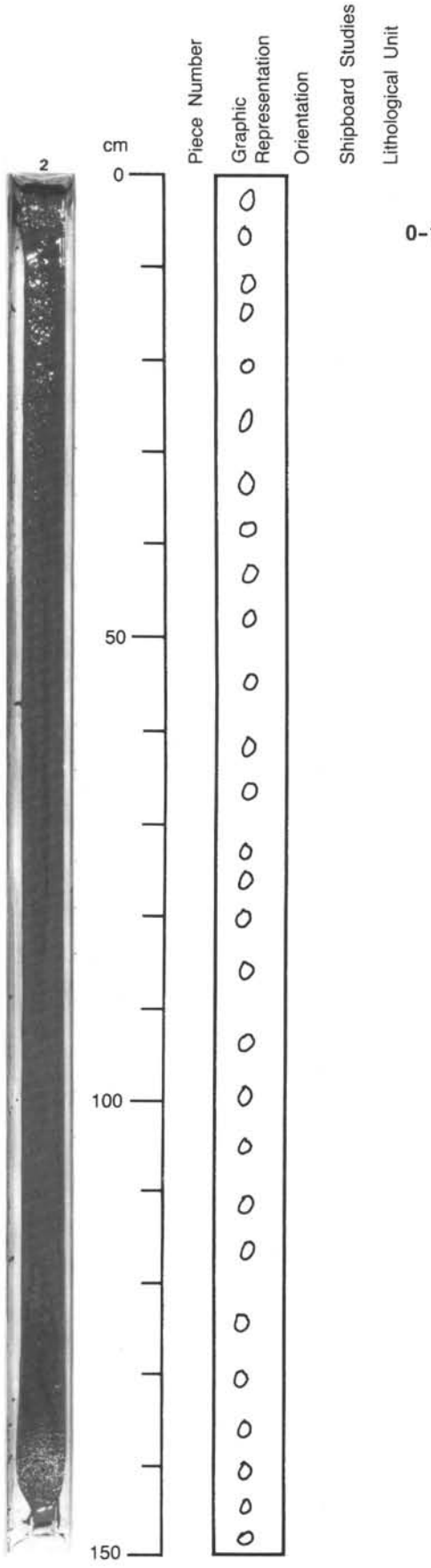


**114-698A-27R-2**

**0-150 cm: DRILLING SLURRY**

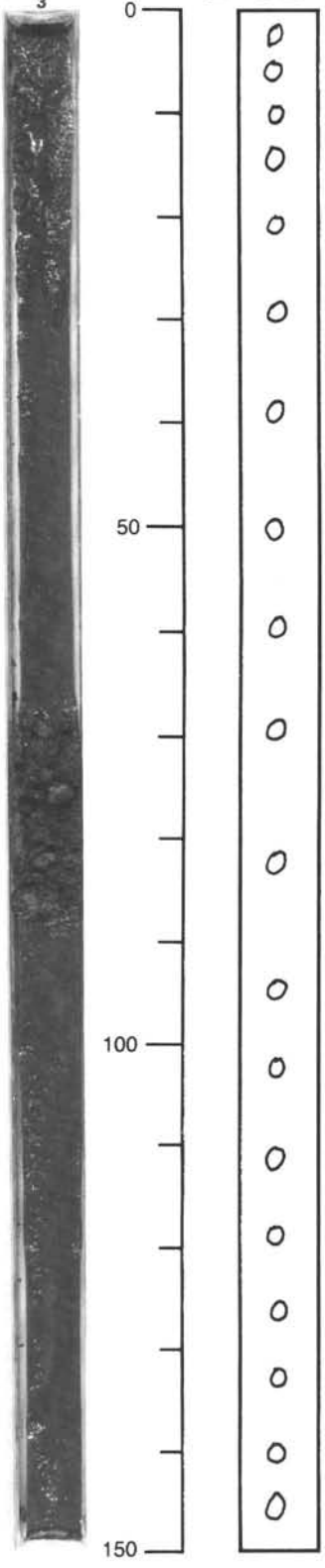


**114-698A-27R-3**

**0-150 cm: DRILLING SLURRY**

**STRUCTURE:** Contains some pieces of weathered basalt.

**PHYSICAL PROPERTIES:**

| | | | 3, 78 |
|---|---|---|---|
| $\phi$ | (%) | = | 53.72 |
| $\rho_g$ | (g/cm$^3$) | = | 3.11 |

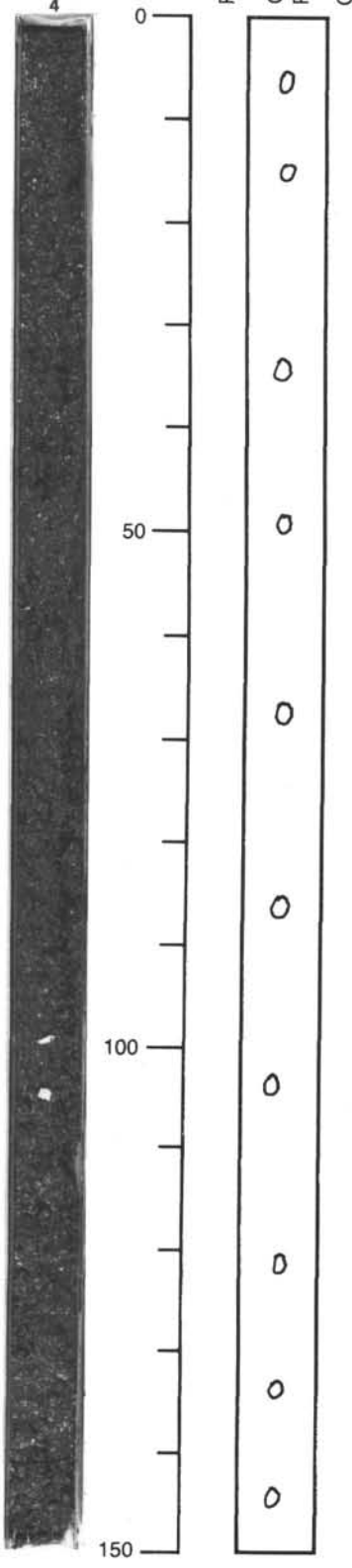


**114-698A-27R-4**

**0-110 cm: DRILLING SLURRY**

**PHYSICAL PROPERTIES:**

| | | | 4, 100 |
|---|---|---|---|
| $\phi$ | (%) | = | 53.15 |
| $\rho_g$ | (g/cm$^3$) | = | 2.92 |

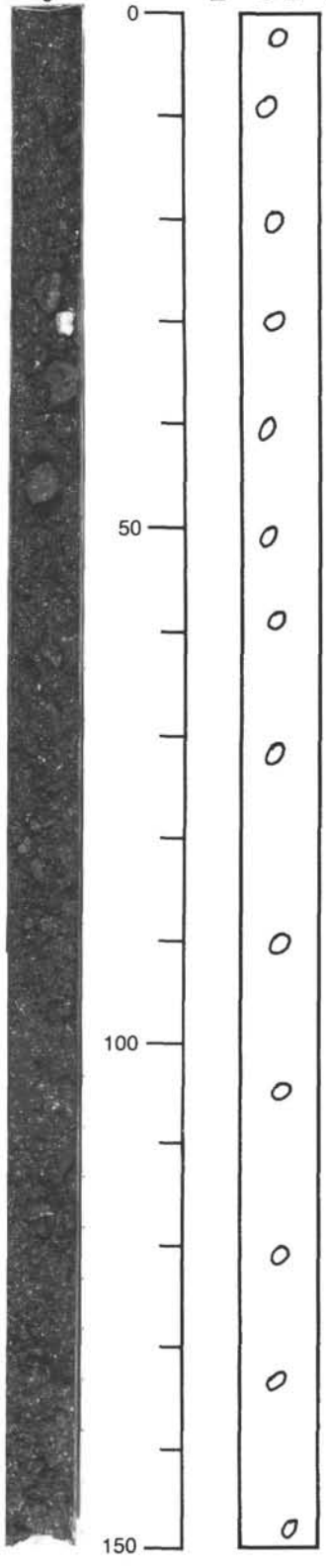


**114-698A-27R-5**

## 0-150 cm: DRILLING SLURRY

**STRUCTURE:** Contains pieces of weathered basalt. Some of those pieces come from a vesicular, fine-grained, very dark gray (8.5YR N3/) basalt.

**ALTERATION:** Weathering consists of an alteration of Fe-Mg minerals, giving iron oxides as limonite or even goethite (see smear slide data), and with a probable phase of alkalization, some of these later filling vesicles.

**PHYSICAL PROPERTIES:**

| | | | 5, 100 |
|---|---|---|---|
| $\phi$ | (%) | = | 69.17 |
| $\rho_g$ | (g/cm$^3$) | = | 2.99 |

**NOTE:** Contamination by downhole fragments, such as chert.


cm
0
50
100
150

Piece Number
Graphic Representation
Orientation
Shipboard Studies
Lithological Unit

**114-698A-27R-6**

**0-54 cm: DRILLING SLURRY**

**PHYSICAL PROPERTIES:**

| | | | |
|---|---|---|---|
| | | | 6, 30 |
| $\phi$ | (%) | = | 80.04 |
| $\rho_g$ | (g/cm$^3$) | = | 2.82 |

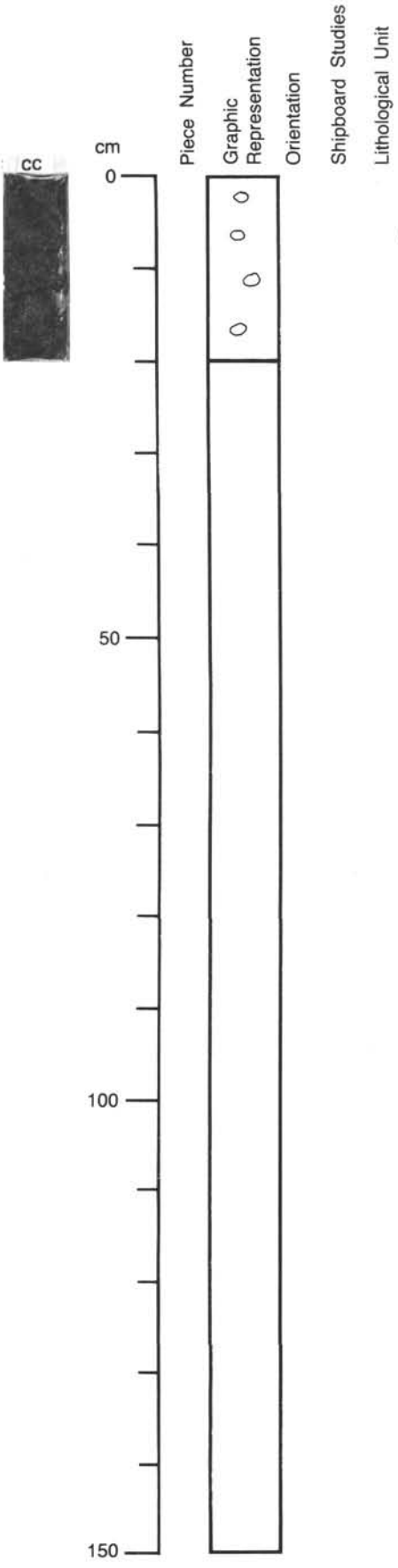


**114-698A-27R-CC**

**0–150 cm: DRILLING SLURRY**

**PHYSICAL PROPERTIES:**

| | | | CC, 10 |
|---|---|---|---|
| $\phi$ | (%) | = | 46.76 |
| $\rho_g$ | (g/cm$^3$) | = | 2.80 |